

GBA2-deficiency and the effect on sphingolipid metabolism in hereditary spastic paraplegia type 46

Dissertation

zur Erlangung des Grades eines Doktors
der Naturwissenschaften

der Mathematisch-Naturwissenschaftlichen Fakultät
und
der Medizinischen Fakultät
der Eberhard-Karls-Universität Tübingen

vorgelegt von

Ulrike Ulmer
aus Sindelfingen,
Deutschland

2024

| | |
|-----------------------------------|---|
| Tag der mündlichen Prüfung: | 05.12.2024 |
| Dekan der Math.-Nat. Fakultät: | Prof. Dr. Thilo Stehle |
| Dekan der Medizinischen Fakultät: | Prof. Dr. Bernd Pichler |
| 1. Berichterstatter: | Prof. Dr. Stefan Liebau |
| 2. Berichterstatter: | Prof. Dr. Rebecca Schüle-Freyer |
| Prüfungskommission: | Prof. Dr. Stefan Liebau Prof. Dr. Rebecca Schüle-Freyer Prof. Dr. Doron Rapaport PD Dr. Christian Johannes Gloeckner |

Erklärung / Declaration:

Ich erkläre, dass ich die zur Promotion eingereichte Arbeit mit dem Titel:

„GBA2-deficiency and the effect on sphingolipid metabolism in hereditary spastic paraplegia type 46”

selbständig verfasst, nur die angegebenen Quellen und Hilfsmittel benutzt und wörtlich oder inhaltlich übernommene Stellen als solche gekennzeichnet habe. Ich versichere an Eides statt, dass diese Angaben wahr sind und dass ich nichts verschwiegen habe. Mir ist bekannt, dass die falsche Abgabe einer Versicherung an Eides statt mit Freiheitsstrafe bis zu drei Jahren oder mit Geldstrafe bestraft wird.

I hereby declare that I have produced the work entitled

„GBA2-deficiency and the effect on sphingolipid metabolism in hereditary spastic paraplegia type 46”

submitted for the award of a doctorate, on my own (without external help), have used only the sources and aids indicated and have marked passages included from other works, whether verbatim or in content, as such. I swear upon oath that these statements are true and that I have not concealed anything. I am aware that making a false declaration under oath is punishable by a term of imprisonment of up to three years or by a fine.

Hamburg, den

Datum / Date

.....

Unterschrift /Signature

Table of Contents

| | |
|---|-----------|
| Table of Contents | V |
| Abstract | 7 |
| Introduction | 8 |
| Hereditary spastic paraplegia | 8 |
| Pathogenic variants affecting lipid metabolism | 9 |
| Bi-allelic <i>GBA2</i> variants cause complicated HSP and spastic ataxia | 9 |
| β-glucosidases in the mammalian cells | 10 |
| Lysosomal β -glucosidase | 10 |
| Klotho-related protein..... | 11 |
| Sphingolipidoses are caused by inherited defects of sphingolipid metabolism | 12 |
| Disease and control models for <i>GBA2</i>-deficiency | 14 |
| <i>In vitro</i> and <i>in vivo</i> models to study <i>GBA2</i> function..... | 14 |
| Induced pluripotent stem cells as a disease model..... | 16 |
| CRISPR/Cas9 genome editing to generate gene-corrected isogenic controls | 19 |
| Introduction to gene editing..... | 19 |
| Material & Methods | 22 |
| Human cell culture | 22 |
| iPSC reprogramming..... | 22 |
| iPSC cell culture | 22 |
| Characterization of induced pluripotent stem cells..... | 23 |
| Cortical differentiation, immunostaining and compound treatment..... | 25 |
| CRISPR/Cas9-mediated gene editing | 27 |
| Establishing a <i>GBA2</i> and <i>GBA1</i> enzymatic activity assay | 31 |
| Western Blot analysis of <i>GBA2</i>-deficient and corrected cell lines | 32 |
| Lipid mass spectrometry to assess changes in the lipid metabolism | 32 |
| Results | 34 |
| Cell lines used in this project and iPSC generation | 34 |
| Characterization of reprogrammed iPSC | 35 |
| Differentiation of iPS cells into cortical neurons | 37 |
| Experimental approach to <i>GBA2</i> gene correction | 37 |
| Functional characterization of isogenic controls | 39 |
| Gene correction restores protein expression..... | 40 |
| Gene correction restores enzymatic function of <i>GBA2</i> | 41 |
| Regulatory interaction between <i>GBA1</i> and <i>GBA2</i> activity..... | 43 |
| Lipidomic studies in <i>GBA2</i>-deficient cells and their isogenic controls | 45 |
| Lipidomics in cortical neurons reveals hexosylceramide accumulation | 45 |
| Validation of glucosylceramide accumulation in human biofluids | 47 |
| Proof-of-principle treatment trials: correction of HexCer accumulation | 49 |
| Discussion | 52 |
| iPSC generation, validation and cortical differentiation | 52 |
| <i>GBA2</i> disease modeling using iPSC | 53 |
| iPSC-derived disease models and isogenic controls | 53 |
| Abbreviations: | 59 |
| Statement of contributions | 61 |

References.....62
List of figures74
List of tables75
Acknowledgements77

Abstract

Bi-allelic, pathogenic variants in the *GBA2* gene cause hereditary spastic paraplegia subtype 46, complicated by cerebellar ataxia. The *GBA2* gene encodes the non-lysosomal β -glucosidase, also known as GBA2. This enzyme is involved in the sphingolipid metabolism and catalyzes the breakdown of glucosylceramide into glucose and ceramide.

To assess consequences of the disturbed sphingolipid metabolism, we have reprogrammed patient-derived fibroblasts into induced pluripotent stem cells and differentiated these induced pluripotent stem cells into cortical neurons. These patient-derived cells carry three different pathogenic variants: Patient 1 carries compound heterozygous variants, comprising of a missense variant in exon 7 and a nonsense variant in the last exon, exon 17. Two siblings are the carriers of the third pathogenic variant studied in this work. Both patients carry a bi-allelic premature stop codon variant in exon 4. As a part of the thesis, I generated isogenic controls by using the CRISPR-Cas9 technique and thereby restored the enzymatic activity of GBA2 in these patient-derived cells. This technology allows creating isogenic controls by the correction of the disease-causing variants while preserving the genetic background of the donor cells.

To reveal differences in the sphingolipid metabolism in a disease-specific background and a disease relevant cell type, I differentiated patient-derived induced pluripotent stem cells into cortical neurons and analyzed these neurons via lipid mass spectrometry.

Two lipid classes were increased in patient-derived cortical neurons, these lipids belong either to the class of dihydro-mono-hexosylceramides or mono-hexosylceramides. To verify the relevance of these results *in vivo*, we analyzed biofluids, collected from the same patients we obtained fibroblast for reprogramming induced pluripotent stem cells. Six different hexosylceramide species were measured in plasma and cerebrospinal fluid samples. Two hexosylceramide species were increased in cerebrospinal fluid samples and one hexosylceramide species was elevated in the plasma samples. The same species were elevated in iPSC-derived neurons, demonstrating the relevance of our cell-based disease model.

As a proof of principle study, I treated patient-derived cortical neurons with different compounds to decrease hexosylceramide levels in these cells. One compound was Miglustat, an approved treatment for substrate reduction therapy in Gaucher disease. This glucosylceramidase inhibitor decreased hexosylceramide levels in cortical neurons originated from two different patients after a four-day treatment.

These results improve the understanding of implicated mechanisms in this rare subtype of hereditary spastic paraplegia and present a strategy to lower the hexosylceramide burden in patient-derived cortical neurons.

Introduction

Hereditary spastic paraplegia

Hereditary spastic paraplegias (HSP) are a heterogeneous group of inherited disorders with the pathological hallmark of progressive lower limb weakness and spasticity caused by degeneration of upper motor neurons. Taken together, these rare neurodegenerative diseases have a prevalence of about 2-10 per 100.000. More than 100 genomic loci are known to be associated with HSP (**s**pastic **p**araplegia **g**ene: SPG1 – SPG83). Autosomal-dominant and autosomal-recessive modes of inheritance predominate, but a few X-linked and mitochondrial transmitted genes are also known. Age of onset can be quite variable and ranges from congenital forms of the disease well into older age (8th decade) (Schüle et al. 2016; Erfanian Omidvar et al. 2019; Wagner et al. 2019).

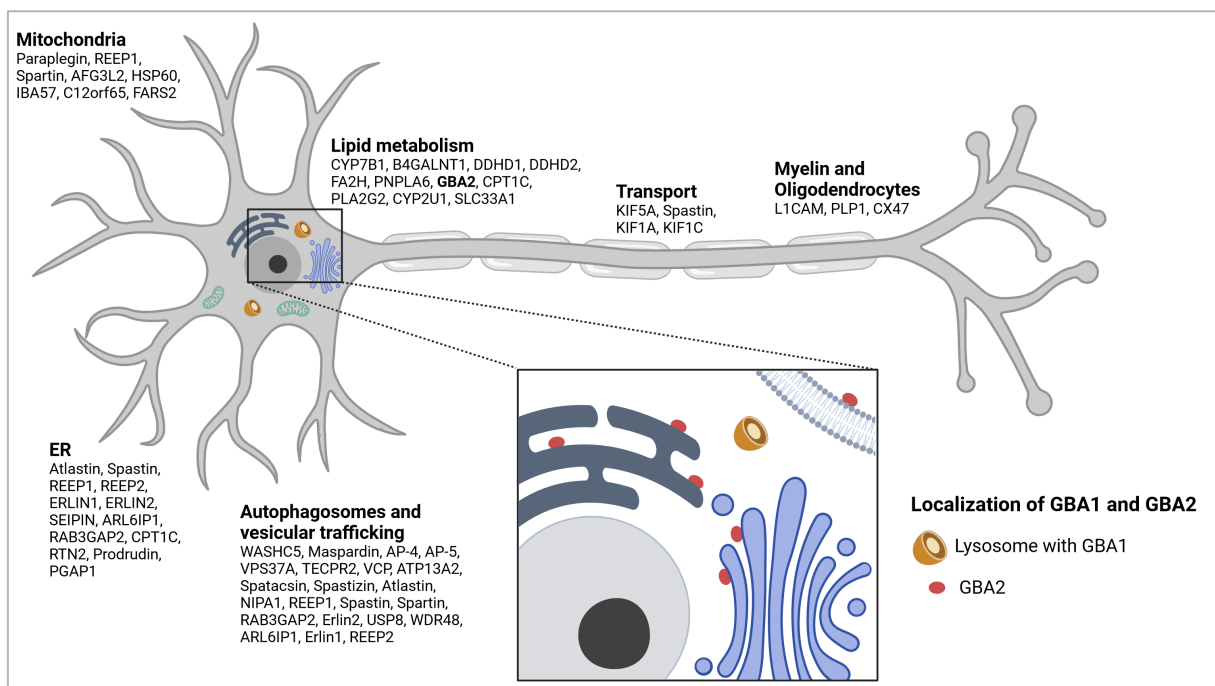


Fig. 1: Overview of the most frequent pathways disturbed in hereditary spastic paraplegia with examples of affected proteins. A detailed look presents the localization of GBA1 and GBA2: two enzymes involved in the lipid metabolism and important for this thesis. Bi-allelic, pathogenic variants in the genes encoding GBA1 and GBA2, cause either Morbus Gaucher or SPG46, respectively. Created with BioRender.com, modified from Blackstone 2018.

The clinical phenotype of HSPs is heterogenic; accordingly, HSPs can be classified as either pure or complicated forms. Pure HSPs are characterized mainly by weakness and spasticity of the lower limbs whereas in complicated forms spasticity is accompanied by additional signs and symptoms. These additional features can include ataxia, cataract, cognitive decline, movement disorders, epilepsy, peripheral neuropathy, thin corpus callosum, skeletal abnormalities, amyotrophy and optic atrophy

among others and indicate affection of neuronal systems other than the pyramidal tracts (Lo Giudice et al. 2014; Erfanian Omidvar et al. 2019; Martin et al. 2013).

Despite the enormous genetic heterogeneity of HSPs, cellular pathways disturbed in the majority of HSPs converge onto a number of common themes, including lipid metabolism, axonal transport, endoplasmic reticulum (ER) morphogenesis and endosomal trafficking (Fig. 1).

Pathogenic variants affecting lipid metabolism

Disturbances of the lipid metabolism are an emerging and unifying theme among several HSP subtypes (Fig. 1). HSP-genes encoding proteins regulating distinct pathways in lipid metabolism can be classified into different functional groups. One subset of genes (*PNPLA6*, *CYP2U1*, *DDHD1* and *DDHD2*) is involved in *phospholipid remodeling*; *CYP2U1* additionally plays a role in *fatty acid hydroxylation* (Lo Giudice et al. 2014; Tesson et al. 2012; Citterio et al. 2014; Synofzik et al. 2014; Schubert, Hoffjan, and Dekomien 2016). Another affected biological function is *sterol metabolism*; pathogenic variants in the *CYP7B1* gene, encoding oxysterol 7- α -hydroxylase, lead to SPG5, an autosomal-recessive form of HSP (Schöls et al. 2017; Schubert, Hoffjan, and Dekomien 2016). *SLC33A1* encodes an ER membrane acetyl-coenzyme, a transporter mutated in autosomal-dominant SPG42 (Peng et al. 2014; Lin et al. 2008). Disturbances of the *sphingolipid metabolism* are another emerging theme. Sphingolipid dysregulations are not only restricted to HSP but are also discussed with high interests in other motor neuron diseases (Dodge et al. 2015). Pathogenic variants in *FA2H*, *B4GALNT1* and *GBA2* result in a dysfunctional sphingolipid homeostasis (Peng et al. 2014; Garcia-Cazorla et al. 2014; Blackstone 2018).

Bi-allelic *GBA2* variants cause complicated HSP and spastic ataxia

Pathogenic variants in the *GBA2* gene cause an autosomal-recessive HSP complicated with cerebellar ataxia (SPG46, OMIM #614409 (Martin et al. 2013; Hammer et al. 2013; Citterio et al. 2014; Votsi et al. 2014; Boukhris et al. 2010; Yang et al. 2016; Coarelli et al. 2018)). The disease mainly manifests during infancy and early childhood. A lower-limb predominant pyramidal syndrome with lower limb weakness, spasticity and brisk reflexes is commonly accompanied by a cerebellar syndrome with dysarthria, cerebellar oculomotor disturbances, limb stance and gait ataxia. Additionally, axonal neuropathy, cataract and a mild to moderate mental impairment followed in later stages by cognitive decline have been described (Hammer et al. 2013; Martin et al. 2013; Boukhris et al. 2010). *GBA2* is located on chromosome 9p13.3 and encodes the non-lysosomal β -glucosidase (*GBA2*). *GBA2* catalyzes the breakdown of glucosylceramide (GlcCer) into glucose and ceramide (Cer) *in vitro* and *in vivo*. Glucosylceramide is a precursor for sphingolipids and plays a pivotal role in glycosphingolipid metabolism (R. K. Yu, Nakatani, and Yanagisawa 2009; van Meer, Wolthoorn, and Degroote 2003). Originally, *GBA2* was identified as bile acid β -glucosidase (Matern et al. 1997; Boot et al. 2007). Recently it was discovered, that *GBA2* displays transglucosylation activity towards cholesterol (Marques et al. 2016).

The physiological function of *GBA2* is incompletely understood. The *GBA2* gene comprises 17 exons and the protein consists of 927 amino acids forming a protein with a predicted molecular weight of

105kDa and a C-terminal catalytic domain. The GBA2 protein is conserved among multiple vertebrate species (Aureli et al. 2016; Woeste, Stern, Diana Raju, et al. 2019). *GBA2* mRNA is expressed ubiquitously, with highest expression levels found in human brain, heart, skeletal muscle, kidney and placenta (Matern et al. 2001). Expression increases during neuronal development. This was shown *in vitro* in isolated granule cells from mice and rats, but also in human neuroblastoma SH-SY5Y cells during retinoic acid induced differentiation (Aureli et al. 2011; Aureli, Gritti, et al. 2012; Aureli et al. 2016, 2013). Localization studies have revealed that the enzyme is associated to the cytosolic side of the endoplasmic reticulum (ER) membrane and the *cis*-Golgi membrane. Additionally, GBA2 activity can be measured on the external side of plasma membranes, thus suggesting additional localization of GBA2 on the external leaflet of the plasma membrane (Körschen et al. 2013; Aureli, Loberto, et al. 2012) (Fig. 1).

β-glucosidases in the mammalian cells

Three functional enzymes are known to catabolize GlcCer in mammals: GBA1, GBA2 and GBA3. Although they all share the same enzymatic function, they differ in their nucleotide and amino acid sequence, their structure as well as their cellular localization (Körschen et al. 2013).

Lysosomal β-glucosidase

GBA1 was the first β-glucosidase to be identified and is the primary catabolic enzyme for GlcCer located in the lysosome; it has therefore also been described as lysosomal β-glucosidase (Van Weely et al. 1990; Brady, Kanfer, and Shapiro 1965).

GBA1 in Gaucher disease:

Bi-allelic, pathogenic variants in the *GBA* gene, encoding GBA1 protein, lead to Gaucher disease (GD), an autosomal-recessive lysosomal storage disorder (Fig. 1). Deficiency of lysosomal β-glucosidase leads to accumulation of GlcCer in lysosomes. Especially in macrophages, these GlcCer accumulations become apparent and cause pathognomonic characteristically enlarged substrate-laden cells known as Gaucher cells. Typically Gaucher cells accumulate in organs, in particular in spleen and liver, causing organomegaly, a characteristic hallmark of the disease (Ellen Sidransky 2004; Boven et al. 2004; Zimran and Elstein 2015).

The phenotypic variability of Gaucher disease is striking and disease severity ranges from completely asymptomatic bi-allelic variant carriers to neonatal death (Ellen Sidransky, Sherer, and Ginns 1992; Berrebi, Wishnitzer, and Von-der-Walde 1984). More than 300 disease-causing variants in the *GBA* gene are known. However, many studies demonstrated that there is neither a consistent genotype-phenotype correlation nor a convincing correlation between the residual enzymatic activity of GBA1 and the clinical phenotype (Smith, Mullin, and Schapira 2017; Goker-Alpan et al. 2005; Biegstraaten et al. 2010; Ellen Sidransky 2004). Morbus Gaucher is classically categorized into three subtypes based on their clinical manifestation and presence or absence of neurological involvement:

- Type I is classified as non-neuronopathic form. This is the most frequent disease condition and is characterized by a mild phenotype restricted to visceral manifestations including: organomegaly, anemia, thrombocytopenia and bone involvement.
- Type II is the most severe subtype of Gaucher disease with a progressive neurological disease manifestation. This acute neuronopathic form leads in many cases to an early death within 9 months.

- Type III is described as chronic neuronopathic form, with a milder progression than type II but still with distinctive neurological involvement (Mignot, Gelot, and De Villemeur 2013; Ellen Sidransky 2004; Grabowski 2008).

GBA1 in Parkinson disease:

The assumption that Gaucher disease type I is limited to extra-neurological disease manifestations was challenged when studies revealed an increased likelihood of patients with Gaucher disease type I as well as their relatives to develop Parkinson’s disease (PD) (Westbroek, Gustafson, and Sidransky 2011; Hruska et al. 2008; E. Sidransky et al. 2009; Ellen Sidransky 2004). Heterozygous variants in the *GBA* gene are now known to be the most frequent genetic risk factor for PD (Goker-Alpan et al. 2004; E. Sidransky et al. 2009; Lwin et al. 2004), 5-12 % of idiopathic PD patients carry a pathogenic *GBA* variant (Mullin et al. 2019; Avenali, Blandini, and Cerri 2020).

The lipid profile in these patients reflects the impaired enzymatic function of GBA1. Fibroblasts from GBA-PD patients showed higher level of sphingolipids compared to fibroblasts from healthy donors and idiopathic PD donors without pathogenic *GBA* variants. Within the sphingolipid profile an increase of short chain sphingomyelin, ceramide and hexosylceramide was measured in GBA-PD patient-derived fibroblasts, compared to control and idiopathic PD fibroblasts (without pathogenic *GBA* variants) (Galvagnion et al. 2022). Patients with pathogenic *GBA* variants respond well to Levodopa treatment (C. Ran et al. 2016; Aasly 2020) but several therapeutic approaches specific to target GBA1-deficiency are tested in ongoing clinical trials (Tab. 1).

Tab. 1: Selection of therapeutic approaches to target GBA1-deficiency in GBA-PD (adapted and modified from (Schneider and Alcalay 2020)).

| Compound | ClinicalTrials.gov identifier (NCT number) | Mechanism |
|---------------------------|--|---|
| Ambroxol | NCT04388969 NCT02941822 NCT02914366 | Pharmaceutical chaperon |
| Venglustat (GZ/SAR403671) | NCT02906020 | Substrate reduction / GlcCer-synthase inhibitor |
| PR001 | NCT04127578 | AAV9-based gene therapy |

Klotho-related protein

Klotho-related protein (GBA3) is a cytosolic enzyme most abundantly expressed in liver, kidney and small intestine and has marginal impact on bulk GlcCer degradation (Dekker et al. 2011; Yahata et al. 2000). It has been suggested to be involved in detoxification of plant glycosides (De Graaf et al. 2001) but may also contribute to neutral GlcCer catabolism (Hayashi et al. 2007). GBA3 has not been associated to any human disease yet.

Sphingolipidoses are caused by inherited defects of sphingolipid metabolism

The majority of sphingolipid catabolizing enzymes are localized in lysosomes; in consequence, pathogenic variants in genes encoding these enzymes commonly lead to substrate accumulation in lysosomes. Inherited defects of sphingolipid metabolism have therefore been classified as lysosomal storage disorders, with Gaucher disease being one of the most frequent representative of this group. More than ten distinct human single-gene disorders are known to result from defective sphingolipid metabolism. Hereby, pathogenic variants affecting sphingolipid-catabolizing pathways are more frequent than deficits in sphingolipid biosynthesis (Tab. 2). In the majority of cases, pathogenic variants in genes encoding enzymes involved in sphingolipid metabolism, lead to autosomal-recessive inherited diseases with a severe neurological phenotype (Kolter and Sandhoff 2006; Sun 2018).

Tab. 2: Overview of diseases resulting from disturbances of the sphingolipid metabolism (modified from (Platt 2014) and complemented by (Kolter and Sandhoff 2006)).

| Disease | OMIM # | Gene | Protein | Biochemical consequences | Major symptoms | Metabolic function |
|--|---------------------------------|----------------------------|---|---|---|---------------------------|
| Farber lipogranulomatosis, spinal muscular atrophy with progressive myoclonic epilepsy | #228000, #159950 | <i>ASAH1</i> | Acid ceramidase | Ceramide accumulation | Joint deformation, lipogranulomas and hoarseness | Catabolic |
| Niemann-Pick type C | #257220, #607625 | <i>NPC1</i> <i>NPC2</i> | NPC1 NPC2 | Storage of all GSLs, cholesterol, sphingomyelin and sphingosine | Progressive neurodegeneration | Trafficking and fusion |
| Krabbe | #245200 | <i>GALC</i> | Glactosylceramide- β -galactosidase | Accumulation of galactosylceramide resulting in demyelination | Progressive neurodegeneration | Catabolic |
| Metachromatic Leukodystrophy | #250100 | <i>ASA</i> | Arylsulfatase A | Accumulation of sulfatides resulting in demyelination | Progressive neurodegeneration and mental regression. | Catabolic |
| Fabry | #301500 | <i>GLA</i> | α -Galactosidase | Gb3 storage | Renal, cardiovascular and peripheral pain | Catabolic |
| Gaucher Types 1,2 and 3 | #230800, #230900, #231000 | <i>GBA</i> | β -Glucoserebrosidase | GlcCer accumulation and storage | Hepatosplenomegaly, hematological defects, inflammation, bone disease and CNS involvement (types 2 and 3) | Catabolic |
| Sandhoff | #268800 | <i>HEXB</i> | B-Hexosaminidase β -subunit | GM2 ganglioside accumulation and storage | Progressive neurodegeneration | Catabolic |
| Tay-Sachs | #272800 | <i>HEXA</i> | B-Hexosaminidase α -subunit | GM2 ganglioside accumulation and storage | Progressive neurodegeneration | Catabolic |
| GM1-Gangliosidosis | # 230500 | <i>GLB1</i> | β -Galactosidase | GM1 ganglioside accumulation and storage | Progressive neurodegeneration | Catabolic |
| GM2 synthase deficiency (SPG26) | #609195 | <i>B4GALNT1</i> | GM2/GD2 synthase | Loss of GM2 and downstream gangliosides | Spastic paraplegia | Biosynthetic |
| GM3 synthase deficiency (Salt and pepper developmental regression syndrome) | # 609056 | <i>ST3GAL5</i> | GM3 synthase | Loss of GM3 and downstream gangliosides | Infantile onset epilepsy with developmental retardation and blindness | Biosynthetic |

Disease and control models for GBA2-deficiency

***In vitro* and *in vivo* models to study GBA2 function**

The role of GBA2 has been studied in different cell culture systems as well as animal models and the importance of GBA2 during neuronal differentiation and in neuronal cells was demonstrated (Aureli et al. 2011; Aureli, Gritti, et al. 2012; Aureli et al. 2016). Both, *in vitro* and *in vivo* model systems, have clear advantages but also distinctive limitations.

In vitro models:

The consequences of GBA2-deficiency and overexpression were studied in various *cancer and immortalized cell lines* including SH-SY5Y, HEK, HeLa, COS-7, CHO and HAP1 cells (Schonauer et al. 2017; Aureli et al. 2013; Woeste, Stern, Diana Raju, et al. 2019; Körschen et al. 2013; Sultana et al. 2015; Boot et al. 2007). Besides, *in vitro* cultured cells from GBA2 knock-out (KO) mice were analyzed to reveal the function of GBA2 (Raju et al. 2015; Schonauer et al. 2017; Woeste, Stern, Diana Raju, et al. 2019; Körschen et al. 2013).

In a GBA2-overexpression study using SH-SY5Y cells it was demonstrated, that GBA2 overexpression promotes neuronal differentiation (Aureli et al. 2013). But most studies were performed on GBA2-deficient cells with following results:

Loss of GBA2 leads to an accumulation of GlcCer in testis, brain, liver, sperm cells and dermal fibroblasts obtained from mice (Raju et al. 2015; Yildiz et al. 2006). These GlcCer accumulations change the cytoskeletal dynamics and lead to an increase of actin polymerization. Moreover, the lipid packaging is altered in giant plasma membrane vesicles (GPMV) derived from mouse fibroblasts. Both, a genetic deletion and a chemical inhibition of GBA2 resulted in reduced membrane fluidity in these GPMV (Raju et al. 2015). Protein overexpression studies of wild-type (wt) and mutant mouse GBA2 in CHO cells, revealed an oligomer formation of wt-mouse GBA2. Some nonsense variants diminished the oligomerization of GBA2 proteins, compared to missense variants, which mostly formed oligomers. The use of *in vitro* cultured cells from mice, allows the direct comparison between *in vitro* and *in vivo* results, but species specific variation is apparent not only in phenotypic differences but also in GBA2 function (Woeste, Stern, Diana Raju, et al. 2019).

However, the majority of these cell models displays a non-neuronal or non-human origin and thus can only partially mimic the disease-relevant consequences of GBA2 dysfunction. Additionally, various cancer and immortalized cell lines are known to carry a wide range of chromosomal aberrations and rearrangements, hence these data should be interpreted with caution (Thompson and Compton 2011; Frattini et al. 2015; Duesberg and McCormack 2013; Stepanenko and Dmitrenko 2015).

Functional assays in *patient-derived cellular models* allow studying variant-dependent consequences in a disease-related context. Hereby, patient lymphocytes and fibroblasts are among the most easily accessible tissues. Both model systems were used to determine GBA2 enzymatic activity. However, GBA2 expression is rather low in fibroblasts and lymphocytes compared to neuronal cells (Martin et al. 2013; Malekkou et al. 2018; Aureli, Loberto, et al. 2012; Aureli, Bassi, et al. 2012).

Patient-derived lymphoblastoid cells with a pathogenic missense variant in the *GBA2* gene showed *GBA2* mRNA expression, but *GBA2* enzyme activity was highly decreased in cell lysate and at the plasma membrane. GlcCer was elevated in comparison to control cells in this patient-derived lymphoblastoid cell model (Malekkou et al. 2018).

In vivo models:

GBA2-deficiency has been modeled *in vivo* in zebrafish as well as two different mouse models (Martin et al. 2013; Yildiz et al. 2006; Woeste, Stern, Diana Raju, et al. 2019; Raju et al. 2015).

In zebrafish, a commonly used vertebrate model organism was shown, that an *in vivo* antisense-mediated knockdown of the *GBA2*-ortholog resulted in a curly tail phenotype and locomotor defects in some of these morphants.

On a cellular level, abnormal axonal outgrowth and branching was observed in embryos treated with the antisense morpholino oligonucleotide designed to target the *GBA2*-ortholog. This phenotype could be rescued by injecting human wt *GBA2* mRNA, but not with human mRNA carrying a known human-pathogenic variant (c.1888C>T) (Martin et al. 2013).

Primarily, two *GBA2*-deficient mouse models are described and studied in literature. Both *GBA2* KO mice exhibit no *GBA2* activity or *Gba2* expression (Woeste, Stern, Raju, et al. 2019). The first created mouse model deleted *Gba2* exons 5-10 in mice with a C57BL/6J background (Yildiz et al. 2006).

The second characterized KO mouse model is the $Gba2^{tm1a(EUCOMM)Wtsi}$, a mouse line with the genetic background of C57BL/6N and the potential to express the β -galactosidase reporter gene under the endogenous *Gba2* promoter (Woeste, Stern, Raju, et al. 2019).

The first mouse model developed by Yildiz and co-workers aimed to identify the biological function and metabolic relevance of *GBA2*. They showed high *Gba2* mRNA expression in brain and testis, while human have an increased *GBA2* expression in brain, heart, skeletal muscle and kidneys (Yildiz et al. 2006; Matern et al. 2001).

The examination of the *GBA2* KO mouse model revealed no differences to wild-type mice in body weight and life span. Additionally, these mice displayed neither observable neurological symptoms as seen in SPG46 patients nor an enlargement of organs (organomegaly) in contrast to mice and patients with a *GBA1*-deficiency (Enquist et al. 2007; Mistry et al. 2010; Yildiz et al. 2006).

The consequences of a *Gba2* KO in mice resulted in substrate accumulation of GlcCer in testis, brain and liver. Loss of *GBA2* resulted in reproductive impairments and infertile male mice, but not female mice. Further investigations revealed irregular large and round headed sperm (globozoospermia) and motility defects in *GBA2*-deficient mice compared to control mice (Yildiz et al. 2006). These defects were investigated later more closely and it was shown that accumulating GlcCer leads to a more ordered lipid structure in the plasma membrane. This results in an enhanced actin polymerization and cytoskeletal dynamics in different cells of *GBA2* KO mice (Raju et al. 2015).

The second mouse model confirmed the high *GBA2* expression in neurons by visualizing β -gal expression under the endogenous *Gba2* promoter. This enzyme-deficiency influences the glycolipid metabolism in the brain. Overall hexosylceramide (HexCer) levels in P10 and adult mice were unchanged but HexCer levels with a chain length of d18:1 / 18:0 were elevated significantly in *GBA2*-deficient mice. Besides, a slight increase of complex glycosphingolipids such as GM1a, GT1b, GD1b and GM3 were measured in *GBA2*-KO mice compared to their respective wild-type controls.

In behavioral test and locomotion assays a varying degree of impairment was exhibited in mice lacking GBA2.

Phenotypic changes in GBA2-deficient mice comprise reduced muscle strength of front paws and an altered gait pattern. While some mice had more severe impairments, some mice showed mild phenotype. These GBA2-deficient mice do not relate entirely to the human phenotype, emphasizing a different role of GBA2 in human and mice (Woeste, Stern, Diana Raju, et al. 2019).

Induced pluripotent stem cells as a disease model

In 2006 Yamanaka and colleagues first reprogrammed somatic mouse cells into so-called induced pluripotent stem (iPS) cells (iPSC). One year later, two independent laboratories achieved reprogramming of human adult fibroblasts into induced pluripotent stem cells (Takahashi and Yamanaka 2006; J. Yu et al. 2007). This novel technique overcomes the ethical issues being discussed in the context of human embryonic stem cells and enables completely new capabilities for diseases modeling and therapeutic applications.

To reprogram induced pluripotent stem cells, patient-derived somatic cells are forced to transiently express the so-called Yamanaka factors: OCT3/4, SOX2, c-MYC and KLF4. The resulting iPSC are capable of self-renewal and able to differentiate into various tissues of all three germ layers (Takahashi et al. 2007; Takahashi and Yamanaka 2006; J. Yu et al. 2007). The initial method was adapted and improved steadily towards integration free reprogramming methods, including: mostly episomal plasmids (Junying et al. 2009; Okita et al. 2011), recombinant proteins (Zhou et al. 2009; D. Kim et al. 2009), mRNA (Warren et al. 2010) or integration free viruses (Ban et al. 2011; Fusaki et al. 2009). The ability of infinite proliferation holds both challenges and opportunities for new therapeutic advances.

Disease modeling:

iPSC opened up new perspectives in the field of cell culture models systems. Previous inaccessible patient-derived tissues, especially brain cells, heart tissue, hepatic cell and many more, could not be easily obtained without harming a patient. Disease models for example neurological diseases relied on artificial cell models or animal models without a human-specific or patient-specific background. Converting accessible patient-derived tissue such as skin cells or blood cells into iPSC cells allows differentiating these iPSC cells in any tissue of interest while providing a more accurate disease model system (Fig. 2).

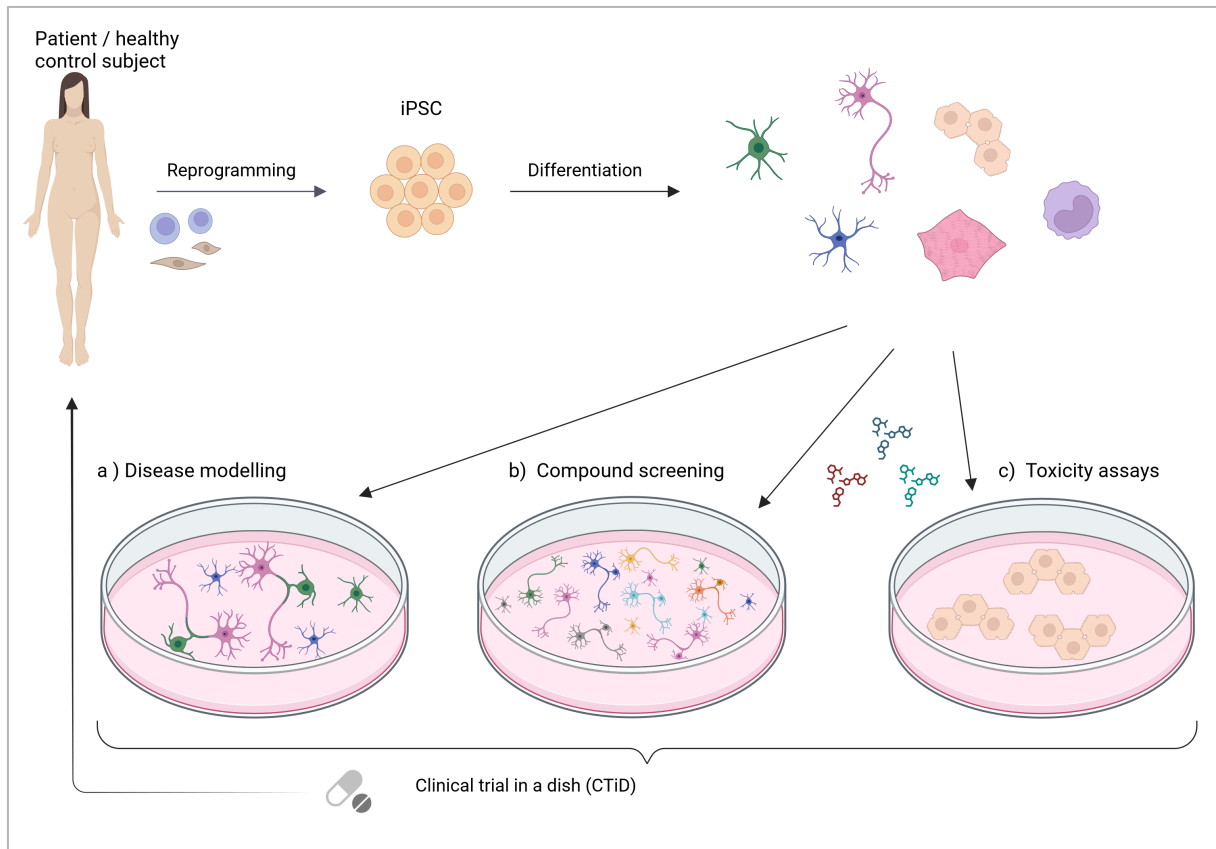


Fig. 2: Application opportunities for iPSC. Somatic cells from either a patient or a healthy control subject can be reprogrammed and differentiated in a second step towards specialized cells. a) These specific cells can be combined to mimic a specific tissue composition or used as a pure cell culture for disease modeling. b) A suitable disease model presenting characteristic hallmarks of the disease allows compound screening and evaluation based on the disease characteristics. c) Additionally, compounds can be tested on several tissues to assess toxicity profiles on defined cell types, e.g. hepatocytes. These models can be a new opportunity to accelerate drug development in a so-called clinical trial in a dish (CTiD) approach or used as therapeutic cell therapy. Created with BioRender.com, adapted from Bellin et al. 2012.

Drug screening:

The recent 'clinical trial in a dish' (CTiD) approach allows testing compounds on a large cohort of donor cells. This method combines the advantages of preserving the human background with the defined pattern of target cells to conduct safety and efficacy tests (Fig. 3). It is possible to combine different cell types to mimic the *in vivo* environment by setting up cultures containing tissue specific cells (e.g. neurons, astrocytes, oligodendrocytes and microglia for brain tissue). CTiD advancement stratifies pharmaceutical development and could be more cost effective in the early stages of drug development and leading to a more specialized treatment of diseases.

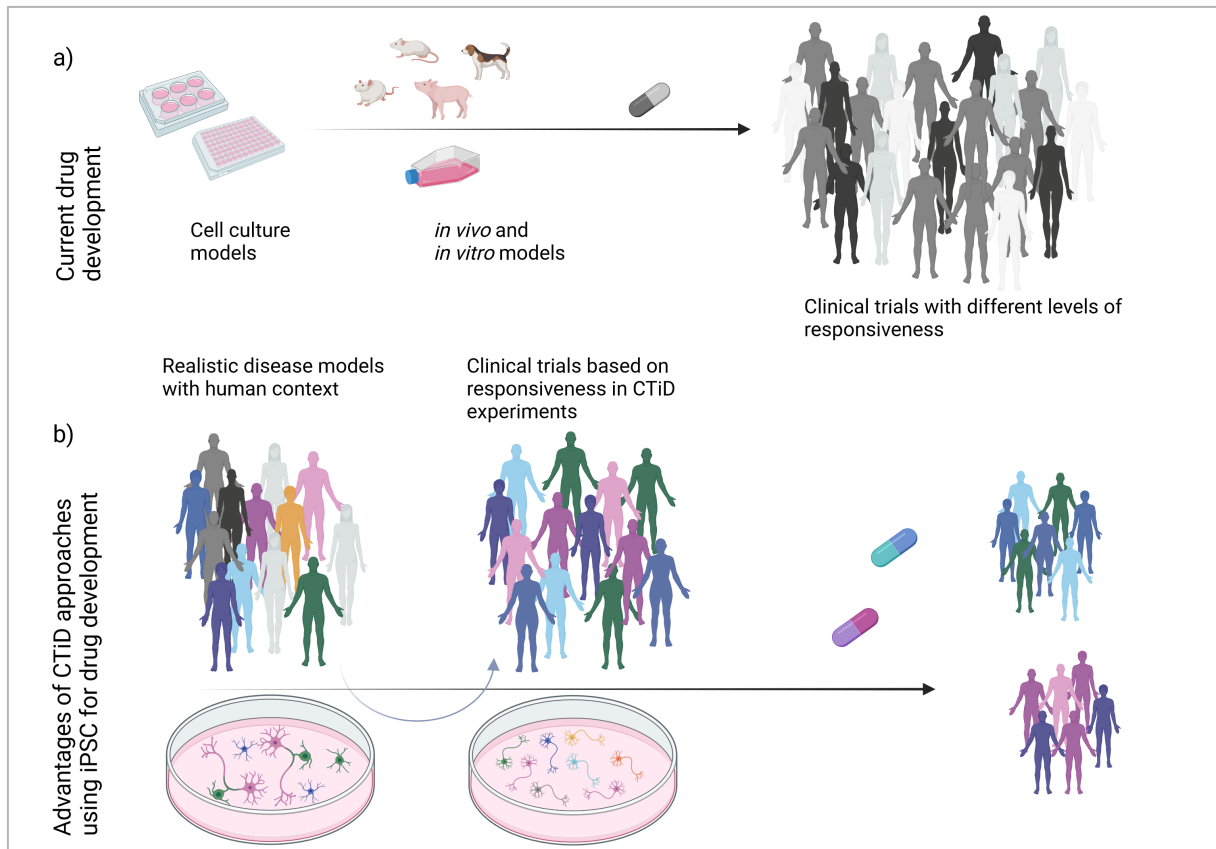


Fig. 3: Comparison of the current drug development approach to a new strategy using iPSC in a clinical trial in a dish (CTiD) approach. a) Artificial cell culture models and animal models are the foundation to screen and test for potential compounds. In a clinical trial period these compounds often fail due to different kinds of responsiveness in large heterogeneous cohorts. b) Using actual human cells collected from large cohorts to model disease-specific features and for toxicity assays can allow to stratify inclusion criteria for more successful clinical trials. Created with BioRender.com, modified from Hnatiuk et al. 2021.

Cell therapy:

Since the discovery of iPSC this powerful method was connected with the hope to repair, substitute or replace damaged or diseased tissue. At the same time new challenges and obstacles needed to be addressed such as: tumorigenicity, immune rejection, heterogeneity and engraftment. In 2014 the first clinical trial using iPSC cells differentiated into retinal pigment epithelium cells was conducted in Japan (Cyranoski 2014). A lot of progress has been made and clinical trials using iPSC as cell replacement therapy are ongoing (Al Abbar et al. 2020; J. Y. Kim et al. 2022).

CRISPR/Cas9 genome editing to generate gene-corrected isogenic controls

To precisely model disease-relevant variants and eliminate the variability introduced by the different genetic background of each individual cell line, we decided to use the Clustered Regularly Interspaced Short Palindromic Repeats (CRISPR) / CRISPR-associated (Cas) genome editing technique to correct the disease-causing variants in GBA2-deficient iPSCs and thus generate so-called isogenic controls.

Introduction to gene editing

Before the introduction of CRISPR/Cas9 mediated gene editing in 2012 (M. Jinek et al. 2012), chimeric nucleases such as zinc finger nucleases (ZFN) or transcription activator-like effector nucleases (TALENs) were utilized to introduce sequence-specific genetic modifications (Fig. 4). These engineered nucleases are composed of a DNA-binding domain fused to FokI, an unspecific restriction enzyme, which can induce a DNA double strand break (DSB) after dimerization (Urnov et al. 2010; Porteus and Carroll 2005; Cermak et al. 2011; Gaj, Gersbach, and Barbas 2013; Bibikova et al. 2002). These DSBs trigger two different DNA repair mechanisms in the cell; either the error-prone non-homologous end joining (NHEJ) repair or the precise homology-directed repair (HDR) pathway (Fig. 4). To generate gene knock-out models the NHEJ repair pathway is employed. Hereby, the often-imperfect end joining of DNA ends introduces small insertion or deletion (indel) variants. Indels can result in a shift of the reading frame resulting in a premature stop codon variant. To trigger the HDR instead, which is necessary for specific and precise gene editing, a repair template, either encoded by a plasmid or a single stranded oligonucleotide (ssODN) needs to be provided simultaneously (F. Ran et al. 2013; Richardson et al. 2016; Symington and Gautier 2011; Lieber 2010).

The more recent CRISPR/Cas9 approach greatly accelerates and facilitates gene editing. In contrast to ZFN and TALENs, the CRISPR/Cas9 system relies on RNA-DNA base pairing.

Originally, the CRISPR/Cas9 system contributes to the acquired immunity in bacteria and archaea. Three types of CRISPR/Cas systems are described to be part of the adaptive immune system; gene editing utilizes components of the CRISPR/Cas type II system (Terns and Terns 2011; M. Jinek et al. 2012).

This RNA-directed gene editing system is composed of the CRISPR RNA (crRNA), a trans-activating crRNA (tracrRNA) and the Cas9 endonuclease. Precise gene editing is achieved by the sequence specificity of the crRNA containing a 20-nucleotide guide sequence complementary to the targeted genomic region. To constitute the guide RNA, another part of the crRNA forms a duplex with the tracrRNA, necessary for target recognition and as a scaffold to guide the Cas9 to their destined target. The endonuclease Cas9 is only catalytically active, if the target DNA sequence is followed by a 5'-protospacer adjacent motif (PAM). The Cas9, most commonly used for gene editing is derived from *Streptococcus pyogenes* with the PAM sequence 5'NGG, other Cas9 orthologs require different PAM motifs (Esvelt et al. 2013; Martin Jinek et al. 2013; M. Jinek et al. 2012; F. Ran et al. 2013; Mali et al. 2013).

One of the first described CRISPR/Cas9 gene editing approaches for mammalian cells was a vector-based strategy coding for a human codon optimized and modified Cas9 and a single transcript guide RNA (gRNA) comprising tracrRNA and crRNA (F. Ran et al. 2013; M. Jinek et al. 2012; Martin Jinek et

al. 2013; Cong et al. 2013). This versatile and easy applicable approach nevertheless harbors the risk of unintentional plasmid integration and an increased risk for off-target effects due to peak and prolonged plasmid expression (Liang et al. 2015). More recent approaches circumvent these risks by delivering either a ribonucleoprotein (RNP) or a Cas9-coding mRNA in combination with the chimeric tracrRNA:crRNA duplex (S. Kim et al. 2014; Liang et al. 2015).

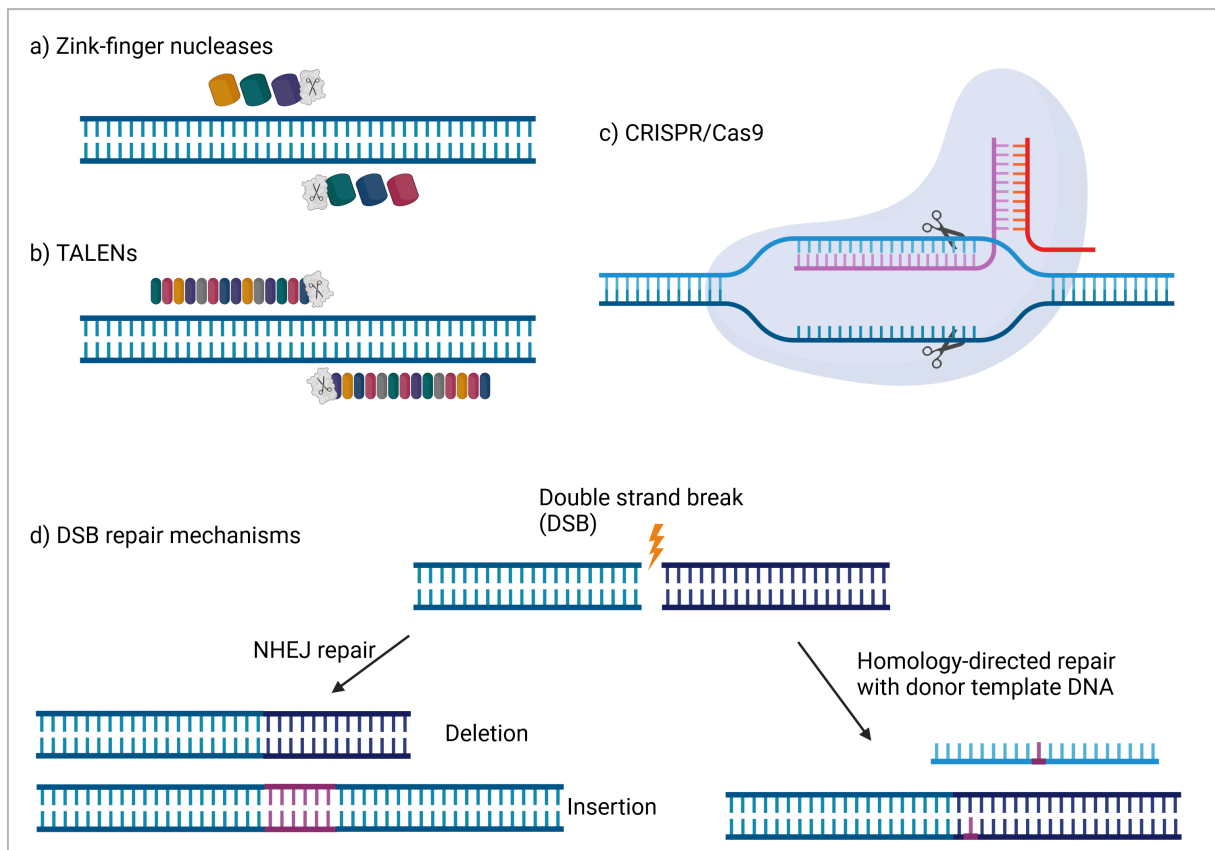


Fig. 4: Schematic representation of different gene editing approaches. a) Two zinc finger nucleases bind sequence specific to the DNA and allow the unspecific endonuclease FokI to dimerize and thereby introduce a double strand break (DSB) into the DNA. b) Two transcription activator-like effector proteins (TALEN) bind sequence specific to target region on DNA, dimerizing FokI nucleases introduce a DSB into the DNA. c) In the CRISPR/Cas9 system, the Cas9 endonuclease introduces a DSB into the DNA target region by sequence specific guide RNA complexed to the Cas9 protein. d) Repair: The introduced DSB can be repaired by two different mechanisms in the cell. Either the non-homologous end joining (NHEJ) mechanism, that frequently leads to an introduction of insertions or deletions (indel), which can result in a premature stop codon, or the homology-directed repair (HDR) resulting in a precise gene editing by simultaneous addition of a donor repair template. Created with BioRender.com, adapted from Li et al. 2020.

As seen after the discovery of reprogramming iPS cells, the expectations and concerns about the CRISPR technique were comparable. New opportunities but also new hurdles are associated with this new gene editing method. The first impact and application were the generation of new and more precise disease models, which led to models for drug and toxicity testing.

CRISPR is not the first method used to edit genes, but compared to TALEN and ZFN, it is by far faster, more specific, cheaper and more efficient. Through this advancement, disease models became more

specialized and it is feasible to generate larger cohorts. The importance of isogenic controls in understanding specific genetic variations and their effect in the metabolism are indispensable. Keeping the genetic background the same and only introducing or correcting one variant allows pointing at the effect to this particular variant. Especially in drug testing distinct variants can help to explain the molecular mechanism behind effectiveness of drugs or their potential side effects. High expectations and hopes are pinned to the combination of reprogramming somatic cells in association with the opportunity to create specific genetic modifications (e.g. correcting a pathogenic variant) and re-introducing these cells to cure the patient.

Material & Methods

Human cell culture

iPSC reprogramming

All cells were cultured at 37°C and 5% CO₂. Human iPSC were reprogrammed using an episomal plasmid approach described by Okita et al. (Nagel et al. 2019; Okita et al. 2011). Fibroblasts were cultured in Dulbecco's Modified Eagle's Medium (Life Technologies) supplemented with 10% fetal calf serum (FCS) (Life Technologies). At a confluence of 80% fibroblasts were collected for electroporation. 1 µg of each plasmid (pCXLE- hUL, ID: #27080; pCXLE-hSK, ID: #27078 and pCXLE-hOCT3/4, ID: 27076; Addgene) was mixed with 82 µl Human Dermal Fibroblast Nucleofactor solution and 18 µl supplement solution to resuspend 10⁵ human fibroblasts. The suspension was transferred to a cuvette for the Amaxa 2b nucleofactor. Cells were electroporated using program P-022 (Human Dermal Fibroblast Nucleofection Kit VPD-1001, Lonza). Prior to electroporation, matrigel-coated (Corning) 6-well plates (1:60) with fibroblast culture medium were prepared to gently distribute the fresh electroporated cells. On the following day, medium was changed using fibroblast medium supplemented with 2 ng/ml fibroblast growth factor 2 (FGF2) (Peprotech). The following medium changes were performed with medium suited for arising iPS cells: E8 medium (DMEM/F12 (Life Technologies), 64 mg/l L-ascorbic acid-2-phosphate magnesium (Sigma-Aldrich, St), 1% ITS-Supplement 100× (Life technologies), 100 µg/l FGF2, 2 µg/l Transforming Growth Factor Beta 1 (TGFβ1) (Peprotech), supplemented with 100 µM Sodium Butyrate (Sigma-Aldrich). Medium was changed every other day. After eight days, the first iPSC colonies appeared. Colonies were monitored until ready for picking. Dependent on the growth, colonies were picked manually after 2-3 weeks and seeded for singularization one by one into matrigel-coated 12-well plates (1:60). After expansion up to 80% confluency, iPSC were passaged onto matrigel-coated 6-well plates (1:60) in a ratio of 1:6 to 1:12. On the day of passaging, E8 medium was supplemented with 1 µM Rock inhibitor Y-27632 (Abcam Biochemicals) for 24 h after passaging. Medium was changed daily until cells were ready for cryopreservation using 50% E8, 40% KnockOut Serum Replacement (KO-SR, Life Technologies), 10% DMSO (Sigma-Aldrich) and 1 µM Y-27632. Prior to freezing, Mycoplasma contamination of each line was excluded by a PCR Mycoplasma Test Kit (AppliChem) following manufacturer's recommendations.

iPSC cell culture

iPSC were cultivated in E8 medium on matrigel-coated plates (1:60). Medium was changed every day, after reaching 80% confluence cells were split in a 1:12 ratio using 0.02% EDTA in phosphate buffered saline (PBS). Medium was supplemented with 1 µM Rock inhibitor Y-27632 for 24 hours after passaging.

Ethical approval by the Institutional Review Board at the University of Tübingen Medical School, Germany, approval number 819/2016A (2016/12/21) and (054/2013BO1).

Characterization of induced pluripotent stem cells

Generated iPSC were characterized and validated for genomic integrity as well as pluripotency before used for any following experimental setups (Nagel et al. 2019).

Genomic integrity:

Cells were analyzed after at least five passages; therefore DNA was extracted using GeneJET-Genomic DNA Purification Kit (Thermo Fisher Scientific). All lines were confirmed for their specific variants via Sanger Sequencing using 3130xl Genetic Analyzer (Applied Biosystems). *GBA* has a highly similar pseudogene. A nested PCR was performed for pathogenic variants in exon 9 and 10 to ensure specificity (Tab. 3).

Tab. 3: Primers used to verify pathogenic *GBA* variants in reprogrammed iPSC via Sanger Sequencing.

| Primer for <i>GBA</i> variants | | |
|--|---|----------------|
| Target (NM_000157.4) | Forward / reverse Primer (5'-3') | Product length |
| <i>GBA</i> Exon 6 | CTCTGGGTGCTTCTCTCTTC/ ACAGATCAGCATGGCTAAAT | 271 bp |
| <i>GBA</i> Exon 8-11 (PCR for <i>GBA</i> -specific amplicon) | TGTGTGCAAGGTCCAGGATCAG / ACCACCTAGAGGGGAAAAGTG | 1682 bp |
| <i>GBA</i> Exon 9 | CACAGGGCTGACCTACCCAC / GCTCCCTCGTGGTGTAGAGT | 307 bp |
| <i>GBA</i> Exon 10 | CAGGAGTTATGGGGTGGGTC / GAGGCACATCCTTAGAGGAG | 329 bp |

Unintentional plasmid integration was excluded via PCR with specific primers for reprogramming factors on the episomal vectors (Tab. 4). To demonstrate the genomic integrity of the iPSC cells, a whole-genome Single nucleotide polymorphisms (SNP) Array (Infinium OmniExpressExome-8 BeadChip, Illumina) was performed.

Tab. 4: Primers used to exclude unintentional plasmid integration.

| Target | Forward / reverse primer (5'-3') | Product length |
|----------------|--|----------------|
| KLF4_plasmid | CCACCTCGCCTTACACATGAAG / TAGCGTAAAAGGAGCAACATAG | 156 bp |
| OCT3/4_plasmid | CATTCAAAGTGGTAAGGG / TAGCGTAAAAGGAGCAACATAG | 124 bp |
| L-MYC_plasmid | GGCTGAGAAGAGGATGGCTAC / TTTGTGTTGACAGGAGCGACAAT | 122 bp |
| SOX2_plasmid | TTCACATGTCCCAGCACTACCAG / TTTGTGTTGACAGGAGCGACAAT | 111bp |

By comparing the SNPs to the corresponding fibroblast lines, the parentage was additionally confirmed. Fibroblast DNA was also used for an STR analysis, since balanced translocations are not detected via SNP genotyping. iPS cells and their corresponding fibroblasts were compared and varied with six short tandem repeats (STR) loci (D6S1624; D6S265; D10S537; D10S606; D10S1730; D10S605).

Pluripotency:

First, immunohistochemistry and an alkaline phosphatase (AP) staining demonstrated the pluripotency of the generated iPS cells. For this purpose, iPSC were fixed with 4% paraformaldehyde (PFA), 1 min at room temperature (RT) for AP staining and 15 min at RT for immunocytochemical analysis. For AP staining, cells were washed three times after fixation with PBS, before incubated with the staining solution (20 µl naphthol AS-MX phosphate alkaline solution (Sigma-Aldrich) and 500 µl Fast Red (1 mg/ml, Sigma-Aldrich)) for 30 min at RT. Cells for immunostaining were permeabilized with 0.1% triton X (Carl Roth), blocked with 5% bovine serum albumin (BSA) (Thermo Fisher Scientific) in PBS for 1 h at RT and stained with specific primary antibodies over night at 4°C (Tab. 6). Specific primary antibodies were visualized by using Alexa Fluorophore-coupled secondary antibodies for 1 h at RT (Tab. 6). For nuclear counterstaining Hoechst 33342 (1:10.000, Invitrogen) in PBS was applied for 5 min at RT. Before mounting the cells using ProLong Gold Antifade Reagent (Life Technologies), stained cells were washed thrice with PBS. Images were obtained using AxioImager Z1 with ApoTome (Zeiss).

Second, RNA was extracted using the High Pure RNA Isolation Kit (Roche) followed by reverse transcription of RNA to cDNA (Transcriptor First Strand cDNA Synthesis Kit, Roche) to evaluate expression levels of pluripotency markers (Tab. 5) on transcriptional level. RT-qPCR was performed using Light Cycler 480 SYBR Green I Master (Roche). GAPDH served as a housekeeping gene to normalize the data set. For analysis, $2^{-\Delta\Delta Ct}$ method was used to compare expression patterns from reprogrammed iPSC to a human embryonic stem cell line HUES 6 (HUES 6 cDNA was provided with kind permission of the MPI for Molecular Medicine, Münster, Germany).

Tab. 5: RT-qPCR primer to compare pluripotency marker on a transcriptional level.

| Target | Forward / reverse Primer (5'-3') |
|---------------------------|---|
| KLF4 | CCCCAAGATCAAGCAGGAGG / GGGCAGGAAGGATGGGTAAT |
| OCT4 | GGAAGGTATTCAGCCAAACG / CTCCAGGTTGCCTCTCACTC |
| C-MYC | ATTCTCTGCTCTCCTCGACG / CTGTGAGGAGGTTTGCTGTG |
| SOX2 | AGCTCGCAGACCTACATGAA / CCGGGGAGATACATGCTGAT |
| NANOG | CAAAGGCAAACAACCCACTT / TCGGTCACACCATTGCTATT |
| DNMT38 | ACGACACAGAGGACACACAT / AAGCCCTTGATCTTTCCCA |
| TDGF1 | GGTCTGTGCCCATGACA / AGTTCTGGAGTCTGGAAGC |
| GAPDH (housekeeping gene) | TCACCAGGGCTGCTTTAAC / GACAAGCTTCCCGTTCTCAG |

To further demonstrate pluripotency of the reprogrammed iPS cells, the differentiation potential toward cells of each germ layer was shown by an embryoid-body (EB)-based differentiation protocol. Embryoid-bodies were formed using EB-culture medium (80% DMEM/F12, 20% KO-SR, 1 x NEAA

(Sigma-Aldrich), 1× penicillin-streptomycin (Merck), 2mM L-glutamine (Life technologies), 0.1 mM β -mercaptoethanol (Merck) in an AggreWell 800 Plate (Stemcell Technologies). Medium was gently changed on day two before EBs were collected on day four. For ectodermal differentiation, EBs were cultivated on matrigel-coated coverslips (1:30) in ectodermal differentiation medium (50% DMEM/F12 with N-2 supplement (Life Technologies), 50% Neurobasal medium (Life Technologies) 1% NEAA, 1% B27-supplement with retinoic acid (Life Technologies), 1% penicillin/streptomycin, 1mM L-glutamine) for 14 days. Mesodermal differentiation was induced by plating EBs on 0.1% gelatin-coated coverslips in mesodermal differentiation medium (82% DMEM high glucose (Life Technologies), 16% FCS, 1% penicillin-streptomycin, 1% NEAA, 55 μ M β -mercaptoethanol, 0.0004% α -thioglycerol (Sigma-Aldrich)) for 2 weeks. Endodermal differentiation was performed according to a protocol described by Carpentier and colleagues until definitive endoderm (Carpentier et al. 2014). Cells were fixed for immunohistochemistry staining with 4% PFA to visualize germ layer specific markers: TUJ, SMA and FOXA2 (Tab. 6) for ectoderm, mesoderm and endoderm, respectively.

Tab. 6: Antibodies used to demonstrate pluripotency of generated GBA1-deficient iPSC by immunohistochemistry staining.

| | Antibody, Company, Catalogue number | Dilution |
|-----------------------------|--|-----------------|
| Pluripotency marker | Goat anti-OCT4, Santa Cruz, sc-8628 | 1:100 |
| | Mouse anti-TRA-1-81, Millipore, MAB4381 | 1:500 |
| | Mouse anti-SSEA-4, Abcam, ab16287 | 1:500 |
| Germ layer marker | Mouse anti- β -Tubulin III (TUJ) Sigma-Aldrich, T8660 | 1:1000 |
| | Mouse anti-SMA, Dako, M0851 | 1:100 |
| | Rabbit anti-FOXA2, Millipore, 07-633 | 1:300 |
| Secondary antibodies | Alexa Fluor 488 donkey anti-goat IgG Thermo Fisher, A11055 | 1:500 |
| | Alexa Fluor 488 donkey anti-mouse IgG Thermo Fisher, A21202 | 1:500 |
| | Alexa Fluor 488 goat anti-rabbit IgG Thermo Fisher, A11008 | 1:500 |
| | Alexa Fluor 488 goat anti-mouse IgG Thermo Fisher, A11001 | 1:500 |

Cortical differentiation, immunostaining and compound treatment

To create a disease-relevant and biological background to investigate the impact of GBA2- and GBA1-defective enzymes, I differentiated the characterized iPSC towards cortical neurons of layer V and layer VI. On this account, a differentiation protocol published by Rehbach and colleagues (Rehbach et al. 2019) was utilized.

Differentiation:

The differentiation protocol is based on a dual SMAD-inhibition of confluent cells using 10 μ M SB-431542 (Sigma-Aldrich), and 500nM LDN-193189 (Th. Geyer) in 3N medium (1:1 DMEMF12 / N2:Neurobasal / B27). Medium was changed daily, supplemented with 20ng/ml FGF2 on day 9 after induction (DAI). Cells were dissociated with Accutase (Gibco) on DAI 10 and replated 1:3 on matrigel-

coated plates (1:30). FGF2 was withdrawn on DAI 12; 3N medium was changed every other day. To promote neural rosette formation 100 ng/ml heparin was supplemented on DAI 14 and DAI 16. Cells were frozen on DAI 20 and defined aliquots were thawed for every experiment. For the final maturation step, cells were dissociated with Accutase on DAI 27 and a defined amount was plated for further experiments. On DAI 28 and DAI 30 medium was supplemented with 10 μ M DAPT (Sigma) and 10 μ M PD0325901 (R&D System).

Immunostaining:

Cortical differentiation was validated by immunostaining for a general neuronal marker (TUJ) and for a marker of the cortical layer V. Cortical neurons were washed twice on DAI 37 with PBS, before they were fixed with 4% (w/v) paraformaldehyde (Merck) for 15 min at RT. PFA was removed, cells were washed three times with PBS. Afterwards cortical neurons were incubated with 5% BSA supplemented with 0.1% Triton X in PBS (PBS-T) to block and permeabilize these cells for 1 h at RT. Subsequently the first antibody was incubated in 5% BSA in PBS-T. As a neuronal marker TUJ was used, cortical layer V was stained using CTIP2 (Tab. 7). After washing thrice with PBS-T, secondary antibody was diluted in 5% BSA in PBS-T. As secondary antibodies Alexa fluorophores were used (Tab. 7). Cells were washed three times with PBS-T, for nuclear staining neurons were incubated with Hoechst 33342 (1:10.000) for 5 min at RT. Before mounting the cells with Dako (Agilent, S3023), coverslips were washed three times with PBS. Images were acquired using Axio Imager Z1 with ApoTome.

Tab. 7: Antibodies used for immunohistochemistry to stain neuronal markers.

| | Antibody, Company, Catalogue number | Dilution |
|-----------------------------|--|-----------------|
| Neuronal marker | Mouse anti-TUJ, Sigma-Aldrich, T8660 | 1:1000 |
| | Rat anti-CTIP2, abcam, ab18465 | 1:500 |
| Secondary antibodies | Alexa Fluor 488 goat anti-mouse IgG Thermo Fisher, A11001 | 1:1000 |
| | Alexa Fluor 568 goat anti-rat IgG Thermo Fisher, A-11077 | 1:1000 |

Compound treatment:

To assess possible changes in the lipid metabolism and lipid content of iPSC-derived neurons after compound treatment, cells were treated and prepared for lipid mass spectrometry. Individual treatment duration for each compound: neurons were incubated for three days with 300 μ g/ml Aminoglycoside G418 (Sigma); four days of treatment with 50 μ M Migulstat (Cayman Chemical) and neurons were incubated for seven days with 400 μ M Arimocloamol (MedChemExpress). All neurons were harvested on DIV37 and pelleted for further MS sample preparation.

CRISPR/Cas9-mediated gene editing

To specifically target and edit the point mutations in patient-derived iPSC sequence specific crRNAs were designed using <http://crispr.mit.edu/> and <http://crispor.tefor.net/>.

Tab. 8: CRISPR approach and sequence-specific parts of the gRNA to correct pathogenic *GBA2* variants (NM_020944.3) in patient-derived iPSC cells (PAM-sequence in grey).

| Exon | Specific sequence of gRNA for editing | CRISPR approach |
|---------|--|---------------------------------------|
| Exon 4 | CAGTCCAGGCTCAGGGATAG AGG | Cas9 Protein Atto-labeled tracrRNA |
| Exon 7 | Top : CACCgTTTAGCTCCAACCATGATCC Bottom: AAACGGATCATGgTTGGAGCTAAAc | Plasmid |
| Exon 17 | TCCGCTCACTGGCCTACATG CGG | Cas9 Protein |

iPSC were singularized by Accutase before 10^5 up to $3 \cdot 10^5$ iPSC were electroporated with either 8 μ g CRISPR Plasmid (Addgene: #48139) pSpCas9(BB)-2A-Puro (PX459) or a preformed RNP complex, containing the sequence specific crRNA annealed to (ATTO 550-labeled) tracrRNA (4 μ g duplex) and 20 μ g Cas9 protein (all Integrated DNA Technologies). A single strand oligonucleotide was provided simultaneously in the electroporation mix (1 μ M) as a repair template. To enhance HDR efficiency an asymmetric designed ssODN was used for the two approaches (Richardson et al., 2016; CRISPR knockin tool by deskgen.com). Electroporated (Amaxa 2b, B-16, Human Stem Cell Nucleofactor Kit 2, Lonza) cells were seeded as single cells on matrigel-coated 10cm dishes (1:30), E8 medium was supplemented with 10 μ M γ -27632 and 1% penicillin/streptomycin.

Tab. 9: ssODNs used as repair templates to correct patient-specific variants in *GBA2*-deficient iPSC.

| Exon <i>GBA2</i> (NM_020944.3) | ssODN Sequence (5'-3'): |
|-----------------------------------|---|
| 4 | GACTGTGTACCAGCAAGTCCTGTCCCTGGAGCGCCCAAGTGTCTCCGCAGCTGGA ACTGGGGCCTGTGTGGGTA CTTTGTCTTCTACCATGCACTCTATCCCCGAGCCTGGA CTGTCTATCAGCTTCTCT |
| 7 (wt/R870*) | CCAGTGCCGCCTGGAGTTTTCACTGGCTTGGGACATGCCGAGGATCATGTTTGGAG CTAAAGGCCAAGTCCACTACAGgtgaggggaccaagaaag |
| 7 (wt/wt) | AGGAGTAGGCATTGCTGGAGCTGTGTGTGTTTCCAGCAAGTTGCGACCTCGAGGCC AGTGCCGCCTGGAGTTTTCACTGGCTTGGGACATGCCGAGGATCATGTTTGGAGCT AAAGGCCAAGTCCACTAC |
| 17 | CTGGCCTTCCAGACCCAGAGGCATACTGCCAGCAGCGAGTGTTCCGCTCACTGGCC TACATGCGCCCACTGAGCATATGGGCCATGCAGCTAGCCCTGC |

For cells electroporated with the fluorescent tracrRNA, single cells were sorted using the SH800 Cell Sorter (Sony) into E8 supplemented with 1% penicillin/streptomycin and 10 μ M γ -27632. Afterwards, cells were plated as outlined above. Single cell colonies were picked manually, screened via

restriction fragment length polymorphism (RFLP) and validated by Sanger sequencing. Sequencing was performed for the loci of interest and potential off-target effects (Tab. 10, Tab. 11, Fig. 5).

Screening strategy for:

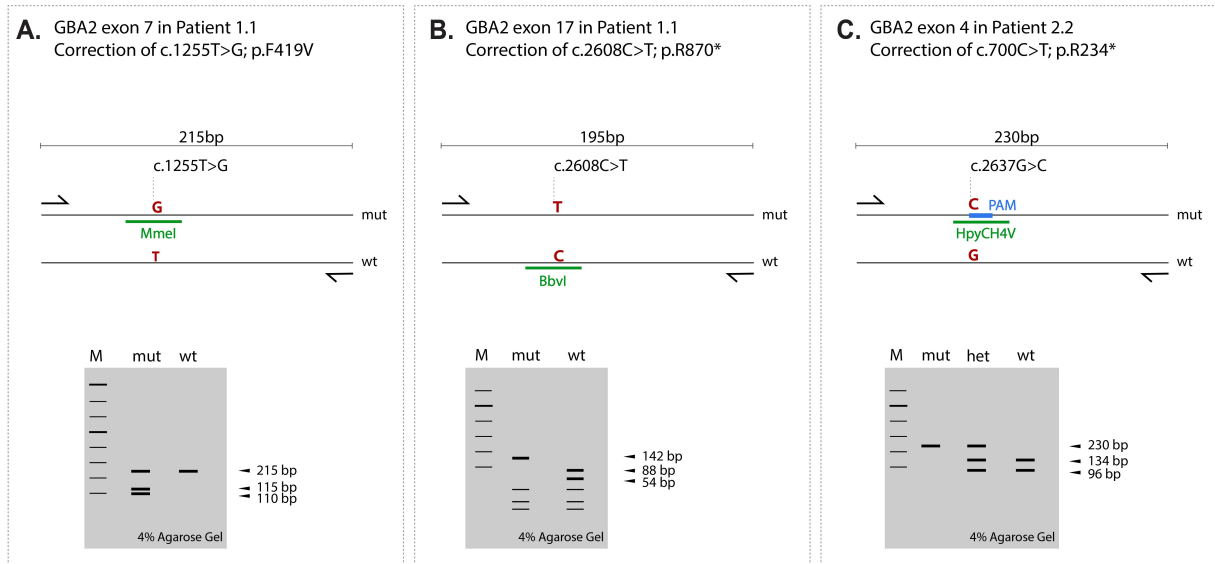


Fig. 5: Restriction fragment length polymorphism strategy to pre-screen picked iPSC colonies after each CRISPR approach. Highlighted red letters indicate the silent variant change to introduce or abolish a cleavage site. Restriction enzyme used for each experiment indicated in green. The expected pattern for each restriction fragment length polymorphism condition is shown.

Tab. 10: Primers used in this study to pre-screen via RFLP, to confirmed variants in patient-derived cells and check for unintentional plasmid integration.

| Primer (<i>GBA2</i> : NM_020944.3) | Sequence (5'-3') |
|-------------------------------------|--|
| <i>GBA2</i> Exon 7 | TCCCCTCACCTGTAGTGGAC ACCCCTACGCAGAAAGGAGT |
| <i>GBA2</i> Exon 7 RFLP | CACCCCTACGCAGAAAGGAG AGGATGAACACAAGCCCCAG |
| <i>GBA2</i> Exon 17 | CCTGTGCCCTGTTTGACTTT GACAGCTGAAGGCTGCTACC |
| <i>GBA2</i> Exon 4 | GGAGGGCAATGGAAGATACA GGCAGACTGTGTACCAGCAA |
| Plasmid integration #1 | CAGAGCTTCATCGAGCGGAT CGAACAGGTGGGCATAGGTT |
| Plasmid integration #2 | ACCCAGAAACGCTGGTGAAA TCCGGTCCCAACGATCAAG |
| Plasmid integration #3 | CAGAGCTTCATCGAGCGGAT CGAACAGGTGGGCATAGGTT |

By introducing a specific silent nucleotide change in the repair template, a restriction enzyme cleavage site was introduced or destroyed. This RFLP method pre-selects generated CRISPR clones cost and time efficient. Clones with the anticipated RFLP-pattern were analyzed further by Sanger sequencing (Fig. 5, Tab. 10).

Tab. 11: Locus and primers used to confirm potential predicted off-target sites.

| Locus for potential predicted off-target effects | Sequence off-target site | Primer sequence (5'-3') |
|--|-----------------------------|--|
| Off targets crRNA E4 (CRISPOR) | | |
| <i>CALCB-INSC</i> (intergenic) | TAGTTTAGGCTCAGGGATAA GGG | AGAAGAGTGTGACAGTTGCCT CTACCTAGAGTCCACACGGC |
| <i>WDR1-RP11-480G3.1</i> | CTGTCCAGGCTCAGGAAAAG GGG | GCTCTGAGTCCTGGCTTCTA CAGCGCTACCCTTGCATAG |
| <i>TFDP2</i> | TAGTACAGACTCAGAGATAG AGG | AGCCTCACCACCATGCTAAC CTGTCACCTCCCCAGTGTTT |
| <i>RP11-701P16.1</i> (LincRNA) | CTGACCTGGTTCAGGGATAG AGG | TTGCCTGCACTACTACCTCC TGGAGAGGACTGGCATGAAG |
| <i>KCNT1</i> | CTGTCCAGGCCCGGGGACAG CGG | GTTCTCGGAGGGATGAGCTG TGCACACACCTGCAGATTCA |
| <i>AC068137.5</i> | CAGTGCATGAGCAGGGATAG TGG | ACTGTTGACTGTTCTCAGCCA GCCTGGTAAGATGAGAGAGACTT |
| <i>AC073869.7</i> | CAGTGCATGAGCAGGGATAG TGG | TAAAGTTAATAGCACCTGCCTCT GACGGGACTTAAACCCACGA |
| <i>PRAMENP/IGLVI-70</i> | AAGTTCAGGCCCAGGGATAG CAG | GTGGGGGTTTCAACTGGGAA GTGAGAAGCTGGAGGAGGAG |
| <i>RABL2B</i> | CGGTTCAAGCTCAGGGCTAG GGG | CCTCCAAAGTGTCTAGCCCA CTTCTGCCACCTCTTGAGA |
| <i>KMT2D</i> | GAGACCAGGCTGAGGGACAG GGG | GGAAGTTCCTGTGGCTACT CAATTTTGTCCGGTCCCCTG |
| <i>FOXP4</i> | CAGCCCAGGGTCAGGGAGAA GGG | AGAAAGGAGGGGAGAAAGCG TATGAGCATCCGATACGCC |
| <i>RP11-83N9.5</i> | CAGGCCAGGCACAGGGATGC TGG | GTTCTGCGAATCCCTTACC GTGGTGAGGTCCCTGTCC |
| <i>C17orf96</i> | CACCCCAGCCTCAGGGATTG CGG | GATCCAGGCCTATCTACCC GGAAACAAAACAAGCTGCACT |
| <i>RAB13</i> | CCGCCAGGCTCCGGGAAAG AGG | ACCGATGGTGGAGATGTAAGTG AGAGGGGAGCTACAATTACCGA |
| <i>FBXO39</i> | CATCCCAGGCTCCGGGATAG AGG | TGTAGCTTTGGGTATCTGCAC CCTGGCTCACTCTTCTCTT |
| <i>PPP6R1</i> | CAGTCCTGGCGCAGGGACTG TGG | GCAACAGATGCTTGTGGCAA AGCTAGCCTTAGGGGTTCCA |

| | | |
|---|--------------------------|--|
| <i>RP11-48B3.3</i> | CACTCCAGCCTGAGGGACAG AGG | TCCCCTGATATTTCTAAGTCACTGT GCAGTTAATATGTGGTAGCATCAGG |
| <i>ST3GAL4</i> | CAGTCCGGGCGCAGGGCTGG GGG | TCCCTGGACCAGATTTTCGC CTCCCACTGACAACCTCCACC |
| <i>MANBAL</i> | CATTCCAGGCTCAGGGTCTG AGG | TGTGAACAAGAGGCCAAGA AGAGGAAGTGGTGGATTGCC |
| <i>CRCP</i> | CACTCCAGGCTTAGTGACAG TGG | GGCCAATCCTTCAACAGCTC ACTGTTGTGCAAATGAGGCT |
| Off targets crRNA E7 (Zhang Lab, MIT) | | |
| <i>CDRT4</i> | CATGGCTCCTACCATGATCC CAG | AAAGACCCTGGGCATCAAGG GGACAGTCTCTGGAATCCGC |
| <i>TMEM150C</i> | TTTGGGTTCAACCATGATCA AAG | GGGGCAGTGAAGGTATGGTT AGGAAGGGTATTCTTTAATTGGCT |
| <i>PLXNA3</i> | TTTACCTACTACCCTGATCC CAG | ACCCTGATGAGTTTGGCTTCC CTTCAGCCCAGGACTCTCCAC |
| <i>LRRC8A</i> | TTTAGGTTGAACCATGATTC CGG | AGGAGTTCCCGATTGCTCTTAC CCCCGAAGACGGCAATCAT |
| <i>ZDHC2</i> | TTTACCTCCAGACATGGTCC TGG | ACAGACTTGCCACGTTTCA TGTGCCACAGTGCTATTCTG |
| <i>TMEM140</i> | TTCAGTTCCAACCATGGTCA GAG | GGTTTCTAGCTCTGGGCAGC GGAGCTGGAGATCAGCGTTA |
| <i>MIPEP</i> | TTTACCTTCAACCATGAGCA TGG | CTGTGCAAGCAGGAGTCTGT ACTTAGGACACAGTGAGACAGATG |
| <i>MESTIT1</i> | TTAAGCTCCTACCATGAGCA TGG | ACGAAGGGGTTTTGGTTGAGA AGCTGCCGTATCTCTCTCTG |
| <i>DNM1P46</i> | TTTAGCACCGACCATGTGCC GAG | GGCCCAGGCACTATCAACTT TCACTCCAGCCAACCTGAAGC |
| <i>TPH2</i> | TTCAGCTCCACCCATGTGCC AGG | GGAAGAAGGCAAGGGTGGTC AAAGCATTGCAGCACAGAACA |
| <i>XPNPEP1</i> | TTTAACTCCAGCCCTGGTCC CAG | GGCCTCCTGCCTGTTTAAAGT AGCACTCACACGCAATCTCA |
| Chr6: -51925144 (intergenic) | TTGAGCTTCTACCATGATCC AGG | ACCAACAAATGACTGCCCTTG GGAACCACAAGCCAGGTAGT |
| Off targets crRNA E17 (Zhang Lab, MIT) | | |
| <i>TMEM185A</i> | ACTGCTCGCCGGCCTACATG GGG | TGTGTCAGAGGCTGCAAGTT CCCCAAAGAGAACAGGGCTT |
| <i>SLC4A11</i> | TGAGCTCCCTGCCCTACATG AGG | AGATCCACTACTTCACGGGC CCCATTCTCCACACCTAGACT |
| <i>CXCL10</i> | TCCCATCACTTCCCTACATG GAG | GGGGAGCAAATCGATGCAG GCAGCTGATTTGGTGACCATC |

| | | |
|-----------------|--------------------------|---|
| <i>TSC22D1</i> | TGCGCTTAGTGTCTACATG GGG | CTGTGTGCCTTTCCATCCCT TCCCAGCTACCTGTCACCAT |
| <i>TNKS1BP1</i> | TCCTCTCACTGGCCTCGATG CAG | CCAAGTGTGGAAGACAGCCT TTCCCAGGAGGCACAAAGTG |
| <i>EPG5</i> | TCCGCTCGCTGGGCTTCATG TGG | CACAATGCACTCACGTAGCC TTGGTGCATAAGAAGAGTTCACA |
| <i>NPTXR</i> | TCCGCACGCGGGCGTACATG TAG | TTTCTGAAGTGTGCCCTGTCC CAGGCGGTGAATGCGTAGAG |
| <i>NUTF2</i> | ACCCCTCACTGGCCTTCTG GAG | TCCTAGCACTGGTCTGGCTT CTCCATTCTGGAGCGTCAC |

Establishing a GBA2 and GBA1 enzymatic activity assay

To demonstrate the restoration of GBA2 activity in gene-corrected iPSC-derived neurons I established a widely used assay to measure GBA1 and GBA2 enzymatic activity in our lab.

To establish the best working condition to measure GBA2 activity two different published assay buffer and conditions and a more physiological condition were compared to each other. The assay is based on the specific inhibition of either GBA1 or GBA2. Calculating the difference allows to determine the respective enzyme activity.

Two different buffer compositions, 0.2 M Acetate buffer and McIlvain buffer, with varying pH values were tested, namely: Acetate buffer pH 5.2 and pH 5.8 (Sultana et al. 2015; Aureli et al. 2015; Haugarvoll et al. 2017; Aureli, Loberto, et al. 2012), McIlvain buffer pH 4 und pH 6 (Körschen et al. 2013) and a more physiological condition of McIlvain buffer of pH 5 and pH 7. Using conditions of acetate buffer pH 5.2 and 5.8 revealed to be a more suitable condition to measure GBA2 activity, for GBA1 activity no difference between buffer conditions was apparent. According to this outcome, acetate buffer pH 5.2 and pH 5.8 were used in all further GBA1 and GBA2 enzymatic assays.

GBA2 is mainly expressed in neuronal tissue and neurons are the affected cell type, hence all enzymatic activities were measured in lysates of iPSC-derived cortical neurons.

On DAI 34 to 36 differentiated cortical neurons were lysed with purified water supplemented with complete Protease Inhibitor (Roche). Lysates was normalized to 20 µg total cell protein content using the Micro BCA Kit (Pierce Thermo Scientific™ Pierce™).

To measure either GBA2 activity or GBA1 activity in cortical neurons, hypotonic lysates were incubated for 30min at RT with 1,6 mM final concentration of Condurotol B epoxide (CBE) (Cayman Chemical) a specific inhibitor for GBA1 or 7.9 nM N-(5-adamantane-1-yl-methoxy-pentyl)-Deoxyojirimycin (AMP-DNM) (Cayman Chemical), a specific inhibitor for GBA2 (Overkleeft et al. 1998; Witte et al. 2010).

To adjust the pH value water-soluble 4-methylumbelliferyl-b-D-glucopyranoside (4MU) (Glycosynth) was solved in a final concentration of 1.8 mM in 0.2 M acetate buffer of pH 5.2 / pH 5.8. and added to the lysates. The reaction was stopped after 2 h at 37°C by adding 9 parts 0.2 M Glycinbuffer (pH 10.2). Fluorescence was measured using the Spectramax M2 (Molecular Devices) with filters of

355nm/460nm for excitation and emission, respectively. Statistical analysis was done using Dunnett's test; outliers were removed.

For regulatory interaction studies between GBA1 and GBA2 the chemical inhibition of the two enzymes was performed during cell culture. 48h prior to the assay, neurons were cultured with the specific inhibitor for each enzyme. GBA1 was inhibited by a final concentration of 25 μ M CBE, GBA2 was chemically blocked using 10 μ M AMP-DNM (Overkleeft et al. 1998), supplemented to the neuronal medium. Medium was refreshed after 24 h, to prevent potential loss of inhibitory capacity. After 48 h, cortical neurons were lysed and measured as described above.

Western Blot analysis of GBA2-deficient and corrected cell lines

Cortical neurons were lysed on DAI 33 to 36 using RIPA buffer (Sigma) containing complete Protease Inhibitor. The protein amount was determined using the Pierce™ BCA Protein Assay Kit (Thermo Scientific). 40 μ g protein was loaded onto a 8% Bis-Tris gel, transferred on a Nitrocellulose membrane (GE Healthcare Amersham™ Protran™). Antibodies for GBA2 and β -actin (Tab. 12) were diluted in 5% non-fat milk in Tris-buffered saline supplemented with 0.1% Tween 20 (TBS-T) and incubated overnight at 4°C. On the next day, membrane was washed three times with TBS-T and incubated with Horseradish peroxidase-coupled secondary antibody (Tab. 12) in 5% non-fat milk in TBS-T for 1h at RT. Blots were washed thrice with TBS-T before development using ECL (Milipore) and Biorad ChemiDoc MP developing system and software.

Tab. 12: Antibodies used in GBA2 Western Blot analysis.

| | Antibody, Company, Catalogue number | Dilution |
|-----------------------------|---|-----------------|
| Primary antibodies | Mouse anti-GBA2, Santa cruz, D-10 sc-393782 | 1:1000 |
| | Mouse anti- β -actin, Sigma, Clone AC-15, A5441 | 1:50000 |
| Secondary antibodies | Goat anti-mouse peroxidase-conjugated AffiniPure, Jackson Immuno Research | 1:10000 |

Lipid mass spectrometry to assess changes in the lipid metabolism

Lipid extraction was performed as described previously (Pellegrino et al. 2014) with some modifications. To 20 μ l of the sample, 1 ml of a mixture of methanol: MTBE: chloroform (MMC) 1.33:1:1 (v/v/v) was added. The MMC was fortified with the SPLASH mix of internal standards (Avanti Lipids). After brief vortexing, the samples were continuously mixed in a Thermomixer at 25°C (950rpm, 30min). Protein precipitation was obtained after centrifugation for 10min, 16000g, 25°C. The single-phase supernatant was collected, dried under N₂ and stored at -20°C until analysis. Before Analysis, the dried lipids were re-dissolved in 100 μ L MeOH:Isopropanol (1:1).

Liquid chromatography was done as described previously (Cajka and Fiehn 2016) with some modifications. The lipids were separated using C18 reverse phase chromatography. Vanquish LC pump (Thermo Scientific) was used with the following mobile phases; A) Acetonitrile:Water (6:4) with 10 mM ammonium acetate and 0.1% formic acid and B) Isopropanol: Acetonitrile (9:1) with 10 mM ammonium acetate and 0.1% formic acid. The Acquity BEH column (Waters) with the dimensions 100mm * 2.1mm * 1.7 μ m (length*internal diameter*particle diameter) was used. The following gradient was used with a flow rate of 0.6ml/minute; 0.0-2.0 minutes (isocratic 30% B), 2.0-2.5 minutes (ramp 30-48% B), 2.5-11 minutes (ramp 48-82% B), 11-11.5 minutes (ramp 82-99%), 11.5-12 minutes (isocratic 100% B), 12.0-12.1 minutes (ramp 100-30% B) and 12.1-15 minutes (isocratic 30% B).

The liquid chromatography was coupled to a hybrid quadrupole-orbitrap mass spectrometer (Q-Exactive HFX, Thermo Scientific). A full scan acquisition in negative and positive ESI was used. A full scan was used scanning from 200-2000 m/z at a resolution of 120000 and automatic gain control (AGC) Target 1e6, max. Injection time 200 ms, while data-dependent scans (top10) were acquired using normalized collision energies (NCE) of 20, 30, 50 and a resolution of 15,000 and AGC target of 1e5.

Identification of the lipids was achieved using following criteria: high accuracy and resolution with an accuracy within m/z within 5 ppm shift from the predicted mass and a resolving power 70000 at 200 m/z. The fragmentation pattern matching to the *in silico* LipidBlast lipid fragmentation database. Mass spectrometric data analysis was performed in Compound Discoverer software 3.3 (Thermo Scientific) for peak picking, annotation and matching to LipidBlast.

Quantification was done using single point calibration by comparing the area under the peak to the area under the peak of SPLASH internal standard closed in time s to the area under the peak of the internal standard and then normalized to protein concentration.

Lipid mass spectrometry was done in cooperation with Dr. Alaa Othman, see statement of contributions (page 61). The material and method description for lipid mass spectrometry was kindly provided by Dr. Alaa Othman.

Subjects

The study was conducted in line with the Declaration of Helsinki and approved by the local institutional review board at the University of Tübingen, Germany (054/2013BO1). All patients/controls gave written informed consent for clinical data collection, collection and storage of biological samples, experimental analyses and the publication of relevant findings.

Results

Cell lines used in this project and iPSC generation

To study GBA1- and GBA2-dysfunction in a human neuronal cell system, we created iPSC models from patient-derived fibroblasts with Gaucher disease (GBA1-deficiency) and GBA2-associated HSP (GBA2-deficiency). I included three different patients carrying three different pathogenic variants in the *GBA2* gene and two patient-derived lines harboring different pathogenic variants in the *GBA* gene (Tab. 13). One patient with GBA1-deficiency carries the common bi-allelic p.(L483P) (historic nomenclature: p.(L444P)). The other patient displays compound heterozygous amino acid change of the p.(N409S) and the p.(W223R) variant (p.(N409S) historic nomenclature: p.(N370S)) (Nomenclature, Dimitriou et al. 2020).

Tab. 13: List of patients from which skin-derived iPSCs were generated in this project.

| Affected gene | Pathogenic variants | Phenotype |
|---------------------------|--|------------------|
| <i>GBA2</i> (Patient 1.1) | c.1255T>G, p.(F419V) and c.2608C>T, p.(R870*) compound heterozygous | Complicated HSP |
| <i>GBA2</i> (Patient 2.1) | c.700C>T, p.(R234)* homozygous | Complicated HSP |
| <i>GBA2</i> (Patient 2.2) | c.700C>T, p.(R234)* homozygous | Complicated HSP |
| <i>GBA</i> | c.1448T>C, p.(L483P) (L444P) homozygous | Neuronopathic GD |
| <i>GBA</i> | c.667T>C, p.(W223R) and c.1226A>G, p.(N409S) (N370S) compound heterozygous | Neuronopathic GD |

*Variant positions annotated according to the following transcripts: GBA: ENST00000368373.8 / NM_000157.4; GBA2: ENST00000378103.7 / NM_020944.3. *GBA* nomenclature: Human Genome Variation Society (HGVS) recommends numbering the codons beginning with the first ATG, historic nomenclature of *GBA* starts 39 codons downstream of the first ATG (Dimitriou et al. 2020).

While generation and characterization of GBA1-deficient iPSC cells was part of this thesis, GBA2-deficient iPSCs were already available (created by Stefan Hauser and Stefanie Schuster, see statement of contribution, page 61). Patients with pathogenic, bi-allelic *GBA2* variants were described previously (Martin et al. 2013; Sultana et al. 2015).

To generate GBA1-deficient iPSCs, patient-derived fibroblasts were reprogrammed using episomal vectors encoding the Yamanaka factors: OCT4, KLF4, L-MYC, SOX2 and LIN28 (Okita et al. 2011). Initial appearing of iPSC-like colonies were visible eight to ten days after nucleofection. Colonies were observed until large enough to pick and selected according to their morphology and growth rate. Each colony was manually picked for singularization around day 20 to day 25. After five passages cells were assumed to be transgene free and the characterization was initiated.

Characterization of reprogrammed iPSC

First, we confirmed the genomic integrity before demonstrating the pluripotency of the reprogrammed iPS cells.

Genomic integrity:

iPSC were passaged for at least five times before DNA was extracted. During these cultivation steps, iPS cells were monitored and evaluated based on their morphology and growth rate. Only cells that displayed the expected morphology and growth behavior were further analyzed. The criteria comprised dense and uniformly packed colonies with a distinct and sharp border. We aimed for a split ratio of approximately 1:12 every 5 days.

Selected iPS cells were negative in the PCR for unintentional plasmid integration, whereas positive plasmid controls showed an unambiguous band for the expected size (Fig. 6 E). In parallel, all pathogenic variants were re-evaluated via Sanger Sequencing (Fig. 6 C, D). The parentage of each fibroblast line with their reprogrammed iPSC line was confirmed by a STR analysis. All six STR markers identified the origin of each iPSC line from their respective fibroblast line. In addition the whole genome SNP analysis confirmed genomic integrity as well as the parentage by comparing fibroblast to their corresponding iPS cell line (Fig. 6A).

Demonstration of pluripotency:

Pluripotency is defined by the ability of self-renewal and the capacity to develop into cells of all three germ layers.

All generated iPSC cells are positive for an alkaline phosphatase staining and for specific pluripotency markers, which were verified by immunocytochemistry. We stained for the surface markers TRA-1-81 and SSEA4 as well as for the transcription factor OCT4 (Fig. 6 F). The expression of pluripotency markers was demonstrated by two different methods: immunohistochemistry staining against the target and on a transcriptional level. Transcript expression levels of pluripotency genes: *OCT4*, *SOX2*, *KLF4*, *C-MYC*, *NANOG*, *DNMT3B* and *TDGF1* in the generated GBA1-deficient iPSC were similar to the expression profile of HUES 6, a human embryonic stem cell line (Fig. 6 H). Differentiation potential in all three germ layers was confirmed using an embryoid body-mediated differentiation protocol for mesodermal and ectodermal markers. For endodermal differentiation, a protocol to differentiate hepatocytes was followed for the first days (Carpentier et al. 2014). Morphological changes in the differentiating endodermal 2D culture were visible within the first days. The usually small and densely packed iPS cells became flatter, bigger and more spread in the well. Characteristic markers for each layer were demonstrated by immunohistochemistry staining for mesodermal, endodermal and ectodermal by SMA, FOXA2 and TUJ, respectively (Fig. 6 G). Pluripotency for our reprogrammed iPS cells was demonstrated by these experiments. The generation of these iPSC-lines was published by our lab (Nagel et al. 2019).

All validated iPSC were expanded in young passages and cryopreserved for following experiments.

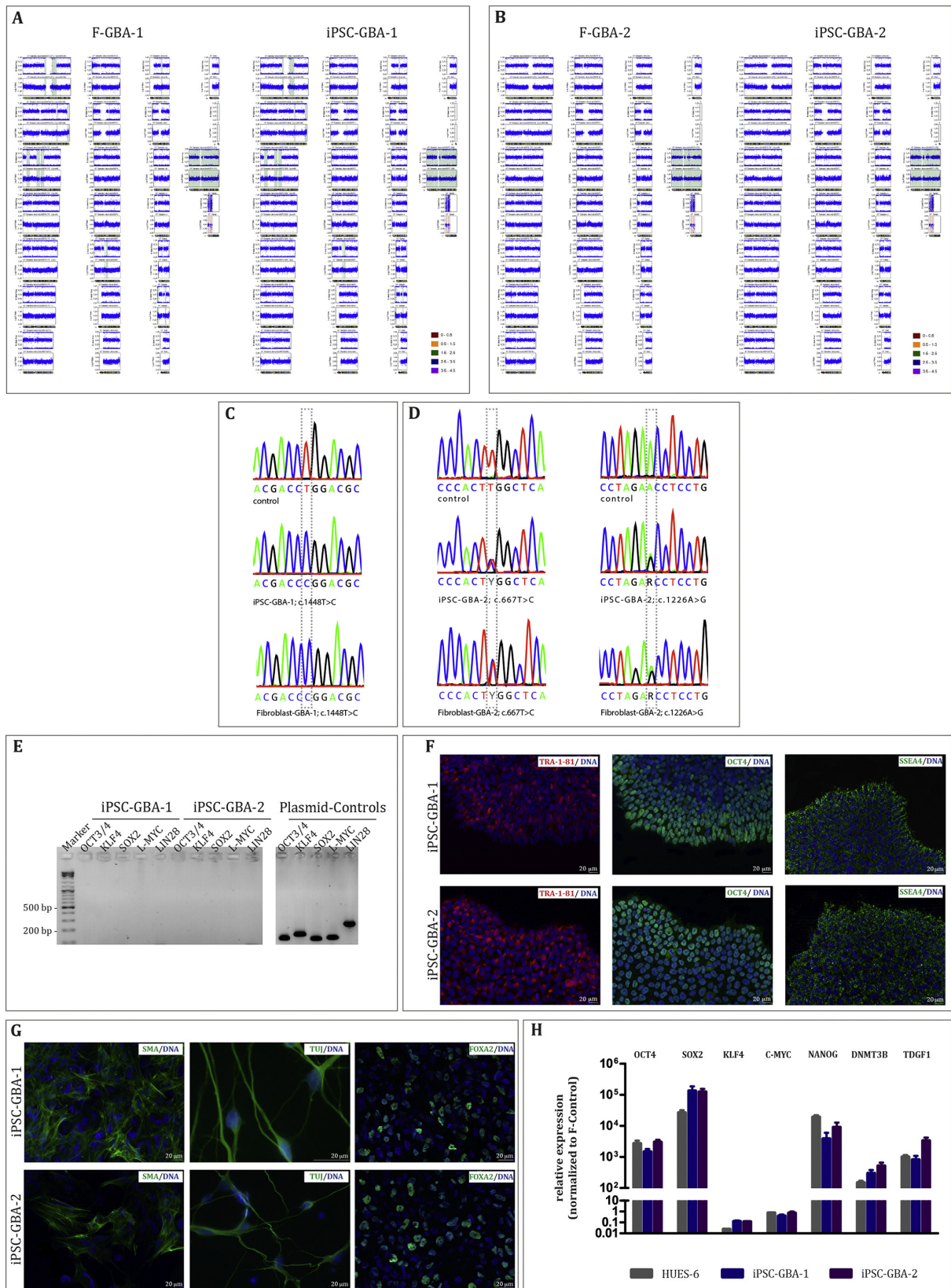


Fig. 6: Characterization and validation of genomic integrity and pluripotency of reprogrammed iPSC from GBA1-deficient fibroblasts. Two iPSC lines with three different pathogenic variants in the *GBA* gene were analyzed (iPSC-GBA-1: c.1448T>C; p.(L483P), homozygous; iPSC-GBA-2: c.667T>C, p.(W223R) and c.1226A>G, p.(N409S) (compound heterozygous). Figure from Nagel et al. 2019.

Differentiation of iPSC cells into cortical neurons

To model one of the affected cell types in GBA2-associated HSP, patient-derived iPSC were differentiated towards cortical neurons of layer V and VI (Yichen Shi et al. 2012; Schöls et al. 2017; Rehbach et al. 2019). Cortical differentiation was recapitulated using a protocol based dual SMAD inhibition to stimulate neural induction. FGF2 withdrawal on day 12 promoted cortical neurogenesis. Neural rosettes appeared, which are characteristic for cortical neuroepithelium. The differentiation process comprises 37 days, staining for neuronal and cortical marker revealed an almost pure culture of TUJ positive cells and the specific marker expression for cortical layer V (CTIP2) of over 75% (Schuster et al. 2020). Astrocytes were excluded by immunofluorescence staining; differentiated cultures presented no GFAP positive cells.

Experimental approach to *GBA2* gene correction

To generate isogenic controls for two GBA2-deficient iPSC lines (Tab. 13) a precise gene editing strategy was necessary. To design the sequence specific crRNA, online tools of the Zhang lab and the CRISPOR tool (<http://crispor.tefor.net/>) were used. crRNAs targeting the following variants were designed (Fig. 7) (F. Ran et al. 2013; Haeussler et al. 2016):

- c.1255T>G, p.(F419V) (exon 7) and c.2608C>T, p.(R870*) (exon 17) (Patient 1.1)
- c.700C>T, p.(R234)* (exon 4) (Patient 2.2)

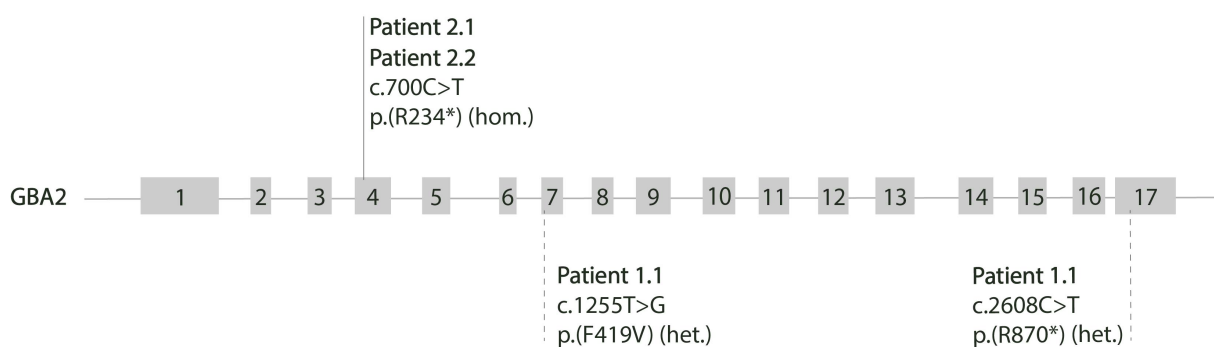


Fig. 7: Summary of pathogenic *GBA2* variants present in iPSCs generated from two unrelated families. Patient 1.1 carries compound heterozygous variants in *GBA2*, a missense variant in exon 7 and a nonsense variant in exon 17. Patient 2 (two siblings, P2.1 and P2.2) show a bi-allelic nonsense variant in exon 4, leading to a premature stop codon. GBA2: ENST00000378103.7 / NM_020944.3.

Over time the CRISPR technique improved continuously and thereby the development was directed towards a more efficient and integration free editing approach. The original protocol used a plasmid-based approach, with the drawback of unintentional plasmid integration (F. Ran et al. 2013). The advancement of *in vitro* assembly of the RNP allowed a faster, more flexible and safer editing process. Since only Cas9 protein and the RNA duplex is used for gene editing, the risk of unintentional plasmid integrations is prevented. In this project, both methods were applied (Tab. 8).

Specific requirements for designing the crRNA and ssODN were fulfilled. Firstly, the crRNA should span the targeted variant on the affected allele. This was applicable for two variants, but not for variant c.2608C>T, p.(R870)* (Patient 1.1), consequently, a sequence downstream of the variant locus was selected. Secondly, the repair template should contain an additional silent variant in the PAM sequence to prevent the Cas9 from repeated cutting after successful gene correction. Thirdly, an additional consideration was to introduce or remove an enzymatic restriction site to facilitate the screening for potential positive clones (Tab. 14, Fig. 5). The optimized protocol for correcting GBA2-specific variants relied on the RNP approach.

In the first step of assembling the RNP, the sequence-specific crRNA and scaffolding tracrRNA were annealed to form the gRNA. In the second step, the annealed gRNA was combined with the Cas9 protein to form the RNP. Hereby, we used a fluorescently labeled (ATTO 550) tracrRNA to allow FACS sorting of successfully transfected cells and thus increase the efficiency of gene editing. The RNP was assembled outside the cells and then electroporated into iPSC.

iPSC were pre-selected with an RFLP approach (Fig. 5) and positive clones validated further via Sanger sequencing. After confirming the successful genetic editing, off-target effects of the most likely predicted coding sites were excluded by direct Sanger sequencing (Tab. 11). To predict the off-target sites the same online tools were utilized as for designing the crRNAs (Zhang lab and the CRISPOR tool (<http://crispor.tefor.net/>)).

Tab. 14: Overview and efficiency of CRISPR experiments to generate isogenic controls.

| Generated genotype with CRISPR/Cas9 | Number of single-cell colonies screened by restriction digest | Number of clones with restriction digest pattern suggestive of variant correction | Number of clones with variant and PAM correction confirmed by Sanger sequencing | Total efficiency |
|--|--|--|--|-------------------------|
| CRISPR wt / R870* (P1.1) | 85 | 5 | 1 | 1.18% (1/85) |
| CRISPR F419V / wt (P1.1) | 105 | 2 | 1 | 0.95% (1/105) |
| CRISPR wt / wt (P1.1) | 142 | 11 | 1 | 0.70% (1/142) |
| CRISPR R234* / wt (P2.2) | 176 | 8 | 5 | 2.84% (5/176) |
| CRISPR wt / wt (P2.2) | 213 | 5 | 2 | 0.94% (2/213) |

Despite all advancements, the efficiency of gene editing remains low (Tab. 14) and the feasibility of creating large cohorts and patient-derived iPSC studies remain difficult in practical application. This highlights the value of these generated isogenic controls.

Functional characterization of isogenic controls

To validate the generated isogenic controls, GBA2 was assessed on a protein level by Western Blot analysis and for functionality by measuring GBA2 enzyme activity. All cell lines used in the following experiments are listed in Tab. 15.

Tab. 15: Overview over iPSC cell lines used in this study.

| Name | Parent cell line | Variant status |
|-------------------------------------|--|--|
| iPSC F491V/R870* | Patient-derived (P1.1) | GBA2: c.1255T>G, p.(F491V); c.2608C>T, p.(R870*) (compound heterozygous) |
| iPSC wt/R870* | Gene-corrected from iPSC F491V/R870* | GBA2: c.1255T, p.(F491); c.2608C>T, p.(R870*) (heterozygous) |
| iPSC F491V/wt | Gene-corrected from iPSC F491V/R870* | GBA2: c.1255T>G, p.(F491V); c.2608C, p.(R870) (heterozygous) |
| iPSC wt/wt | Gene-corrected from iPSC wt/R870* = isogenic control | GBA2: c.1255T, p.(F491); c.2608C, p.(R870) (GBA2 wt) |
| iPSC R234*/R234* | Patient-derived (P2.1) | GBA2: c.700C>T, p.(R234*); (homozygous) |
| iPSC R234*/R234* | Patient-derived (P2.2) | GBA2: c.700C>T, p.(R234*); (homozygous) |
| iPSC R234*/wt | Gene-corrected from iPSC R234*/R234* (P2.2) | GBA2: c.700C>T, p.(R234*); (heterozygous) |
| iPSC wt/wt | Gene-corrected from iPSC R234*/wt (P2.2) | GBA2: c.700C, p.R234; (GBA2 wt) |
| iPSC control 1-3 (Co-1, Co-2, Co-3) | Derived from unrelated healthy controls | GBA2 wt |
| Gaucher 1 (L483P/L483P) | Derived from unrelated GBA1 patient | GBA1: c. 1448 T > C, p.(L483P); (homozygous), (GBA2 wt) |
| Gaucher 2 (W223R/N409S) | Derived from unrelated GBA1 patient | GBA1: c.667 T > C p.(W223R), c.1226A > G p.(N409S); compound heterozygous), (GBA2 wt) |
| SPG5 | Derived from unrelated SPG5 patient | CYP7B1: c.1484C>T, p.(R486C); (homozygous), (GBA2 wt) |

*Variant positions annotated according to the following transcripts: *GBA*: ENST00000368373.8 / NM_000157.4; *GBA2*: ENST00000378103.7 / NM_020944.3. *GBA* nomenclature: Human Genome Variation Society (HGVS) recommends numbering the codons beginning with the first ATG, historic nomenclature of *GBA1* starts 39 codons downstream of the first ATG (Dimitriou et al. 2020).

Gene correction restores protein expression

WB analysis demonstrated full restoration of GBA2 protein expression in isogenic control neurons compared to the corresponding patient cell line (Fig. 8). In the sample of Patient P1.1 a faint signal of GBA2 protein is detectable compared to more intense signals in the heterozygous-corrected samples and the isogenic control. Both siblings (P2.1 and P2.2) carrying the premature stop codon variant p.(R234*) have no detectable full-length GBA2 protein, but full-length GBA2 protein content increases depending on the restored wild-type alleles. The used antibody was raised against amino acids 325 to 574 of the full-length GBA2 protein. Hence this antibody does not allow the detection of a truncated protein due to the nonsense variant in exon 4 (amino acid 234). Quantification of GBA2 levels confirmed restoration of GBA2 protein in isogenic controls compared to unrelated controls.

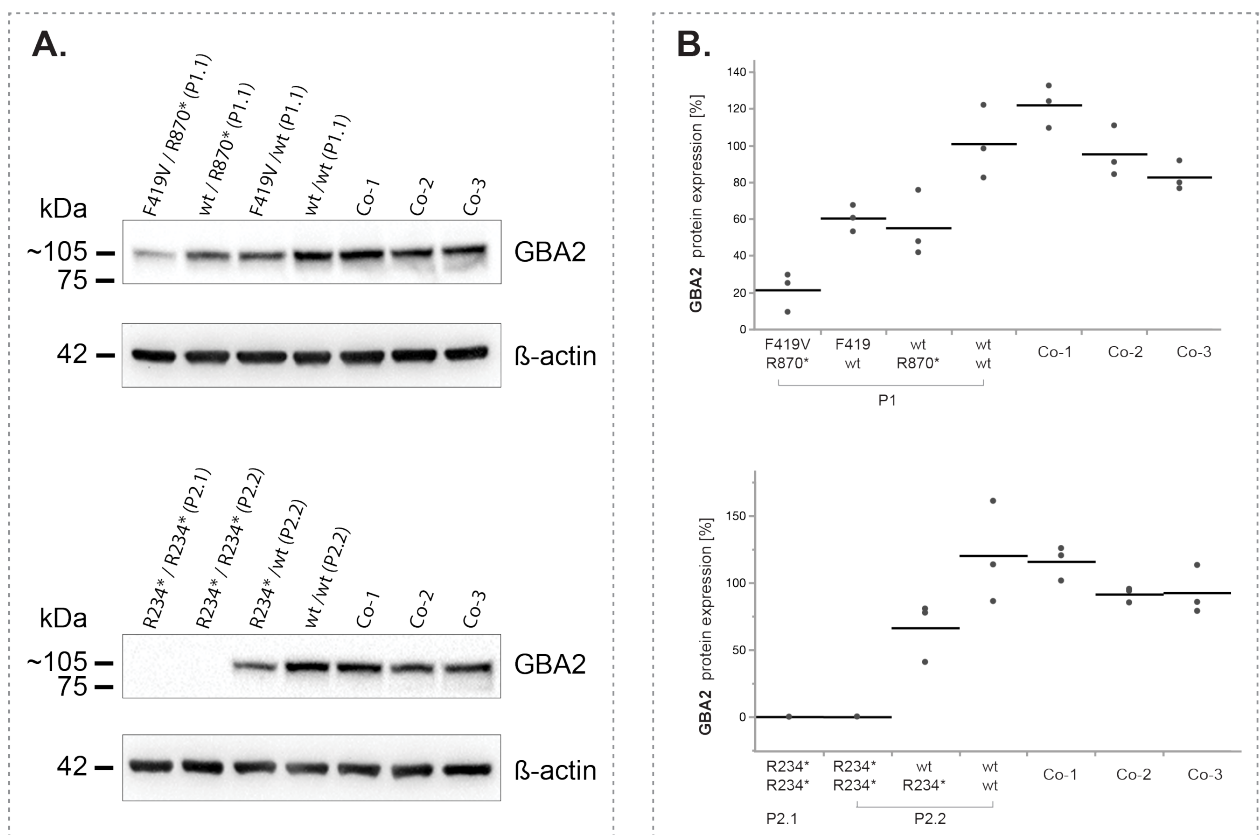


Fig. 8: Western Blot analysis demonstrated restoration of GBA2 protein in isogenic controls of iPSC-derived cortical neurons in three independent lysates. A: 40 μ g protein was loaded and detected with specific antibodies; (GBA2: santa cruz, D-10 sc-393782 and β -actin Clone AC-15, A5441). B: Quantification of GBA2 protein expression in cortical neurons. GBA2 was normalized to the mean GBA2 levels of three unrelated controls (Co1- Co3).

Gene correction restores enzymatic function of GBA2

First, I tested different assay conditions to evaluate the best condition to measure GBA2 activity, since most publications focus on GBA1 activity (Van Weely et al. 1993; Körschen et al. 2013; Aureli et al. 2016; Haugarvoll et al. 2017; Sultana et al. 2015; Aureli et al. 2015; Aureli, Loberto, et al. 2012). To assess the enzymatic function of GBA2 in a disease relevant tissue and concurrently a cell type with a high GBA2 expression, I measured GBA2 activity in iPSC-derived cortical neurons.

The artificial substrate 4-methylumbelliferyl- β -D-glucopyranoside (4MU) is hydrolyzed by GBA1 and GBA2 to 4-methylumbelliferone, a quantifiable fluorescent product. Various conditions for this assay have been described; they differ in their buffer constitution and their pH (Van Weely et al. 1993; Körschen et al. 2013; Aureli et al. 2016; Haugarvoll et al. 2017; Sultana et al. 2015; Aureli et al. 2015; Aureli, Loberto, et al. 2012). In our preparatory assay setup I included three cell lines and three different buffer conditions. Three control lines were tested, two healthy wild-type controls (Co-2 and P1.1 wt/wt) and a cell line with a HSP background (SPG5) as a disease control without a GBA2-deficiency (Tab. 15). The buffer conditions differ in their composition (McIlvain or Acetate) and pH (Fig. 9). Specific inhibitors were used to distinguish between GBA1 and GBA2 activity. CBE is an irreversible inhibitor of the lysosomal GBA1, whereas AMP-DNM is a potent and specific inhibitor of the non-lysosomal β -glucosidase, GBA2 (Boot et al. 2007; Overkleeft et al. 1998).

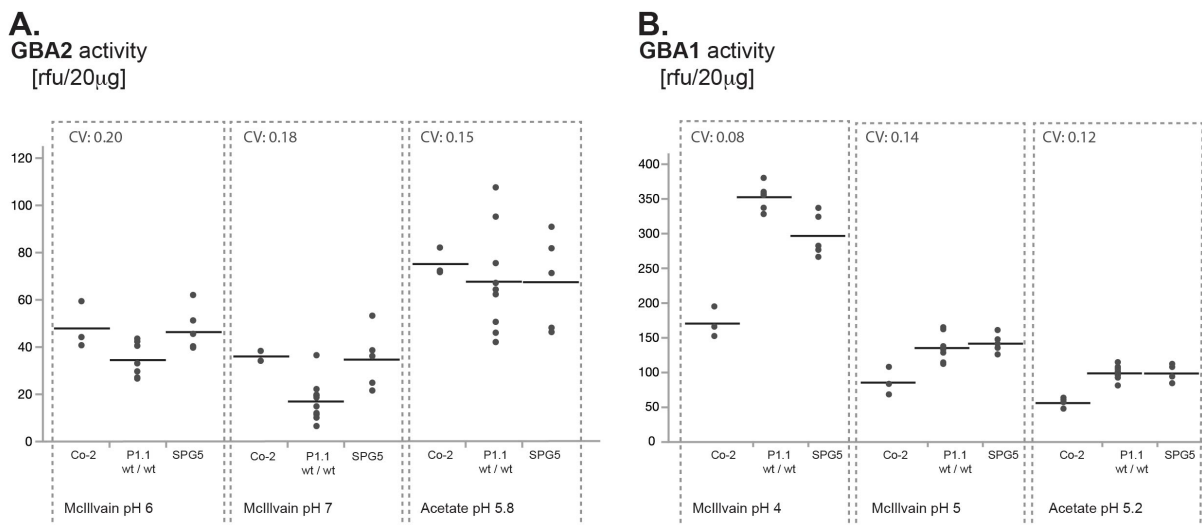


Fig. 9: Comparing assay conditions for measuring GBA2 activity. Three different cell lines, two healthy control lines (Co-2 and P1.1wt/wt) and a disease control line with a SPG5 background were used. Two described assay conditions and a more physiological assay condition were evaluated for GBA2 activity (A) and GBA1 activity (B). Coefficient of Variation (CV) was determined for each buffer composition.

The optimal condition with the lowest coefficient of variation (CV) for GBA2 activity was chosen. The CV of GBA2 is calculated by the ratio of the standard deviation to the mean of all tested measurements for each condition of the three cell lines. All further enzymatic activity assays, the characterization of all isogenic controls and the interaction of GBA1 and GBA2, were measured using acetate buffer pH 5.2 for GBA1 activity and pH 5.8 for GBA2 activity (Condition 3, Tab. 16).

Tab. 16: Evaluation of tested assay conditions to optimize the enzymatic assay for quantification of GBA2 activity.

| Condition | Buffer | pH GBA1 activity | pH GBA2 activity | Coefficient of variation (GBA2) |
|-----------|----------|------------------|------------------|---------------------------------|
| 1 | McIlvain | 4 | 6 | 0.20 |
| 2 | McIlvain | 5 | 7 | 0.18 |
| 3 | Acetate | 5.2 | 5.8 | 0.15 |

I proceeded to demonstrate the recovery of GBA2 enzymatic function in all isogenic control cells and their partially corrected intermediates. In cell lysates from cortical neurons of P1.1 (F419V/R870*) no residual GBA2 activity could be detected, whereas in the isogenic control GBA2 activity was 74.5 [rfu/20mg protein] (Fig. 10A). Correcting the nonsense variant in P1.1 neurons lead to an increase of GBA2 activity to 31.4 [rfu/20mg protein] and restoration of the missense variant resulted in a slightly higher activity 49.8 [rfu/20mg protein].

Tab. 17: GBA1 and GBA2 activity in GBA2-deficient cortical neurons and a chemical GBA2 inhibited (AMP-DNM) control line. Mean and standard deviation (StDev) measured in patient-derived cells.

| | GBA2 genotype | GBA1 | | GBA2 | |
|-------------|----------------|-------|-------|------|-------|
| | | Mean | StDev | Mean | StDev |
| P1.1 | F419V/R870* | 120.1 | 47.9 | -2.5 | 14.7 |
| | F419V/wt | 114.4 | 14.8 | 31.4 | 8.0 |
| | wt/R870* | 99.0 | 20.4 | 49.8 | 19.7 |
| | wt/wt | 111.2 | 27.7 | 74.5 | 19.8 |
| P2.1 | R234*/R234* | 110.5 | 51.6 | 7.1 | 4.1 |
| P2.2 | R234*/R234* | 113.7 | 21.4 | 4.8 | 3.8 |
| | R234*/wt | 99.0 | 12.8 | 37.1 | 8.0 |
| | wt/wt | 102.1 | 10.0 | 67.1 | 12.4 |
| Co-2 | Co-2 | 86.1 | 17.1 | 50.1 | 17.1 |
| | Co-2 + AMP-DNM | 95.1 | 14.0 | 7.8 | 6.1 |

The enzymatic activity of GBA2 was completely abolished in both neuronal cell lines, generated from siblings (P2.1 and P2.2) (Fig. 10A). The enzymatic activity of GBA2 in the isogenic control of P2.2 was 67.1 [rfu/20mg protein], demonstrating the full restoration of GBA2 functionality. Cells with heterozygous gene correction (R234*/wt) showed an enzymatic GBA2 activity of 37.1 [rfu/20mg protein] (Tab. 17). Inter-individual variability of GBA2 activity was observed when comparing the two isogenic GBA2 controls lines with iPSC-derived cortical neurons from a healthy donor (Co-2 in Fig. 10). In conclusion, I could demonstrate full restoration of GBA2 enzymatic activity in gene-corrected isogenic control neurons. AMP-DNM as a specific GBA2 inhibitor showed the same loss in GBA2 activity as the genetic GBA2-deficient cell lines (P1.1 - F419V/R870* and P2.1, P2.2 - R234*/R234*). This demonstrates a complete elimination of GBA2 activity in both model systems of either pharmacological or genetic inhibition.

GBA1 activity was unchanged in GBA2-deficient cells compared to cells with full GBA2 activity (Fig. 10B) leading to the conclusion that GBA1 activity is independent from GBA2 activity.

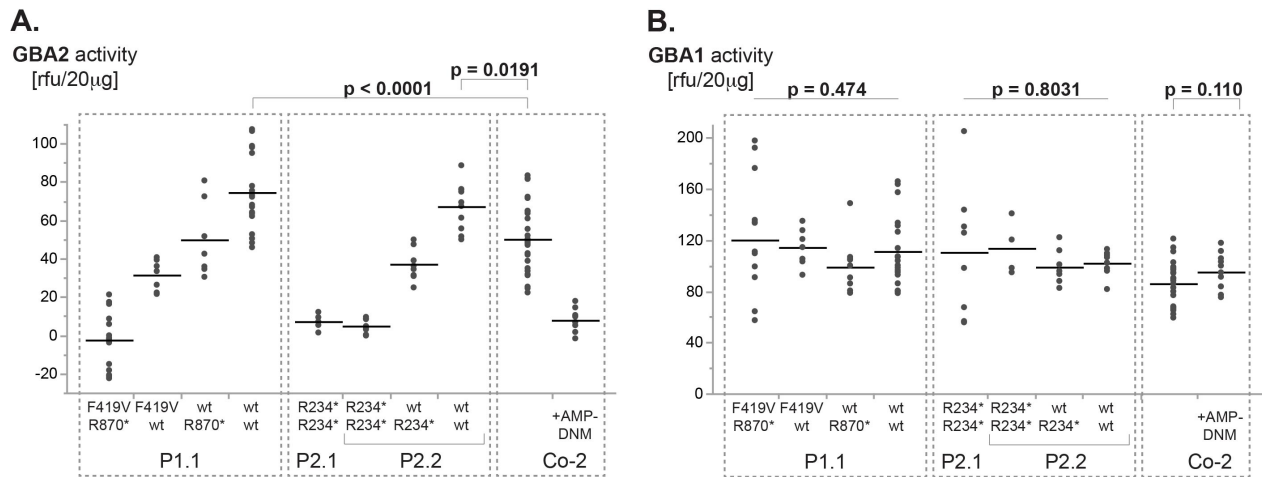


Fig. 10: Enzymatic characterization of patient-derived cortical neurons and their respective isogenic controls. A) Full restoration of GBA2 activity in isogenic controls, complete abolished GBA2 activity in cells treated with AMP-DNM (AMP-DNM, a specific GBA2 inhibitor). B) GBA2-deficiency and the specific GBA2 inhibitor (AMP-DNM) have no effect on GBA1 activity. The specificity of the GBA2 inhibitor AMP-DNM is demonstrated in a healthy wild-type control. Pharmacologic inhibition of GBA2 resulted in an almost complete abolished GBA2 activity (7.8 [rfu/20mg protein]) without affecting GBA1 activity.

Regulatory interaction between GBA1 and GBA2 activity

In literature there are contradictory reports on a regulatory feedback loop between GBA1 and GBA2. Most studies focus on GBA1-deficiency in either artificial, non-human or non-neuronal cell lines without isogenic controls. I investigated the interaction between GBA1 and GBA2 activity in iPSC-derived cortical neurons, a tissue with high GBA1 and GBA2 expression.

Cells from two patients with neuronopathic Gaucher disease were used as a genetic model of GBA1-deficiency. As expected, bi-allelic presence of the common c. 1448 T > C, p.(L483P) variant (historic nomenclature: L444P) in the *GBA1* gene abolished GBA1 activity completely (2.8 [rfu/20mg protein]) (Tab. 18). Low residual GBA1 activity of 24.2 [rfu/20mg protein] was measured in neurons carrying compound heterozygous c.667 T > C p.(W223R) / c.1226A > G p.(N409S) variants (Fig. 11B). GBA2 activity remained unchanged in $GBA^{L483P/L483P}$ neurons compared to controls; surprisingly $GBA^{W223R/N409S}$ neurons, despite their residual GBA1 activity, demonstrated higher GBA2 activity than healthy controls. These results, however, have to be interpreted with caution, as I did not use isogenic controls but unrelated healthy controls and therefore do not control for intra-individual variability of GBA2 activity. CBE is a potent inhibitor of GBA1 and abolished GBA1 activity to the same level as the genetic $GBA^{L483P/L483P}$ model. In accordance with the results in neurons harboring pathogenic *GBA* variants, pharmacologic inhibition of GBA1 enzyme using CBE did not affect GBA2 activity (Fig. 11).

Tab. 18: GBA1 and GBA2 activity in GBA1-deficient cortical neurons and control cells treated with a GBA1 inhibitor (CBE). In these patient-derived cells GBA1 and GBA2 activity are displayed as mean with standard deviation (StDev).

| | GBA genotype | GBA1 | | GBA2 | |
|------------------|--------------|------|-------|------|-------|
| | | Mean | StDev | Mean | StDev |
| Gaucher 1 | L483P/L483P | 2.8 | 4.2 | 45.4 | 4.9 |
| Gaucher 2 | W223R/N409S | 24.4 | 6.6 | 73.0 | 11.0 |
| Co-2 | Co-2 | 86.1 | 17.1 | 50.1 | 17.1 |
| | Co-2 + CBE | 0.3 | 2.8 | 45.9 | 4.8 |

In conclusion, the results show that a complete abolishment of GBA1 activity does not influence GBA2 activity. Both, chemical inhibition (48h CBE treatment prior to lysis) and pathogenic, bi-allelic variants c.1448T>C p.(L483P) reduced GBA1 activity to background level, but resulted in no significant change in GBA2 activity. An increased GBA2 activity was observed in cortical neurons carrying GBA variants causing the amino acid changes p.(W223R)/p.(N409S) while some residual GBA activity was measured. This higher GBA2 activity could be rather explained by high inter-individual variability of GBA2 activity than a regulatory feedback caused by reduced GBA1 activity, taken the data of a complete loss of GBA1 activity into account.

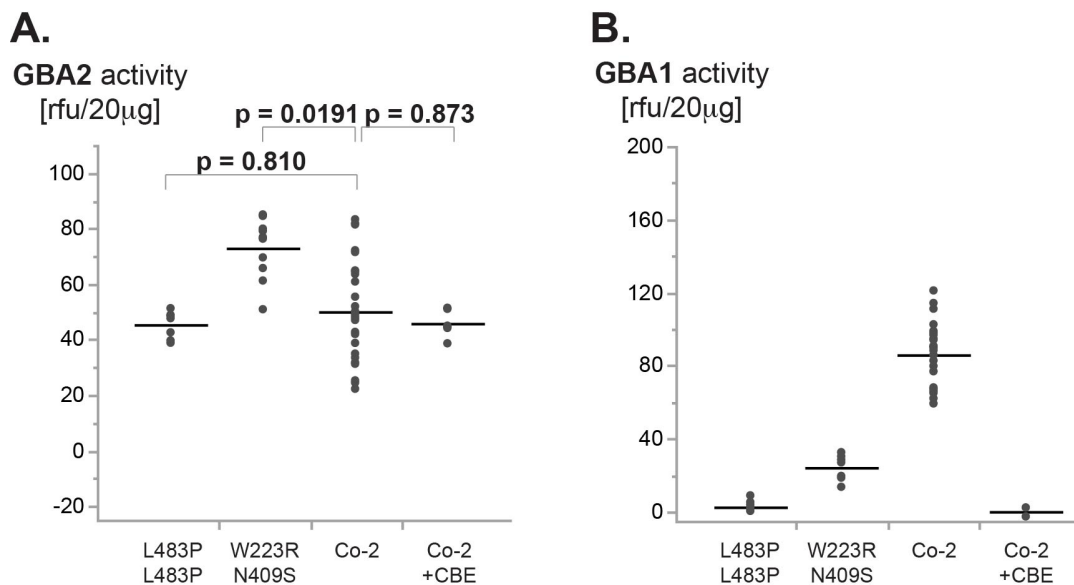


Fig. 11: GBA1 and GBA2 activity in GBA1-deficient neuronal cells. A) CBE (Conduritol B epoxide, a specific GBA1 inhibitor) has no effect on GBA2 activity. B) Complete absence of GBA1 activity in both conditions, either cells carrying bi-allelic p.(L483P) variants or neurons treated with CBE. Some residual GBA1 activity is measurable in cells with the compound heterozygous variants (W223R und N409S), likely reflecting intra-individual variability.

Lipidomic studies in GBA2-deficient cells and their isogenic controls

GBA2 catalyzes the breakdown of GlcCer to glucose and ceramide and is involved in the lipid metabolism. Ceramide plays a pivotal role in the sphingolipid metabolism, since it is the building block for all complex glycosphingolipids (GSL). To reveal the impact of GBA2-deficiency in the context of hereditary spastic paraplegia type 46 we analyzed iPSC-derived cortical neurons from patients and their respective isogenic controls by lipid mass spectrometry.

Lipidomics in cortical neurons reveals hexosylceramide accumulation

Previous studies demonstrated that GBA2-deficiency results in accumulation of GlcCer. Thin-layer chromatography of GBA2 KO mice revealed GlcCer accumulations in testis and fibroblasts (Yildiz et al. 2006; Raju et al. 2015). Furthermore, GlcCer accumulation was shown in patient-derived lymphoblastoid cell lines of three patients carrying the c.1780G>C variant compared to healthy controls using thin layer chromatography (Malekkou et al. 2018).

To analyze lipid metabolism in a more disease relevant cell type iPSC-derived cortical neurons were studied. Patient-derived cortical neurons in combination with their respective isogenic controls represent a solid and robust disease model for HSP type 46. To investigate the consequences of GBA2-deficiency on lipid metabolism we performed lipid mass spectrometry of iPSC-derived cortical neurons from patients compared to their isogenic controls (lipid mass spectrometry was performed in cooperation by Dr. Alaa Othman, see statement of contributions, page 61). Three independent cortical differentiations of patient-derived iPSC cells and their respective isogenic controls were prepared for analysis.

GBA2 is an enzyme involved in the sphingolipid metabolism and is also called the non-lysosomal β -glucosidase. GBA2 catabolizes GlcCer into glucose and ceramide. GlcCer and galactosylceramide are the simplest glycosphingolipids; both are formed by adding a sugar residue (glucose or galactose, respectively) to ceramide. With classical mass spectrometry both glycosphingolipids (GlcCer and galactosylceramide) are indistinguishable.

All GSL have this basic building block in common; they all derive from the simple sphingolipid ceramide. Ceramide is composed of a sphingoid base N-acylated to a fatty acid. While the sphingoid backbone can differ in carbon chain length, hydroxylation and number of double bonds, the N-linked fatty acid can vary in carbon chain length and their number of double bonds. Responsible for the N-acylation is the ceramide synthase (CerS). In mammals, six distinct CerS are known (CerS1-6), every CerS has a particular substrate specificity towards the length of a fatty Acyl-Co-enzyme A. In neurons the predominant CerS is the CerS1, linking fatty acids with a carbon length of C18 to the sphingoid base (Merrill 2011; Kitatani, Idkowiak-Baldys, and Hannun 2008; Ben-David and Futerman 2010; Spassieva et al. 2016; Levy and Futerman 2010).

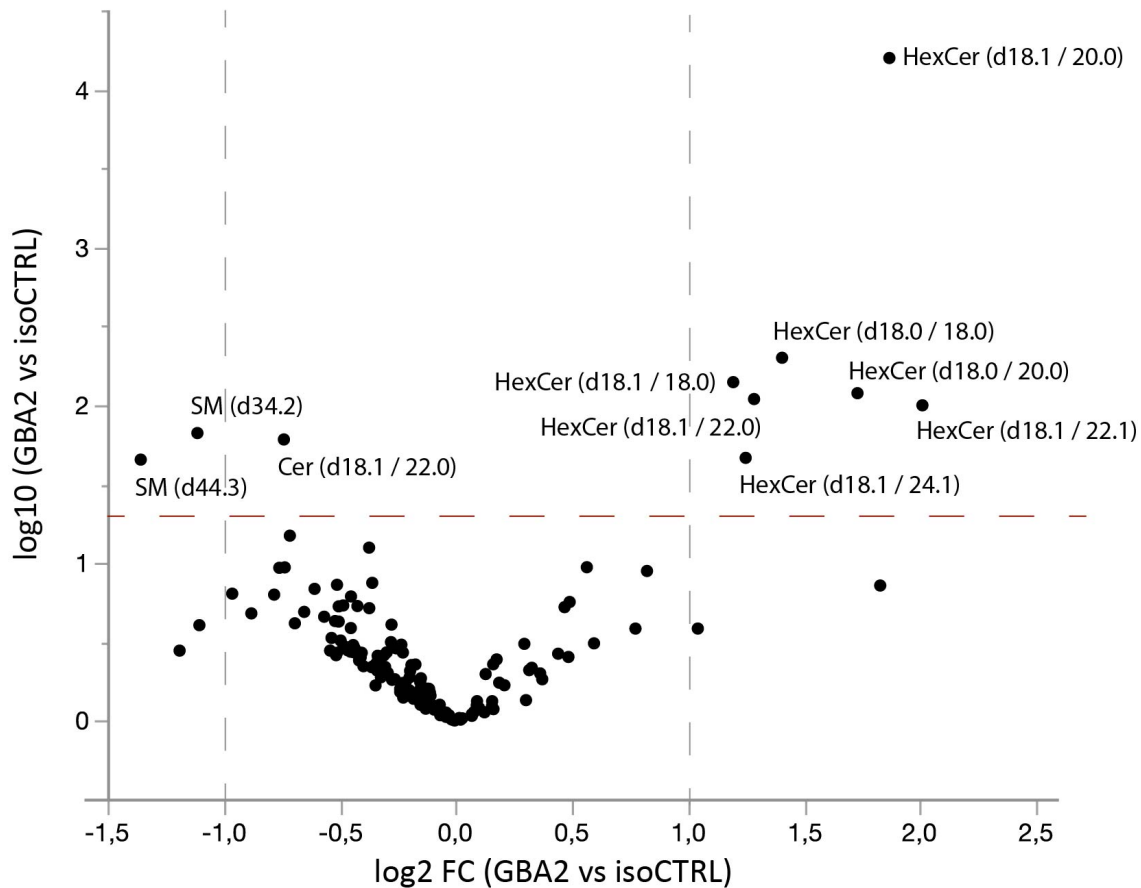


Fig. 12: Mass Spectrometry data of three independent lysates of cortical neurons depicted in a Volcano Blot analysis. Comparison of patient-derived cells versus their isogenic controls. Seven lipid species from two lipid classes were increased: dihydro-monohexosylceramide and monohexosylceramide (HexCer), whereas two sphingomyelin (SM) and one ceramide (Cer) species were decreased. P-Value of 0.05 indicated as red line.

Analysis of the different lipid species in patient-derived samples revealed ten single lipid species differentially regulated (p -value < than 0.05; p -value = red line in Fig. 12), seven lipid species were elevated whereas 3 lipid species were decreased in comparison to the isogenic control cells.

These seven elevated lipid species in patient-derived cortical neurons belong to two lipid classes: dihydro-monohexosylceramide and monohexosylceramide; both are HexCer. Both classes distinguish themselves by the present (monohexosylceramide, e.g. sphingosine d18.1) or absence (dihydro-monohexosylceramide, e.g. sphinganine d18.0) of a double bond in the sphingosine base.

In patient-derived cells, three lipid species were down regulated compared to isogenic controls, two sphingomyelin (SM) species and a ceramide species (Fig. 12). SM is the most abundant complex sphingolipid in mammalian cells and involved in signaling pathways of the cell. The other lipid species reduced in patient-derived cells is ceramide, which is the essential building block for all complex sphingolipids in the cell and ceramide itself is a bioactive sphingolipid and regulates various cellular processes (Gault, Obeid, and Hannun 2010; Slotte 2013; Chakraborty and Jiang 2013; Stith, Velazquez, and Obeid 2019; Merrill 2011; Adada, Luberto, and Canals 2016).

Combining single lipid species into groups (Tab. 19) revealed two enriched lipid groups in patient-derived cortical neurons compared to their isogenic controls. The lipid classes of monohexosylceramides and dihydro-monohexosylceramides are increased in these cells, indicating the importance of GBA2 for catalyzing the breakdown of these two lipid species.

The effect of decreased SM and ceramide species was not severe enough to contribute to a fold change greater than -2 in these groups.

Tab. 19: Lipid classes and their respective fold changes in patient-derived cortical neurons versus isogenic controls are measured in a lipid mass spectrometry approach. Lipid classes with a fold change greater than two are highlighted.

| Group | Measured lipid classes | Fold Change (GBA2/isogenic controls) |
|-------|---------------------------------------|--------------------------------------|
| 1 | Acyl Carnitine | 1.4 |
| 2 | Dihydroceramide | 0.77 |
| 3 | Ceramide (Cer) | 0.71 |
| 4 | Deoxydihydroceramide | 1.12 |
| 5 | Dihydro-monohexosylceramides (HexCer) | 2.63 |
| 6 | Monohexosylceramide (HexCer) | 2.39 |
| 7 | GM2 Gangliosides | 1,41 |
| 8 | Lysophosphatidylcholine | 0,98 |
| 9 | Lysophosphatidylethanolamine | 1.02 |
| 10 | Phosphatidylcholine | 0.87 |
| 11 | Phosphatidylethanolamine | 0.89 |
| 12 | Sphingomyelin (SM) | 0.7 |

Validation of glucosylceramide accumulation in human biofluids

To validate our *in vitro* model of GBA2-deficiency and to gain further insights in the lipid metabolism of SPG46 patients we analyzed patient-derived cerebrospinal fluid (CSF) and plasma. These biofluids were compared to healthy control subjects (Tab. 20).

Tab. 20: Overview of measured biofluid samples via mass spectrometry of GBA2-deficient patients and matching controls.

| Sample | Variant status GBA2 | Sex | Fasted |
|-----------|---------------------|-------------------------|-------------|
| P1.1 | F419V/R870* | Male | Yes |
| P2.1 | R234*/R234* | Female | Yes |
| P2.2 | R234*/R234* | Female | Yes |
| P3.1 | V394Ffs*28/L554P | Female | No |
| Control A | wt/wt | Male | Yes |
| Control B | wt/wt | Female | Yes |
| Control C | wt/wt | Female (sister of P1.1) | Only Plasma |

In various neurological diseases such as Alzheimer's' disease as well as Niemann-Pick Disease Type C, disturbances in the sphingolipid metabolism are described and investigated by lipid mass spectrometry (Fan et al. 2013; Mielke et al. 2014). Especially measuring patient-derived CSF can be a powerful and credible source to reveal pathological changes in the brain. The linkage between brain and CSF allows access to the brain. Even in plasma samples a changed lipid metabolism is detectable, in patients carrying pathogenic variants in the *GBA* gene, resulting in either Gaucher disease or Parkinson's disease. Glucosylceramide levels were increased in patient-derived plasma samples from *GBA1*-deficient patients (Groener et al. 2008; Mielke et al. 2013).

Six hexosylceramide species were measured in patient-derived plasma and CSF samples (Fig. 13). In CSF, two out of six measured hexosylceramide species were significantly elevated (HexCer: d18:1 / 18:0 and d18:1 / 20:0). These species consist of a sphingosine backbone N-acylated to a fatty acid comprising C18 and C20 carbon chains (Fig. 13).

In patient-derived plasma samples one hexosylceramide species was elevated (d18:1 / 18:0), containing a C18 carbon chain length fatty acid N-linked to the sphingosine backbone. Both of these species (d18:1 / 18:0 and d18:1 / 20:0) were also elevated in iPSC-derived neurons (Fig. 12).

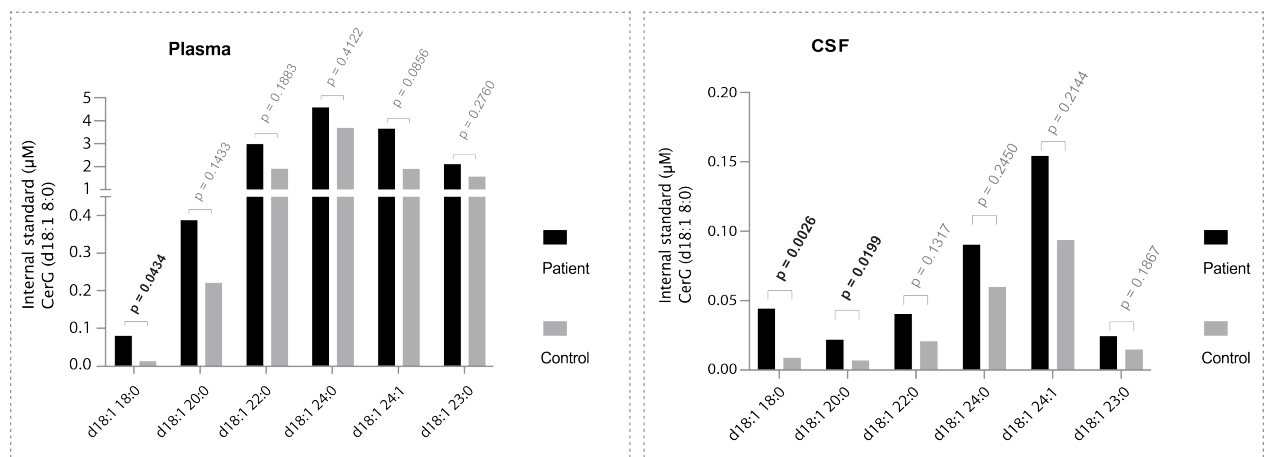


Fig. 13: Comparison of hexosylceramide levels in plasma and CSF derived from different patients carrying bi-allelic *GBA2* variants to age and sex matched healthy control samples. The average of each lipid species was set side by side. P-values (t-test) in bold indicate significant differences between patient and control samples.

Proof-of-principle treatment trials: correction of HexCer accumulation

Dysregulated lipid metabolism was shown in patient-derived neurons and in biofluids from patients with a GBA2-deficiency.

To restore lipid homeostasis in patient-derived neurons I pursued three different approaches: two patient-specific strategies, targeting the different consequences of their *GBA2* variants and one general approach of substrate reduction.

Translational read-through:

Aminoglycosides such as G418 facilitate translational read-through of premature termination codons (PTC). Distinct administration of G418 *in vitro* proved suppression of termination codons and restored expression of full length protein (Heier and DiDonato 2009; Azimov et al. 2008; Howard, Frizzell, and Bedwell 1996).

Patient-derived neurons carrying a premature stop codon variant in exon 4 (P2.2) were treated with aminoglycoside G418 for three days before cell lysis and lipid mass spectrometry analysis.

Proper protein folding by chaperon induction:

Heat shock proteins play an important role in proper protein folding and protein homeostasis. This cytoprotective aspect is an emerging therapeutic approach to induce a heat shock response by the use of small molecules (Kalmar, Lu, and Greensmith 2014; Fog et al. 2018; Kirkegaard et al. 2016).

Arimoclomol is a heat shock protein amplifier and currently tested in clinical trials for Amyotrophic Lateral Sclerosis (clinicaltrials.gov identifier: NCT03836716, phase 3), Inclusion Body Myositis (clinicaltrials.gov identifier: NCT04049097, phase 3), Niemann-Pick Disease, Type C (clinicaltrials.gov identifier: NCT02612129, phase 2/3) and Gaucher disease (type 1 and type 3) (clinicaltrials.gov identifier: NCT03746587, phase 2).

We detected GBA2 protein in WB (Fig. 8), but no residual enzymatic activity (Fig. 10 A) in iPSC-derived neurons from the patient (P1.1) carrying the compound heterozygous variants in the *GBA2* gene.

Due to the existing protein with lacking enzyme activity the hypothesis was, that supporting proper folding by induction of a heat shock response could restore enzymatic activity of the remaining GBA2 enzyme. To test this treatment opportunity, we cultured our iPSC-derived neurons (P1.1) in the presence of the heat shock protein co-inducer Arimoclomol for seven days. Subsequently we determine the lipid profile via mass spectrometry.

Substrate reduction:

Accumulation of toxic metabolites is a common characteristic for inborn errors of metabolism. One unifying theme over these various diseases is the treatment approach to alleviate the burden of toxic metabolites via substrate reduction (Yue, Mackinnon, and Bezerra 2019).

One prominent example for substrate reduction therapy (SRT) is the inhibition of glucosylceramide synthase (GCS) (EC 2.4.1.80). Both glucosylceramide synthase inhibitors, Miglustat and Eliglustat, are an approved treatment for Gaucher disease (Bennett and Turcotte 2015; Aerts et al. 2006).

GBA1 and GBA2 share the same enzymatic function and furthermore, we detected increased hexosylceramide levels in patient-derived neurons and biofluids. Thus, STR outlines a treatment opportunity for both patient-derived neurons; since it is independent of the genomic variants each patient is carrying. Cells were cultured for four days with the glucosylceramide synthase inhibitor Miglustat, before analyzed by lipid mass spectrometry.

Outcome:

Patient-derived neurons harboring a PTC in exon 4 showed no reduction of hexosylceramides under the treatment with aminoglycoside G418 (Fig. 14 A). In addition, there was no obvious effect related to the level of ceramide with G418 treatment (Fig. 14 B).

The treatment approach using the heat shock response amplifier Arimoclomol did not reduce hexosylceramide levels compared to the vehicle in Patient 2.2 (Fig. 14 A). Ceramide levels of treated cells and vehicle control are both increased, most likely due to the induction of a general heat shock response rather a specific effect.

The approach of substrate reduction leads to decreased hexosylceramides levels in both patient-derived neurons (P1.1 and P2.2) (Fig. 14 A). Miglustat, a glucosylceramide synthase inhibitor, blocks the glycosylation of ceramide, resulting in a reduction of measured hexosylceramides and an increase of ceramide levels in all patient-derived cells (Fig. 14 B).

Substrate reduction therapy is one treatment option to decrease GlcCer levels in Gaucher disease type I patients (Ficicioglu 2008; Hollak et al. 2009; Giraldo et al. 2009). Using the same strategy of substrate reduction in patients with a GBA2-deficiency, I reduced the burden of hexosylceramide in iPSC-derived neurons. By blocking the GCS, the amount of accumulating substrate is reduced and at the same time ceramide levels are increasing, due to the inhibition of the biosynthesis step from ceramide to GlcCer. This could create a treatment opportunity for patients with a GBA2-deficiency.

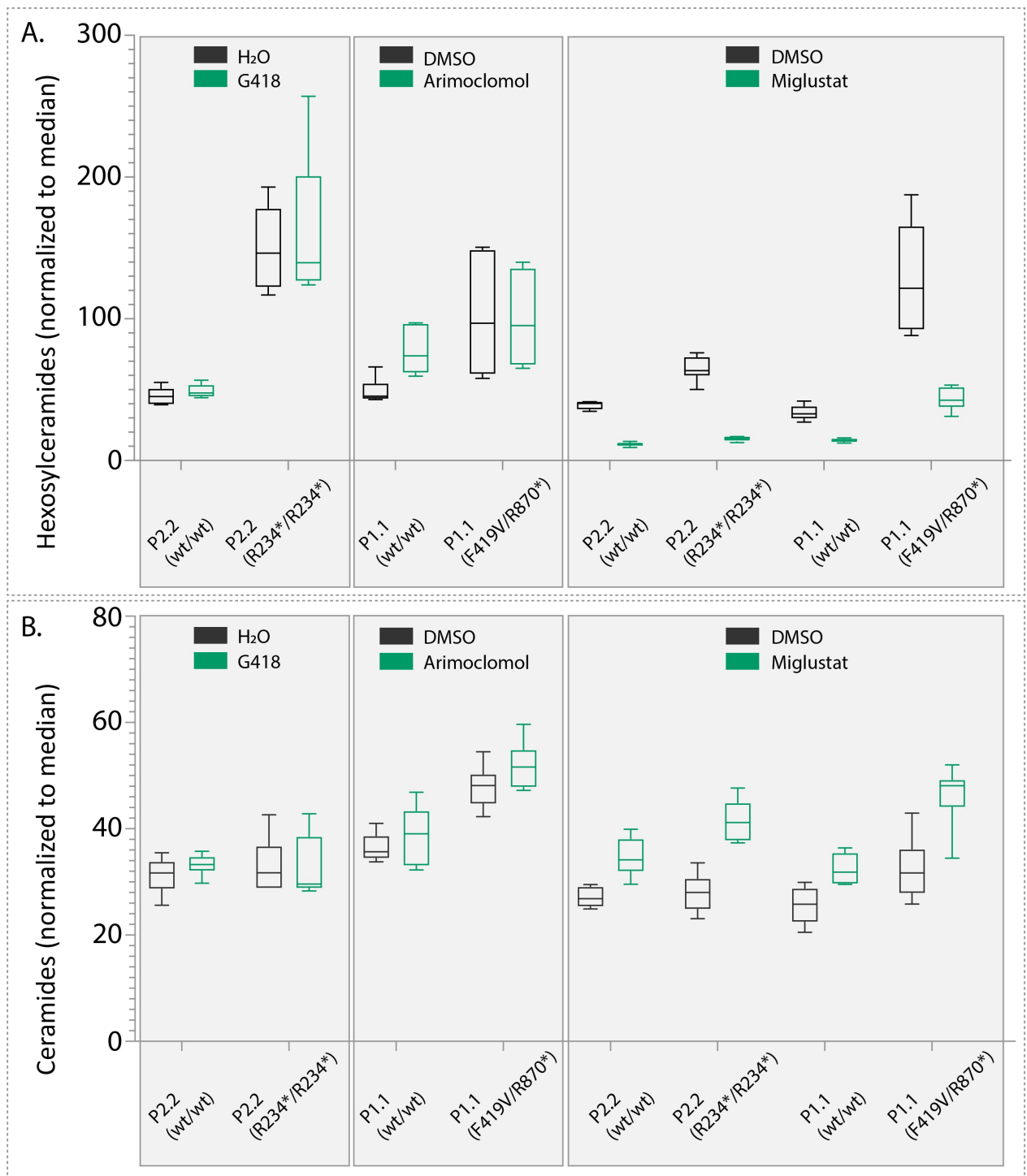


Fig. 14: Lipid mass spectrometry analysis of three independent treatment approaches in cortical neurons with G418, an aminoglycoside for translational read-through; Arimoclomol, as a co-inducer for the heat shock response and Miglustat, as substrate reduction treatment. A) Evaluation of Hexosylceramide levels in patient-derived neurons and their isogenic controls. B) Comparison of Ceramide levels in patient-derived neurons and their isogenic controls.

Discussion

iPSC generation, validation and cortical differentiation

Since 2006, the year Yamanaka and colleagues reprogrammed the first iPS cells, huge advancements were made to improve reprogramming efficiency, applicability and genomic integrity.

Continuous development of reprogramming methods has advanced the technique. Starting from the first application using integrating viruses (retroviral or lentiviral vectors) to non-integrating delivery system, such as episomal vectors, RNA-based techniques and non-integrating viruses (Adeno viruses and Sendai viruses) (Bellin et al. 2012; Cappella, Elouej, and Biferi 2021). Avoiding unintentional vector integrations prepared the basis to use iPSCs in cell-therapeutic applications.

Based on the purpose and research focus a suited strategy for reprogramming should be chosen.

We reprogrammed human fibroblasts by electroporation of episomal vectors. This is a cost-effective and well-described method to introduce the Yamanaka factors into the fibroblasts (Okita et al. 2011; Nagel et al. 2019). With this method we were able to reprogram iPS cells from all patient-derived fibroblast lines planned for this project (Tab. 15). For our model system, it was sufficient enough to exclude unintentional plasmid integrations via PCR.

All generated lines passed our self-imposed validation criteria for iPS cells. The first assessment was morphology-based and a simple but common ALP staining. This preliminary and soft evaluation of morphological and immunohistochemical characteristics, helped to make the first selection of cells to analyze in more detail. The more strict criteria to confirm iPS cells were demonstrated by the immunohistochemical staining of pluripotency markers and the differentiation potential in cells of all three germ layers (mesodermal, endodermal and ectodermal) (Fig. 6). Genomic integrity was shown by a SNP assay in comparison with the corresponding parental line (Fig. 6). If a cell line showed an increased growth rate compared to the other cells, the chances to fail in the SNP analysis were increased. Therefore a well considered cell selection in the early passages facilitated the later outcome. Genomic instability is always discussed in the iPS cell field and raises concerns regarding the application in regenerative medicine. In summary, the reprogramming method, process and all verification criteria should always be considered in relation towards their later application. For our application of iPSC as a disease model, we evaluated our generated cells diligently (Nagel et al. 2019). To examine a neurodegenerative disease, the importance of a suitable model system is indispensable, hence various published protocols are available. These protocols allow to differentiate iPSC towards distinctive neuronal cell types e.g. tyrosine hydroxylase positive neurons, motor neurons or cortical neurons (Maury et al. 2014; Reinhardt et al. 2013; Yichen Shi et al. 2012; Rehbach et al. 2019; Kriks et al. 2011; Schöls et al. 2017).

For modeling hereditary spastic paraplegia forebrain neurons, telencephalic glutamatergic neurons (cortical projection neurons) and cortical neurons positive for cortical layer V and VI (CTP2 and TBR1, respectively) are described (Zhu et al. 2014; Havlicek et al. 2014; Rehbach et al. 2019; Denton et al. 2016; Peotter et al. 2022). I used a differentiation protocol to obtain cortical neurons mainly positive for markers for layer V and layer VI. This differentiation process is robust with comparable outcome providing an essential consistency in all experiments.

GBA2 disease modeling using iPSC

In this thesis, I studied GBA2-deficiency the first time in iPSC-derived cortical neurons from two independent HSP type 46 patients. Loss of GBA2 activity has been studied previously in peripheral tissue of patients, cell models and animal models. Readily accessible patient tissue are lymphocytes. There are two studies of patient-derived lymphoblastoid cells (Martin et al. 2013; Malekkou et al. 2018). These cells have the advantage to originate from SPG46 patients and are facile to sample, however lymphocytes are not the affected tissue nor have the metabolic and structural requirements as the disease-involved neuronal cell types. To recapitulate GBA2-deficiency in previous studies, cell culture models of HAP1 cells and HEK-293 cells were utilized (Schonauer et al. 2017). These artificial cell lines are prone to genetic instability, display chromosomal aberrations and do not resemble the affected neuronal tissue (Duesberg and McCormack 2013; Frattini et al. 2015; Stepanenko and Dmitrenko 2015; Thompson and Compton 2011). The approach to reprogram easy accessible tissue, such as patient-derived fibroblasts, towards iPSC overcame this obstacle since iPSC cells can be differentiated in a second step towards neuronal cells.

In addition, more complex model systems (mouse and zebrafish) were used to assess the physiological interaction caused by bi-allelic variants in the *GBA2* gene.

The zebrafish model was used to demonstrate the pathology caused by variants in the *GBA2* gene. Knock down of *GBA2* ortholog resulted in abnormal motor behavior and was rescued by wild-type human *GBA2* mRNA (Martin et al. 2013). Mouse models allow studying the impact of known pathogenic human variants in a physiological condition, but they reach their limitations, if these genetic changes do not provoke the same phenotype as in human. *GBA2* KO mice display no neurological symptoms (Yildiz et al. 2006) or some inconsistent variety in the Catwalk test (Woeste, Stern, Raju, et al. 2019). However no reliable phenotype resembling the human phenotype was found in mice by today.

Despite the availability of mouse brain tissue, the structure of the corticospinal tract differs in mouse and human, limits the application to model a motor neuron disease (Martin et al. 2013).

For this reason I established iPSC-derived cortical neurons from HSP patients carrying different pathogenic, bi-allelic variants within the *GBA2* gene.

iPSC-derived disease models and isogenic controls

To work with high quality control cells, we generated isogenic control lines for two independent patient cell lines carrying pathogenic, bi-allelic *GBA2* variants; one male (P1.1) and one female (P2.2) cell line. For rare diseases, isogenic controls are crucial, since only a limited number of patients are accessible. With this strategy we can control the genetic background variability among each individual. This inter-individual variety is clearly visibly in the enzymatic activity of GBA1 and GBA2 measurements. Enzymatic activity of GBA2 varies significantly between the isogenic controls and the healthy wild-type control (Fig. 10A). This variability of enzymatic activity between healthy controls was also seen previously (Malekkou et al. 2018).

Although the commonly used GBA1 and GBA2 enzyme assays lack a bit of robustness, if you have a closer look on the standard derivations in many of these assays (Fig. 9, Fig. 10.) (Schonauer et al. 2017), we used the enzyme assay as a proof of principal experiment to verify our isogenic controls

with the expectation of significant changes in GBA2 activity after correcting pathogenic variants in the *GBA2* gene. We expected wild-type levels of GBA2 activity in the isogenic controls and a 50% reduction from the wild-type levels in heterozygous corrected lines. For this purpose, the GBA1 and GBA2 enzyme assay performs stable enough to validate our engineered cell lines (Fig. 8).

These isogenic controls enable us to study the consequences of *GBA2*-variants in patient-derived cells and their corresponding controls harboring the same genetic background. This approach is increasingly used to reveal underlying pathomechanism of different diseases (Schöndorf et al. 2014; Zaslavsky et al. 2019). Although gene-editing methods are improving continuously, the efficiency to correct specific variants or introduce specific changes is still challenging (Tab. 14). However pathophysiological differences could remain unrecognized due to the genetic background of distinctive individuals, which highlights the importance of preserving the patient-specific genetic background (Yanhong Shi et al. 2017). Taking the low editing efficiency into account, this emphasizes the value of these genetic controls even more, but at the same time pointing out, that this process is labor-intensive. Advances in delivery and assembly of these gene-editing tools have been made, nevertheless challenges remain. Not only the success rate of each transfection, but mainly the HDR rate limits the efficiency of editing cells (Khalil 2020; Richardson et al. 2016).

To assess our generated model systems in the context of a potential regulatory feedback loop between GBA1 and GBA2, we compared our genetic and chemical deficiency models.

The literature regarding the interaction and crosstalk between GBA1 and GBA2 are conflicting. There is a broad consensus that loss of GBA2 activity has no influence on GBA1 activity (Körschen et al. 2013; Schonauer et al. 2017; Aureli et al. 2013) (Tab. 17). Except, Malekkou and colleagues found a compensatory mechanism in patient-derived lymphoblastoid cells where GBA2 activity was abolished. They found increased GBA1 activity in cell lysates and at the plasma membrane accompanied with increased GBA1 protein but unchanged levels of GBA1 mRNA (Malekkou et al. 2018). In contrast to that, no compensation for GBA2-deficiency was found in most publications, studying different cell types, comprising HAP1 and HEK293 cells (Schonauer et al. 2017), lymphoblast cells (Martin et al. 2013) and a GBA2 KO mouse model (Körschen et al. 2013; Woeste, Stern, Raju, et al. 2019). I could confirm that loss of GBA2 in cortical neurons did not affect GBA1 activity (Fig. 10), by the use of a genetic and pharmacological approach to monitor GBA1 activity after loss of GBA2 activity. The chemical inhibition using AMP-DNM reduced GBA2 activity almost completely to the same level of patient-derived cells harboring bi-allelic *GBA2* variants. In both conditions GBA1 activity was not changed compared to wild-type GBA2 activity in cortical neurons (Fig. 10). Especially if we compare patient-derived cells to their respective isogenic control, we could not measure significant changes in GBA1 activity, highlighting the importance of a controlled genetic background. In accordance, one study showed, that also overexpression of wild-type GBA2 in SH-SY5Y cells does not affect GBA1 activity (Aureli et al. 2013).

The influence of GBA1-deficiency towards GBA2 activity is more contradictory.

Some studies describe a compensatory effect of GBA2, resulting in an increase of GBA2 activity, mRNA and protein in GBA1-deficient models. In fibroblasts of *GBA* $-/-$ mice an increase of *Gba2* mRNA and GBA2 protein expression was measured (Yildiz et al. 2013). In addition Burke *et al.* compared GBA2 activity in GBA1-deficient mouse brains as well as in leucocytes derived from Gaucher-diseased patients to respective controls. In mouse brains, GBA2 activity was significantly increased in comparison to wild-type mice. Gaucher patient-derived leucocytes displayed a less consistent pattern of GBA2 activity. In 5 out of 13 samples GBA2 activity was increased compared to

healthy control donors. Although GBA2 activity was very variable in these patients (Burke et al. 2013). In accordance with the results reported by Yildiz and – albeit less consistently – Burke et al., Aureli and colleagues detected an increased GBA2 activity in cell lysates and at the plasma membrane of patient-derived fibroblasts including all three types of Gaucher disease (Aureli, Bassi, et al. 2012).

In contrast, a decreased GBA2 activity was measured in human iPSC-derived dopaminergic neurons from Gaucher patients and heterozygous *GBA* variant carriers with PD (Schöndorf et al. 2014). The consequences due to a chemical or a genetic loss of GBA1 were elaborated by Dagmar Wachten's group in various tissues and cell types including: fibroblasts (bi-allelic *GBA* variant carriers from Gaucher disease patients and chemically inhibited GBA1), HAP1 and HEK cells, as well as mouse fibroblasts and brain lysates. In all cell types with a GBA1-deficiency, they observed a decreased GBA2 activity (Schonauer et al. 2017; Körschen et al. 2013).

None of the studies reported here, except Schöndorf and colleagues (Schöndorf et al. 2014), used isogenic controls; results are therefore hampered by the large inter-individual variability of GBA2 activity that others and I observed (Malekkou et al. 2018; Burke et al. 2013). One study analyzed human post mortem brain tissue, in these tissue samples of PD-GBA1 patients GBA2 activity was not significantly affected (Gegg et al. 2012). Hence, I used the generated model system to investigate a possible cross-talk between GBA1 and GBA2 activity.

Accordingly, I analyzed the effect of GBA1-deficiency in iPSC-derived cortical neurons from GD patients and healthy controls with chemical GBA2 inhibition using AMP-DNM. In both conditions I could not detect a cross-regulation between GBA1 and GBA2. I measured variations in GBA2 activity between both Gaucher patients: the patient harboring the pathogenic c.667 T > C p.(W223R) / c.1226A > G p.(N409S) variants displayed around 20% residual GBA1 activity (Fig. 11B), whereas in the patient with the pathogenic, bi-allelic c. 1448T>C p.(L483P) variant barely no GBA1 activity was detectable. On that account we rather would expect a cross-regulation if no residual GBA1 activity is detectable (Tab. 18). Thus I would explain these differences as inter-individual GBA2 activity, these varying GBA2 activities were already detected between control cells (Fig. 10) (Malekkou et al. 2018; Burke et al. 2013).

Little is known about the consequences of GBA2-deficiency and the implications on the lipid metabolism, despite the increase of GlcCer levels (Raju et al. 2015; Woeste, Stern, Diana Raju, et al. 2019; Yildiz et al. 2006; Malekkou et al. 2018).

Hexosylceramides play a pivotal role in sphingolipid metabolism and display the building block for more complex GSL. HexCer are glycosylated (glucose or galactose) ceramides. Ceramide is a crucial lipid in sphingolipid metabolism and is composed of a sphingoid base N-acylated to a fatty acid.

These sphingoid bases can vary in chain length, number of hydroxylation and double bonds. These HexCer species can be classified regarding their double bond in the sphingoid base as dihydro-monohexosylceramide and monohexosylceramide (Kitatani, Idkowiak-Baldys, and Hannun 2008; Merrill 2011).

Furthermore, the N-linked fatty acid can vary in the length of the alkyl chain and their double bonds. In mammals the length of the acylated fatty acid depends on the CerS. The family of CerS comprises six enzymes, specialized for different fatty Acyl-Co-enzymes A. The predominant CerS in neurons is CerS1, adding mainly C18 Acyl-Co-enzymes A to the sphingoid base (Ben-David and Futerman 2010; Spassieva et al. 2016).

Most studies on defective GBA2 function and resulting consequences were performed in mice. These experiments focused on the globozoospermia phenotype, demonstrating increased C16 GlcCer levels (Yildiz et al. 2006; Raju et al. 2015). In one mouse study GBA2 KO mice displayed increased d18 / 10:0 HexCer levels compared to controls (Woeste, Stern, Raju, et al. 2019). In a human model of a transformed lymphoblastoid cell line, C16 GlcCer was the most substantial species, but yet all species were increased in the GBA2-deficient cell line (Malekkou et al. 2018). While in the brain C18 GlcCer species are the most abundant (Levy and Futerman 2010), these species are the most interesting lipids to investigate in the context of GBA2-deficiency in HSP type 46. These HexCer species with C18 fatty acids are increased (d18.0 / 18.0 and d18.1 / 18.0) in iPSC-neurons from GBA2 patients and belong into the group of dihydro-mono-hexosylceramide and mono-hexosylceramide (Fig. 12). Since Galactosylceramide and glucosylceramide are indistinguishable with classical lipid mass spectrometry both are analyzed combined as hexosylceramides (Reza, Ugorski, and Suchański 2021). Galactosylceramide is highly abundant in the brain; hence this lipid will be measured as well in our approach. Previous thin layer chromatography studies on mouse brain, showed that GBA2-deficiency increases GlcCer but not galactosylceramide (Yildiz et al. 2013). In addition, this emphasizes again the value of our GBA2-deficient cell model in combination with their respective isogenic controls. All differences we measured can be traced back to the absence or presence of a functional GBA2 enzyme.

Three lipids species were significantly reduced ($p < 0.05$); two species of sphingomyelin and a ceramide species (Fig. 12). Sphingomyelin is synthesized at the Golgi and the plasma membrane and is the most abundant complex sphingolipid in mammalian cells (Merrill 2011; Chakraborty and Jiang 2013; Adada, Luberto, and Canals 2016). Ceramide is a key lipid in sphingolipid metabolism and a precursor for complex sphingolipids. Apart from this, ceramide itself is a bioactive lipid and plays a pivotal role in regulating cellular processes (Stith, Velazquez, and Obeid 2019; Merrill 2011; Gault, Obeid, and Hannun 2010). Species of these three important sphingolipids, HexCer, sphingomyelin and ceramide, are dysregulated in neurons from patients of SPG type 46. Imbalances of these sphingolipids can cause serious consequences since they are the basis for complex GSL.

To set our results in an even more biological relevant context, we compared HexCer species in biofluids (CSF and plasma) from patients carrying pathogenic, bi-allelic *GBA2* variants, including the same patients used for reprogramming GBA2-deficient iPSC (Tab. 20), allowing a direct comparison between generated cell lines and patient-derived biofluids.

In previous lipidomics studies patient-derived biofluids were measured and changes of sphingolipid levels in plasma and CSF samples of Niemann-Pick Disease, Type C and Alzheimer patients were revealed (Fan et al., 2013; Mielke et al., 2014). Elevated glucosylceramide levels were found in plasma or CSF samples of patients carrying *GBA* variants causing either Gaucher disease or Parkinson's disease (Mielke et al. 2013; Groener et al. 2008; Huh et al. 2021). These studies demonstrate the biological relevance of biofluids; especially CSF samples allow insights into the metabolism in the brain.

HexCer species in biofluids were measured and compared to HexCer species in iPSC-derived neurons. Hexosylceramide species with a N-acyl sphingosine backbone linked to a fatty acid with a carbon chain length of C18 are significantly elevated in plasma and CSF samples. These HexCer species were also significantly up-regulated in neurons differentiated from patient-derived iPSC, with a defective GBA2 enzyme (Fig. 12, Fig. 13)

CerS1 and CerS4 synthesize these HexCer species containing a sphingosine backbone N-linked to fatty acids with a carbon chain of C18. CerS1 is highly expressed in brain tissue, underlining the biological relevance of iPSC-derived neurons as a disease model (Laviad et al. 2007; Ben-David and Futerman 2010; Levy and Futerman 2010). These iPSC-derived model systems could serve as an option to test new compounds on disease-relevant tissues.

Using this cellular model system, I tested three different compounds in patient-derived cortical neurons with the aim to reduce the HexCer burden to a comparable level of HexCer as measured in isogenic controls. This proof of principle study to decrease HexCer levels in iPSC-derived neurons showed no success in reducing HexCer for variant-specific treatment approaches but revealed HexCer reduction for both patients applying a known treatment (Miglustat) to treat Gaucher disease.

It has been known for a long time that aminoglycosides such as G418 facilitate translational read-through. Many studies have proven, that G418 can lead *in vivo* and *in vitro* to compound-induced translational read-through. However, these aminoglycosides demonstrate severe toxicity, especially oto- and nephrotoxicity (Dabrowski, Bukowy-Bieryllo, and Zietkiewicz 2018; Lopez-Novoa et al. 2011). The effect of the translational read-through to restore functional GBA2 enzyme in iPSC-derived cortical neurons was too weak to facilitate a degradation of GlcCer strong enough to observe an effect in HexCer via lipid mass spectrometry.

In the last few years Arimoclomol, a co-inducer of the heat-shock response emerged as a potential candidate to ameliorate diseases such as Niemann-Pick Disease, Type C, Amyotrophic Lateral Sclerosis (ALS), Inclusion Body Myositis and Gaucher disease. Several clinical trials for Arimoclomol were conducted: Niemann-Pick Disease Type C (NCT02612129); ALS (NCT03491462); Inclusion Body Myositis (NCT02753530) and Gaucher disease Type I and Type III (NCT03746587).

Heat shock proteins are molecular chaperones and promote proper protein folding to reduce cellular stress. For this reason I treated iPSC-derived neurons from P1.1 carrying a missense variant on one allele. The WB analysis of this patient displayed a faint band of residual GBA2 protein at the correct size (105kDa) but no GBA2 activity in the assay. This could be an indication of GBA2 dysfunction caused by a miss-folded GBA2 protein. The underlying concept would be to promote proper protein folding to restore proper GBA2 function and thereby alleviating the GlcCer burden. Arimoclomol treatment did not reduce HexCer levels in P1.1. Either protein folding was not enhanced or the amount of restored functional GBA2 protein was not sufficient enough to reduce a measurable amount of HexCer in patient-derived cells. Always taking into account, that we are measuring HexCer (GluCer and GalCer), a small effect in decreased GluCer could be masked by the GalCer content. A more sensitive mass spectrometry technique could discriminate between GalCer and HexCer.

The third tested compound, Miglustat, lead to a reduction in HexCer levels. Miglustat, a GlcCer synthase inhibitor, is an approved substrate reduction medication for Gaucher disease and Niemann-Pick Disease Type C. GlcCer is accumulated in HSP Type 46, hence this could be a promising treatment opportunity independent of the bi-allelic variants affecting the *GBA2* gene. HexCer levels in patient-derived cells are lowered to untreated HexCer stage of isogenic controls. In Miglustat treated isogenic control cells, HexCer levels decreased beyond the untreated isogenic controls, demonstrating that Miglustat lowering HexCer levels to a natural level and not depleting the HexCer content completely.

In parallel, Ceramide levels are increasing in all cells (patient-derived and isogenic controls) when treated with Miglustat. Respecting the biological pathway, higher ceramide levels can be explained by the inhibited synthesis of GlcCer, leaving the substrate unprocessed and therefore ceramide

accumulates in the cells. This effect is investigated primarily in cancer studies, where GCS inhibitors are studied in drug resistant cells to restore ceramide levels (Liu and Li 2013).

Miglustat is used to reduce the GlcCer burden in Gaucher disease type I since the first studies in the year 2000 (Cox et al. 2000). Eliglustat, another GCS inhibitor was developed later and is also a registered drug to treat Gaucher disease type I (Lukina et al. 2014). This medication approach of substrate reduction could be an option to reduce GlcCer in patients with a GBA2-deficiency. Despite different defective enzymes in each disease, both share the same substrate burden.

This first proof of concept study could be a first step toward treating patients with HSP type 46.

Abbreviations:

| | |
|-------------|--|
| 4MU | 4-methylumbelliferyl-b-D-glucopyranoside |
| AGC | Automatic gain control |
| AMP-DNM | N-(5-adamantane-1-yl-methoxy-pentyl)-Deoxynojirimycin |
| AP | Alkaline phosphatase |
| BSA | Bovine serum albumin |
| Cas | CRISPR-associated |
| CBE | Conduritol- β -epoxide |
| Cer | Ceramide |
| CerS | Ceramide synthase |
| CRISPR | Clustered regularly interspaced short palindromic repeat |
| crRNA | CRISPR RNA |
| CSF | Cerebrospinal fluid |
| CTiD | Clinical trial in a dish |
| CV | Coefficient of variation |
| DAI | Dai after induction |
| DSB | Double strand break |
| EB | Embryonic body |
| ER | Endoplasmic reticulum |
| FCS | Fetal calf serum |
| FGF2 | Fibroblast growth factor 2 |
| <i>GBA</i> | Lysosomal β -glucosidase gene (NM_000157.4) |
| <i>GBA1</i> | Lysosomal β -glucosidase (NP_000148) |
| <i>GBA2</i> | Non lysosomal β -glucosidase (NM_020944.3) |
| <i>GBA3</i> | Klotho-related protein |
| GCS | Glucosylceramide synthase |
| GD | Gaucher Disease |
| GlcCer | Glucosylceramide |
| GPMV | Giant plasma membrane vesicles |
| gRNA | Guide RNA |
| GSL | Glycosphingolipid |
| HDR | Homology-directed repair |
| HexCer | Hexosylceramide |
| HGVS | Human Genome Variation Society |
| HSP | Hereditary spastic paraplegia |
| Indel | Insertion or deletion |
| iPS cell | Induced pluripotent stem cell |
| iPSC | Induced pluripotent stem cell |
| KO | Knock out |
| KOSR | Knock-out serum replacement |
| MMC | Methanol: MTBE: chloroform |
| NHEJ repair | Non-homologous end joining repair |

| | |
|---------------|--|
| PAM | Protospacer adjacent motive |
| PBS | Phosphate buffered saline |
| PBS-T | PBS with 0.1% Triton X |
| PD | Parkinson's disease |
| PFA | Paraformaldehyde |
| PTC | Premature termination codon |
| RFLP | Restriction fragment length polymorphism |
| RNP | Ribonucleoprotein |
| RT | Room temperature |
| SM | Sphingomyelin |
| SNP | Single nucleotide variant |
| SPG | Spastic gait locus |
| SRT | Substrate reduction therapy |
| ssODN | Single stranded oligonucleotide |
| STR | Short tandem repeat |
| TALE | Transcription activator-like effector |
| TALEN | Transcription activator-like effector nuclease |
| TBS-T | Tris-buffered saline supplemented with 0.1% Tween 20 |
| TGF β 1 | Transforming Growth Factor Beta 1 |
| tracrRNA | Trans-activating RNA |
| WB | Western Blot |
| Wt | Wild-type |
| ZFN | Zinc finger nuclease |

Statement of contributions

In my doctoral thesis I investigated the impact of GBA2-deficiency in iPSC-derived neurons from patients with hereditary spastic paraplegia Type 46. Fibroblasts were reprogrammed towards iPSC and differentiated into cortical neurons, a disease-relevant cell type in HSP. Isogenic controls were generated using CRISPR/Cas9 and validated by WB and enzymatic activity testing. The lipid profile of patient-derived neurons was compared using lipid mass spectrometry. Hexosylceramide species were increased. These findings were validated using biofluids (Plasma and CSF) from patients carrying bi-allelic *GBA2*-variants. In a small compound treatment study, Miglustat, an approved medication for Gaucher disease, was able to reduce hexosylceramide content in patient-derived neurons.

During the doctoral thesis I was supported by:

Prof. Dr. Rebecca Schüle, as my doctoral supervisor, she was responsible for most of the funding of this project as well as the thematic cornerstones of the thesis. Rebecca Schüle and I were able to raise a smaller amount of additional funding with a grant from the Tom Wahlig Foundation.

Dr. Stefanie Schuster and Dr. Stefan Hauser, both have generated the GBA2-deficient iPS cells used in my project.

Dr. Alaa Othman from ETH Zurich, he performed lipid mass spectrometry measurements and analyzed the generated MS-data.

Alexandra Bentrup, a master student performed enzyme assay optimization experiments during her lab rotation under my supervision.

Dr. Maike Nagel, reprogrammed under my supervision GBA-deficient iPS cells and generated an isogenic control during her lab rotation and master thesis.

The reprogramming of GBA-deficient fibroblast into iPS cells from Gaucher patients resulted in a publication. Figures from this publication were used in this doctoral thesis.

Nagel, M., Reichbauer, J., Bohringer, J., Schelling, Y., Krageloh-Mann, I., Schule, R., & Ulmer, U. (2019). Generation of two iPSC lines derived from two unrelated patients with Gaucher disease. Stem Cell Res, 35, 101336. doi:10.1016/j.scr.2018.10.021

This publication was supported by:

Rebecca Schüle provided the funding.

Maike Nagel, Rebecca Schüle and I, we designed and conceptualized this project.

Maike Nagel and I carried out the experiments, analyzed, interpreted the data and drafted the manuscript.

All revised the manuscript for important intellectual content.

References

- Aasly, Jan O. 2020. "Long-Term Outcomes of Genetic Parkinson's Disease." *Journal of Movement Disorders* 13 (2): 81–96. <https://doi.org/10.14802/jmd.19080>.
- Abbar, Akram Al, Siew Ching Ngai, Nadine Nograles, Suleiman Yusuf Alhaji, and Syahril Abdullah. 2020. "Induced Pluripotent Stem Cells: Reprogramming Platforms and Applications in Cell Replacement Therapy." *BioResearch Open Access* 9 (1): 121–36. <https://doi.org/10.1089/biores.2019.0046>.
- Adada, Mohamad, Chiara Luberto, and Daniel Canals. 2016. "Inhibitors of the Sphingomyelin Cycle: Sphingomyelin Synthases and Sphingomyelinases." *Chemistry and Physics of Lipids*. Elsevier Ireland Ltd. <https://doi.org/10.1016/j.chemphyslip.2015.07.008>.
- Aerts, Johannes M.F.G., Carla E.M. Hollak, Rolf G. Boot, Johanna E.M. Groener, and Mario Maas. 2006. "Substrate Reduction Therapy of Glycosphingolipid Storage Disorders." *Journal of Inherited Metabolic Disease* 29 (2–3): 449–56. <https://doi.org/10.1007/s10545-006-0272-5>.
- Aureli, Massimo, Rosaria Bassi, Nicoletta Loberto, Stefano Regis, Alessandro Prinetti, Vanna Chigorno, Johannes M. Aerts, Rolf G. Boot, Mirella Filocamo, and Sandro Sonnino. 2012. "Cell Surface Associated Glycohydrolases in Normal and Gaucher Disease Fibroblasts." *Journal of Inherited Metabolic Disease* 35 (6): 1081–91. <https://doi.org/10.1007/s10545-012-9478-x>.
- Aureli, Massimo, Sara Grassi, Simona Prioni, Sandro Sonnino, and Alessandro Prinetti. 2015. "Lipid Membrane Domains in the Brain." *Biochimica et Biophysica Acta (BBA) - Molecular and Cell Biology of Lipids*. <https://doi.org/10.1016/j.bbalip.2015.02.001>.
- Aureli, Massimo, Angela Gritti, Rosaria Bassi, Nicoletta Loberto, Alessandra Ricca, Vanna Chigorno, Alessandro Prinetti, and Sandro Sonnino. 2012. "Plasma Membrane-Associated Glycohydrolases along Differentiation of Murine Neural Stem Cells." *Neurochemical Research* 37 (6): 1344–54. <https://doi.org/10.1007/s11064-012-0719-z>.
- Aureli, Massimo, Nicoletta Loberto, Rosaria Bassi, Anita Ferraretto, Silvia Perego, Patrizia Lanteri, Vanna Chigorno, Sandro Sonnino, and Alessandro Prinetti. 2012. "Plasma Membrane-Associated Glycohydrolases Activation by Extracellular Acidification Due to Proton Exchangers." *Neurochemical Research* 37 (6): 1296–1307. <https://doi.org/10.1007/s11064-012-0725-1>.
- Aureli, Massimo, Nicoletta Loberto, Patrizia Lanteri, Vanna Chigorno, Alessandro Prinetti, and Sandro Sonnino. 2011. "Cell Surface Sphingolipid Glycohydrolases in Neuronal Differentiation and Aging in Culture." *Journal of Neurochemistry* 116 (5): 891–99. <https://doi.org/10.1111/j.1471-4159.2010.07019.x>.
- Aureli, Massimo, Maura Samarani, Nicoletta Loberto, Rosaria Bassi, Valentina Murdica, Simona Prioni, Alessandro Prinetti, and Sandro Sonnino. 2013. "The Glycosphingolipid Hydrolases in the Central Nervous System." *Molecular Neurobiology*, 1–12. <https://doi.org/10.1007/s12035-013-8592-6>.
- Aureli, Massimo, Maura Samarani, Nicoletta Loberto, Giulia Mancini, Valentina Murdica, Chiricozzi Elena, Alessandro Prinetti, Rosaria Bassi, and Sandro Sonnino. 2016. "Current and Novel Aspects on the Non-Lysosomal β -Glucosylceramidase GBA2." *Neurochemical Research* 41 (1–2): 210–20. <https://doi.org/10.1007/s11064-015-1763-2>.
- Avenali, Micol, Fabio Blandini, and Silvia Cerri. 2020. "Glucocerebrosidase Defects as a Major Risk Factor for Parkinson's Disease." *Frontiers in Aging Neuroscience* 0 (April): 97. <https://doi.org/10.3389/FNAGI.2020.00097>.
- Azimov, Rustam, Natalia Abuladze, Pagan Sassani, Debra Newman, Liyo Kao, Weixin Liu, Nicholas Orozco, Piotr Ruchala, Alexander Pushkin, and Ira Kurtz. 2008. "G418-Mediated Ribosomal Read-through of a Nonsense Mutation Causing Autosomal Recessive Proximal Renal Tubular Acidosis." *American Journal of Physiology - Renal Physiology* 295 (3). <https://doi.org/10.1152/ajprenal.00015.2008>.
- Ban, Hiroshi, Naoki Nishishita, Noemi Fusaki, Toshiaki Tabata, Koichi Saeki, Masayuki Shikamura,

- Nozomi Takada, et al. 2011. "Efficient Generation of Transgene-Free Human Induced Pluripotent Stem Cells (iPSCs) by Temperature-Sensitive Sendai Virus Vectors." *Proceedings of the National Academy of Sciences of the United States of America* 108 (34): 14234–39. <https://doi.org/10.1073/pnas.1103509108>.
- Bellin, Milena, Maria C. Marchetto, Fred H. Gage, and Christine L. Mummery. 2012. "Induced Pluripotent Stem Cells: The New Patient?" *Nature Reviews Molecular Cell Biology* 13 (11): 713–26. <https://doi.org/10.1038/nrm3448>.
- Ben-David, Oshrit, and Anthony H. Futerman. 2010. "The Role of the Ceramide Acyl Chain Length in Neurodegeneration: Involvement of Ceramide Synthases." *NeuroMolecular Medicine* 12 (4): 341–50. <https://doi.org/10.1007/s12017-010-8114-x>.
- Bennett, Lunawati L., and Kelsey Turcotte. 2015. "Eliglustat Tartrate for the Treatment of Adults with Type 1 Gaucher Disease." *Drug Design, Development and Therapy*. Dove Medical Press Ltd. <https://doi.org/10.2147/DDDT.S77760>.
- Berrebi, A, R Wishnitzer, and U Von-der-Walde. 1984. "Gaucher's Disease: Unexpected Diagnosis in Three Patients over Seventy Years Old." *Nouvelle Revue Francaise d'hematologie* 26 (3): 201–3. <http://www.ncbi.nlm.nih.gov/pubmed/6739289>.
- Bibikova, Marina, Mary Golic, Kent G. Golic, and Dana Carroll. 2002. "Targeted Chromosomal Cleavage and Mutagenesis in Drosophila Using Zinc-Finger Nucleases." *Genetics* 161 (3): 1169–75.
- Biegstraaten, M, I N Van Schaik, J M F G Aerts, M Langeveld, M M A M Mannens, L J Bour, E Sidransky, N Tayebi, E Fitzgibbon, and C E M Hollak. 2010. "A Monozygotic Twin Pair with Highly Discordant Gaucher Phenotypes." <https://doi.org/10.1016/j.bcmed.2010.10.007>.
- Blackstone, Craig. 2018. "Converging Cellular Themes for the Hereditary Spastic Paraplegias." *Current Opinion in Neurobiology*. Elsevier Ltd. <https://doi.org/10.1016/j.conb.2018.04.025>.
- Boot, Rolf G., Marri Verhoeck, Wilma Donker-Koopman, Anneke Strijland, Jan Van Marle, Hermen S. Overkleeft, Tom Wennekes, and J. M F G Aerts. 2007. "Identification of the Non-Lysosomal Glucosylceramidase as ??-Glucosidase 2." *Journal of Biological Chemistry* 282 (2): 1305–12. <https://doi.org/10.1074/jbc.M610544200>.
- Boukhris, Amir, Imed Feki, Nizar Elleuch, Mohamed Imed Miladi, Anne Boland-Augé, Jérémy Truchetto, Emeline Mundwiller, et al. 2010. "A New Locus (SPG46) Maps to 9p21.2-Q21.12 in a Tunisian Family with a Complicated Autosomal Recessive Hereditary Spastic Paraplegia with Mental Impairment and Thin Corpus Callosum." *Neurogenetics* 11 (4): 441–48. <https://doi.org/10.1007/s10048-010-0249-2>.
- Boven, Leonie A., Marjan Van Meurs, Rolf G. Boot, Atul Mehta, Louis Boon, Johannes M. Aerts, and Jon D. Laman. 2004. "Gaucher Cells Demonstrate a Distinct Macrophage Phenotype and Resemble Alternatively Activated Macrophages." *American Journal of Clinical Pathology* 122 (3): 359–69. <https://doi.org/10.1309/BG5VA8JRDQH1M7HN>.
- Brady, Roscoe O, Julian Kanfer, and David Shapiro. 1965. "The Metabolism of Glucocerebrosides I. PURIFICATION AND PROPERTIES OF A GLUCOCEREBROSIDE-CLEAVING ENZYME FROM SPLEEN TISSUE." *THE JOURNAL OF BIOLOGICAL CHEMISTRY*. Vol. 240. <http://www.jbc.org/>.
- Burke, Derek G., Ahad A. Rahim, Simon N. Waddington, Stefan Karlsson, Ida Enquist, Kailash Bhatia, Atul Mehta, Ashok Vellodi, and Simon Heales. 2013. "Increased Glucocerebrosidase (GBA) 2 Activity in GBA1 Deficient Mice Brains and in Gaucher Leucocytes." *Journal of Inherited Metabolic Disease* 36 (5): 869–72. <https://doi.org/10.1007/s10545-012-9561-3>.
- Cajka, Tomas, and Oliver Fiehn. 2016. "Increasing Lipidomic Coverage by Selecting Optimal Mobile-Phase Modifiers in LC–MS of Blood Plasma." *Metabolomics* 12 (2): 1–11. <https://doi.org/10.1007/s11306-015-0929-x>.
- Cappella, Marisa, Sahar Elouej, and Maria Grazia Biferi. 2021. "The Potential of Induced Pluripotent Stem Cells to Test Gene Therapy Approaches for Neuromuscular and Motor Neuron Disorders." *Frontiers in Cell and Developmental Biology* 9 (April): 1–12. <https://doi.org/10.3389/fcell.2021.662837>.
- Carpentier, Arnaud, Abeba Tesfaye, Virginia Chu, Ila Nimgaonkar, Fang Zhang, Seung Bum Lee, Snorri S. Thorgeirsson, Stephen M. Feinstone, and T. Jake Liang. 2014. "Engrafted Human Stem Cell-

- Derived Hepatocytes Establish an Infectious HCV Murine Model." *Journal of Clinical Investigation* 124 (11): 4953–64. <https://doi.org/10.1172/JCI75456>.
- Cermak, Tomas, Erin L Doyle, Michelle Christian, Li Wang, Yong Zhang, Clarice Schmidt, Joshua A Baller, Nikunj V Somia, Adam J Bogdanove, and Daniel F Voytas. 2011. "Efficient Design and Assembly of Custom TALEN and Other TAL Effector-Based Constructs for DNA Targeting." *Nucleic Acids Research* 39 (12): e82. <https://doi.org/10.1093/nar/gkr218>.
- Chakraborty, Mahua, and Xian-Cheng Jiang. 2013. "Lipid-Mediated Protein Signaling." *Advances in Experimental Medicine and Biology* 991: 1–14. <https://doi.org/10.1007/978-94-007-6331-9>.
- Citterio, Andrea, Alessia Arnoldi, Elena Panzeri, Maria Grazia D'Angelo, Massimiliano Filosto, Robertino Dilena, Filippo Arrigoni, et al. 2014. "Mutations in CYP2U1, DDHD2 and GBA2 Genes Are Rare Causes of Complicated Forms of Hereditary Spastic Paraparesis." *Journal of Neurology* 261 (2): 373–81. <https://doi.org/10.1007/s00415-013-7206-6>.
- Coarelli, Giulia, Silvia Romano, Lorena Travaglini, Michela Ferraldeschi, Francesco Nicita, Maria Spadaro, Arianna Fornasiero, et al. 2018. "Novel Homozygous GBA2 Mutation in a Patient with Complicated Spastic Paraplegia." *Clinical Neurology and Neurosurgery* 168 (May): 60–63. <https://doi.org/10.1016/j.clineuro.2018.02.042>.
- Cong, Le, F Ann Ran, David Cox, Shuailiang Lin, Robert Barretto, Patrick D Hsu, Xuebing Wu, Wenyan Jiang, and Luciano a Marraffini. 2013. "Multiplex Genome Engineering Using CRISPR/Cas Systems." *Science (New York, N.Y.)* 339 (6121): 819–23. <https://doi.org/10.1126/science.1231143.Multiplex>.
- Cox, Timothy, Robin Lachmann, Carla Hollak, Johannes Aerts, Sonja Van Weely, Martin Hrebíček, Frances Platt, et al. 2000. "Novel Oral Treatment of Gaucher's Disease with N-Butyldeoxyinosimycin (OGT 918) to Decrease Substrate Biosynthesis." *Lancet* 355 (9214): 1481–85. [https://doi.org/10.1016/S0140-6736\(00\)02161-9](https://doi.org/10.1016/S0140-6736(00)02161-9).
- Cyranoski, David. 2014. "Japanese Woman Is First Recipient of Next-Generation Stem Cells." *Nature*, no. September. <https://doi.org/10.1038/nature.2014.15915>.
- Dabrowski, Maciej, Zuzanna Bukowy-Bieryllo, and Ewa Zietkiewicz. 2018. "Advances in Therapeutic Use of a Drug-Stimulated Translational Readthrough of Premature Termination Codons." *Molecular Medicine* 24 (1). <https://doi.org/10.1186/s10020-018-0024-7>.
- Dekker, Nick, Tineke Voorn-Brouwer, Marri Verhoek, Tom Wennekes, Ravi S. Narayan, Dave Speijer, Carla E.M. Hollak, Hermen S. Overkleeft, Rolf G. Boot, and Johannes M.F.G. Aerts. 2011. "The Cytosolic β -Glucosidase GBA3 Does Not Influence Type 1 Gaucher Disease Manifestation." *Blood Cells, Molecules, and Diseases* 46 (1): 19–26. <https://doi.org/10.1016/j.bcmd.2010.07.009>.
- Denton, Kyle R, Chongchong Xu, Harsh Shah, and Xue-Jun Li. 2016. "Modeling Axonal Defects in Hereditary Spastic Paraplegia with Human Pluripotent Stem Cells." *Frontiers in Biology* 11 (5): 339–54. <https://doi.org/10.1007/s11515-016-1416-0>.
- Dimitriou, Evangelia, Marina Moraitou, Mónica Cozar, Jenny Serra-Vinardell, Lluís Vilageliu, Daniel Grinberg, Irene Mavridou, and Helen Michelakakis. 2020. "Gaucher Disease: Biochemical and Molecular Findings in 141 Patients Diagnosed in Greece." *Molecular Genetics and Metabolism Reports* 24 (March): 1–6. <https://doi.org/10.1016/j.ymgmr.2020.100614>.
- Dodge, James C., Christopher M. Treleaven, Joshua Pacheco, Samantha Cooper, Channa Bao, Marissa Abraham, Mandy Cromwell, et al. 2015. "Glycosphingolipids Are Modulators of Disease Pathogenesis in Amyotrophic Lateral Sclerosis." *Proceedings of the National Academy of Sciences of the United States of America* 112 (26): 8100–8105. <https://doi.org/10.1073/pnas.1508767112>.
- Duesberg, Peter, and Amanda McCormack. 2013. "Immortality of Cancers." *Cell Cycle* 12 (5): 783–802. <https://doi.org/10.4161/cc.23720>.
- Enquist, Ida Berglin, Christophe Lo Bianco, Andreas Ooka, Eva Nilsson, Jan Eric Månsson, Mats Ehinger, Johan Richter, Roscoe O. Brady, Deniz Kirik, and Stefan Karlsson. 2007. "Murine Models of Acute Neuronopathic Gaucher Disease." *Proceedings of the National Academy of Sciences of the United States of America* 104 (44): 17483–88. <https://doi.org/10.1073/pnas.0708086104>.
- Erfanian Omidvar, Maryam, Shahram Torkamandi, Somaye Rezaei, Behnam Alipoor, Mir Davood

- Omrani, Hossein Darvish, and Hamid Ghaedi. 2019. "Genotype–Phenotype Associations in Hereditary Spastic Paraplegia: A Systematic Review and Meta-Analysis on 13,570 Patients." *Journal of Neurology*, November. <https://doi.org/10.1007/s00415-019-09633-1>.
- Esvelt, Kevin M., Prashant Mali, Jonathan L. Braff, Mark Moosburner, Stephanie J. Young, and George M. Church. 2013. "Orthogonal Cas9 Proteins for RNA-Guided Gene Regulation and Editing." *Nature Methods* 10 (11): 1116–23. <https://doi.org/10.1038/nmeth.2681>.
- Fan, Martin, Rohini Sidhu, Hideji Fujiwara, Brett Tortelli, Jessie Zhang, Cristin Davidson, Steven U Walkley, et al. 2013. "Identification of Niemann-Pick C1 Disease Biomarkers through Sphingolipid Profiling." *Journal of Lipid Research* 54 (10): 2800–2814. <https://doi.org/10.1194/jlr.M040618>.
- Ficiocioglu, Can. 2008. "Review of Miglustat for Clinical Management in Gaucher Disease Type I." *Therapeutics and Clinical Risk Management*. Dove Press. <https://doi.org/10.2147/tcrm.s6865>.
- Fog, Cathrine K., Paola Zago, Erika Malini, Lukasz M. Solanko, Paolo Peruzzo, Claus Bornaes, Raffaella Magnoni, et al. 2018. "The Heat Shock Protein Amplifier Arimoclomol Improves Refolding, Maturation and Lysosomal Activity of Glucocerebrosidase." *EBioMedicine* 38 (December): 142–53. <https://doi.org/10.1016/j.ebiom.2018.11.037>.
- Frattini, Annalisa, Marco Fabbri, Roberto Valli, Elena De Paoli, Giuseppe Montalbano, Laura Gribaldo, Francesco Pasquali, and Emanuela Maserati. 2015. "High Variability of Genomic Instability and Gene Expression Profiling in Different HeLa Clones." *Scientific Reports* 5 (1): 1–9. <https://doi.org/10.1038/srep15377>.
- Fusaki, Noemi, Akiyo Nishiyama, Koichi Saeki, and Mamoru Hasegawa. 2009. "Efficient Induction of Transgene-Free Human Pluripotent Stem Cells Using a Vector Based on Sendai Virus, an RNA Virus That Does Not Integrate into the Host Genome." *Proc. Jpn. Acad., Ser. B* 85. <https://doi.org/10.2183/pjab.85.348>.
- Gaj, Thomas, Charles A Gersbach, and Carlos F Barbas. 2013. "ZFN, TALEN, and CRISPR/Cas-Based Methods for Genome Engineering." *Trends in Biotechnology* 31 (7): 397–405. <https://doi.org/10.1016/j.tibtech.2013.04.004>.
- Galvagnion, Cline, Frederik Ravnkilde Marlet, Silvia Cerri, Anthony H.V. Schapira, Fabio Blandini, and Donato A. Di Monte. 2022. "Sphingolipid Changes in Parkinson L444P GBA Mutation Fibroblasts Promote α -Synuclein Aggregation." *Brain* 145 (3): 1038–51. <https://doi.org/10.1093/brain/awab371>.
- Garcia-Cazorla, Àngels, Fanny Mochel, Foudil Lamari, and Jean-Marie Saudubray. 2014. "The Clinical Spectrum of Inherited Diseases Involved in the Synthesis and Remodeling of Complex Lipids. A Tentative Overview." *Journal of Inherited Metabolic Disease* 38 (1): 19–40. <https://doi.org/10.1007/s10545-014-9776-6>.
- Gault, Cr, Lm Obeid, and Ya Hannun. 2010. "An Overview of Sphingolipid Metabolism: From Synthesis to Breakdown Introduction to Sphingolipid Metabolism." *Adv Exp Med Biol* 688: 1–23. <https://www.ncbi.nlm.nih.gov/pmc/articles/PMC3069696/pdf/nihms-283686.pdf>.
- Gegg, Matthew E, Derek Burke, Simon J R Heales, J Mark Cooper, John Hardy, Nicholas W Wood, and Anthony H V Schapira. 2012. "Glucocerebrosidase Deficiency in Substantia Nigra of Parkinson Disease Brains." *ANN NEUROL* 72: 455–63. <https://doi.org/10.1002/ana.23614>.
- Giraldo, Pilar, Pilar Alfonso, Koldo Atutxa, María A. Fernández-Galán, Abelardo Barez, Rafael Franco, Dora Alonso, Alejandro Martin, Paz Latre, and Miguel Pocovi. 2009. "Real-World Clinical Experience with Long-Term Miglustat Maintenance Therapy in Type 1 Gaucher Disease: The ZAGAL Project." *Haematologica* 94 (12): 1771–75. <https://doi.org/10.3324/HAEMATOL.2009.008078>.
- Giudice, Temistocle Lo, Federica Lombardi, Filippo Maria Santorelli, Toshitaka Kawarai, and Antonio Orlacchio. 2014. "Hereditary Spastic Paraplegia: Clinical-Genetic Characteristics and Evolving Molecular Mechanisms." *Experimental Neurology*. Academic Press Inc. <https://doi.org/10.1016/j.expneurol.2014.06.011>.
- Goker-Alpan, O, K S Hruska, E Orvisky, P S Kishnani, B K Stubblefield, and R Schiffmann. 2005. "Divergent Phenotypes in Gaucher Disease Implicate the Role of Modifiers." *J Med Genet*. <https://doi.org/10.1136/jmg.2004.028019>.

- Goker-Alpan, O, R Schiffmann, M E Lamarca, R L Nussbaum, and A Mcinerney-Leo. 2004. "Parkinsonism among Gaucher Disease Carriers." *J Med Genet* 41: 937–40. <https://doi.org/10.1136/jmg.2004.024455>.
- Graaf, Michelle De, Irene C Van Veen, Ida H Van Der Meulen-Muileman, Winald R Gerritsen, Herbert M Pinedo, and Hidde J Haisma. 2001. "Cloning and Characterization of Human Liver Cytosolic β -Glycosidase." *Biochem. J.* Vol. 356.
- Grabowski, Gregory A. 2008. "Phenotype, Diagnosis, and Treatment of Gaucher's Disease." *The Lancet*. [https://doi.org/10.1016/S0140-6736\(08\)61522-6](https://doi.org/10.1016/S0140-6736(08)61522-6).
- Groener, J. E.M., B. J.H.M. Poorthuis, S. Kuiper, C. E.M. Hollak, and J. M.F.G. Aerts. 2008. "Plasma Glucosylceramide and Ceramide in Type 1 Gaucher Disease Patients: Correlations with Disease Severity and Response to Therapeutic Intervention." *Biochimica et Biophysica Acta - Molecular and Cell Biology of Lipids* 1781 (1–2): 72–78. <https://doi.org/10.1016/j.bbali.2007.11.004>.
- Haeussler, Maximilian, Kai Schönig, Hélène Eckert, Alexis Eschstruth, Joffrey Mianné, Jean-Baptiste Renaud, Sylvie Schneider-Maunoury, et al. 2016. "Evaluation of Off-Target and on-Target Scoring Algorithms and Integration into the Guide RNA Selection Tool CRISPOR." *Genome Biology* 17 (1): 148. <https://doi.org/10.1186/s13059-016-1012-2>.
- Hammer, Monia B., Ghada Eleuch-Fayache, Lucia V. Schottlaender, Houda Nehdi, J. Raphael Gibbs, Sampath K. Arepalli, Sean B. Chong, et al. 2013. "Mutations in GBA2 Cause Autosomal-Recessive Cerebellar Ataxia with Spasticity." *American Journal of Human Genetics* 92 (2): 245–51. <https://doi.org/10.1016/j.ajhg.2012.12.012>.
- Haugarvoll, Kristoffer, Stefan Johansson, Carlos E Rodriguez, Helge Boman, Bjørn Ivar Haukanes, Ove Bruland, Francisco Roque, et al. 2017. "GBA2 Mutations Cause a Marinesco-Sjögren-Like Syndrome: Genetic and Biochemical Studies." *PLoS One* 12 (1): e0169309. <https://doi.org/10.1371/journal.pone.0169309>.
- Havlicek, Steven, Zacharias Kohl, Himanshu K Mishra, Iryna Prots, Esther Eberhardt, Naime Denguir, Holger Wend, et al. 2014. "Gene Dosage-Dependent Rescue of HSP Neurite Defects in SPG4 Patients' Neurons." *Human Molecular Genetics* 23 (10): 2527–41. <https://doi.org/10.1093/hmg/ddt644>.
- Hayashi, Yasuhiro, Nozomu Okino, Yoshimitsu Kakuta, Toshihide Shikanai, Motohiro Tani, Hisashi Narimatsu, and Makoto Ito. 2007. "Klotho-Related Protein Is a Novel Cytosolic Neutral β -Glucosylceramidase * \square S." <https://doi.org/10.1074/jbc.M700832200>.
- Heier, Christopher R., and Christine J. DiDonato. 2009. "Translational Readthrough by the Aminoglycoside Geneticin (G418) Modulates SMN Stability in Vitro and Improves Motor Function in SMA Mice in Vivo." *Human Molecular Genetics* 18 (7): 1310–22. <https://doi.org/10.1093/hmg/ddp030>.
- Hnatiuk, Anna P., Francesca Briganti, David W. Staudt, and Mark Mercola. 2021. "Human iPSC Modeling of Heart Disease for Drug Development." *Cell Chemical Biology* 28 (3): 271–82. <https://doi.org/10.1016/j.chembiol.2021.02.016>.
- Hollak, Carla E.M., Derrallynn Hughes, Ivo N. Van Schaik, Barbara Schwierin, and Bruno Bembi. 2009. "Miglustat (Zavesca®) in Type 1 Gaucher Disease: 5-Year Results of a Post-Authorisation Safety Surveillance Programme." *Pharmacoepidemiology and Drug Safety* 18 (9): 770–77. <https://doi.org/10.1002/pds.1779>.
- Howard, Marybeth, Raymond A. Frizzell, and David M. Bedwell. 1996. "Aminoglycoside Antibiotics Restore CFTR Function by Overcoming Premature Stop Mutations." *Nature Medicine* 2 (4): 467–69. <https://doi.org/10.1038/nm0496-467>.
- Hruska, Kathleen S., Mary E. LaMarca, C. Ronald Scott, and Ellen Sidransky. 2008. "Gaucher Disease: Mutation and Polymorphism Spectrum in the Glucocerebrosidase Gene (GBA)." *Human Mutation* 29 (5): 567–83. <https://doi.org/10.1002/humu.20676>.
- Huh, Young Eun, Hyejung Park, Ming Sum Ruby Chiang, Idil Tuncali, Ganqiang Liu, Joseph J Locascio, Julia Shirvan, et al. 2021. "Glucosylceramide in Cerebrospinal Fluid of Patients with GBA-Associated and Idiopathic Parkinson's Disease Enrolled in PPMI." *Npj Parkinson's Disease* 7 (1). <https://doi.org/10.1038/s41531-021-00241-3>.

- Jinek, M., K. Chylinski, I. Fonfara, M. Hauer, J. a. Doudna, and E. Charpentier. 2012. "A Programmable Dual-RNA-Guided DNA Endonuclease in Adaptive Bacterial Immunity." *Science* 337 (6096): 816–21. <https://doi.org/10.1126/science.1225829>.
- Jinek, Martin, Alexandra East, Aaron Cheng, Steven Lin, Enbo Ma, and Jennifer Doudna. 2013. "RNA-Programmed Genome Editing in Human Cells." *ELife* 2013 (2): e00471. <https://doi.org/10.7554/eLife.00471>.
- Junying, Yu, Hu Kejin, Smuga Otto Kim, Tian Shulan, Ron Stewart, Igor I. Slukvin, and James A. Thomson. 2009. "Human Induced Pluripotent Stem Cells Free of Vector and Transgene Sequences." *Science* 324 (5928): 797–801. <https://doi.org/10.1126/science.1172482>.
- Kalmar, Bernadett, Ching Hua Lu, and Linda Greensmith. 2014. "The Role of Heat Shock Proteins in Amyotrophic Lateral Sclerosis: The Therapeutic Potential of Arimocloamol." *Pharmacology and Therapeutics*. <https://doi.org/10.1016/j.pharmthera.2013.08.003>.
- Khalil, Ahmad M. 2020. "The Genome Editing Revolution: Review." *Journal of Genetic Engineering & Biotechnology* 18 (1). <https://doi.org/10.1186/S43141-020-00078-Y>.
- Kim, Dohoon, Chun-Hyung Kim, Jung-Il Moon, Young-Gie Chung, Mi-Yoon Chang, Baek-Soo Han, Sanghyeok Ko, et al. 2009. "Generation of Human Induced Pluripotent Stem Cells by Direct Delivery of Reprogramming Proteins." <https://doi.org/10.1016/j.stem.2009.05.005>.
- Kim, Jennifer Yejean, Yoojun Nam, Yeri Alice Rim, and Ji Hyeon Ju. 2022. "Review of the Current Trends in Clinical Trials Involving Induced Pluripotent Stem Cells." *Stem Cell Reviews and Reports* 18 (1): 142–54. <https://doi.org/10.1007/s12015-021-10262-3>.
- Kim, Sojung, Daesik Kim, Seung Woo Cho, Jungeun Kim, and Jin Soo Kim. 2014. "Highly Efficient RNA-Guided Genome Editing in Human Cells via Delivery of Purified Cas9 Ribonucleoproteins." *Genome Research* 24 (6): 1012–19. <https://doi.org/10.1101/gr.171322.113>.
- Kirkegaard, Thomas, James Gray, David A. Priestman, Kerri Lee Wallom, Jennifer Atkins, Ole Dines Olsen, Alexander Klein, et al. 2016. "Heat Shock Protein-Based Therapy as a Potential Candidate for Treating the Sphingolipidoses." *Science Translational Medicine* 8 (355). <https://doi.org/10.1126/scitranslmed.aad9823>.
- Kitatani, Kazuyuki, Jolanta Idkowiak-Baldys, and Yusuf A. Hannun. 2008. "The Sphingolipid Salvage Pathway in Ceramide Metabolism and Signaling." *Cellular Signalling* 20 (6): 1010–18. <https://doi.org/10.1016/j.cellsig.2007.12.006>.
- Kolter, Thomas, and Konrad Sandhoff. 2006. "Sphingolipid Metabolism Diseases." *Biochimica et Biophysica Acta - Biomembranes* 1758 (12): 2057–79. <https://doi.org/10.1016/j.bbamem.2006.05.027>.
- Körschen, Heinz G., Yildiz Yildiz, Diana Nancy Raju, Sophie Schonauer, Wolfgang Bönigk, Vera Jansen, Elisabeth Kremmer, U. Benjamin Kaupp, and Dagmar Wachten. 2013. "The Non-Lysosomal β -Glucosidase GBA2 Is a Non-Integral Membrane-Associated Protein at the Endoplasmic Reticulum (ER) and Golgi." *Journal of Biological Chemistry* 288 (5): 3381–93. <https://doi.org/10.1074/jbc.M112.414714>.
- Kriks, Sonja, Jae-Won Shim, Jinghua Piao, Yosif M Ganat, Dustin R Wakeman, Zhong Xie, Luis Carrillo-Reid, et al. 2011. "Dopamine Neurons Derived from Human ES Cells Efficiently Engraft in Animal Models of Parkinson's Disease." *Nature* 480 (7378): 547–51. <https://doi.org/10.1038/nature10648>.
- Laviad, Elad L, Lee Albee, Irene Pankova-Kholmyansky, Sharon Epstein, Hyejung Park, Alfred H § Merrill, and Anthony H Futerman. 2007. "Characterization of Ceramide Synthase 2 TISSUE DISTRIBUTION, SUBSTRATE SPECIFICITY, AND INHIBITION BY SPHINGOSINE 1-PHOSPHATE * □ S EXPERIMENTAL PROCEDURES." <https://doi.org/10.1074/jbc.M707386200>.
- Levy, Michal, and Anthony H. Futerman. 2010. "Mammalian Ceramide Synthases." *IUBMB Life* 62 (5): 347–56. <https://doi.org/10.1002/iub.319>.
- Li, Hongyi, Yang Yang, Weiqi Hong, Mengyuan Huang, Min Wu, and Xia Zhao. 2020. "Applications of Genome Editing Technology in the Targeted Therapy of Human Diseases: Mechanisms, Advances and Prospects." *Signal Transduction and Targeted Therapy*. Springer Nature. <https://doi.org/10.1038/s41392-019-0089-y>.
- Liang, Xiquan, Jason Potter, Shantanu Kumar, Yanfei Zou, Rene Quintanilla, Mahalakshmi Sridharan,

- Jason Carte, et al. 2015. "Rapid and Highly Efficient Mammalian Cell Engineering via Cas9 Protein Transfection." *Journal of Biotechnology* 208 (August): 44–53. <https://doi.org/10.1016/j.jbiotec.2015.04.024>.
- Lieber, Michael R. 2010. "The Mechanism of Double-Strand DNA Break Repair by the Nonhomologous DNA End Joining Pathway THE BIOLOGICAL CONTEXT OF NHEJ." *Annu Rev Biochem* 79: 181–211. <https://doi.org/10.1146/annurev.biochem.052308.093131>.
- Lin, Pengfei, Jianwei Li, Qiji Liu, Fei Mao, Jisheng Li, Rongfang Qiu, Huili Hu, et al. 2008. "A Missense Mutation in SLC33A1, Which Encodes the Acetyl-CoA Transporter, Causes Autosomal-Dominant Spastic Paraplegia (SPG42)." *American Journal of Human Genetics* 83 (6): 752–59. <https://doi.org/10.1016/j.ajhg.2008.11.003>.
- Liu, Yong-Yu, and Yu-Teh Li. 2013. "Ceramide Glycosylation Catalyzed by Glucosylceramide Synthase and Cancer Drug Resistance." *Advances in Cancer Research* 117: 59. <https://doi.org/10.1016/B978-0-12-394274-6.00003-0>.
- Lopez-Novoa, Jose M., Yaremi Quiros, Laura Vicente, Ana I. Morales, and Francisco J. Lopez-Hernandez. 2011. "New Insights into the Mechanism of Aminoglycoside Nephrotoxicity: An Integrative Point of View." *Kidney International* 79 (1): 33–45. <https://doi.org/10.1038/KI.2010.337>.
- Lukina, Elena, Nora Watman, Marta Dragosky, Gregory M. Pastores, Elsa Avila Arreguin, Hanna Rosenbaum, Ari Zimran, et al. 2014. "Eliglustat, an Investigational Oral Therapy for Gaucher Disease Type 1: Phase 2 Trial Results after 4years of Treatment." *Blood Cells, Molecules, and Diseases* 53 (4): 274–76. <https://doi.org/10.1016/j.bcmd.2014.04.002>.
- Lwin, Alicia, Eduard Orvisky, Ozlem Goker-Alpan, Mary E. LaMarca, and Ellen Sidransky. 2004. "Glucocerebrosidase Mutations in Subjects with Parkinsonism." *Molecular Genetics and Metabolism* 81 (1): 70–73. <https://doi.org/10.1016/j.ymgme.2003.11.004>.
- Malekkou, Anna, Maura Samarani, Anthi Drousiotou, Christina Votsi, Sandro Sonnino, Marios Pantzaris, Elena Chiricozzi, et al. 2018. "Biochemical Characterization of the GBA2 c.1780G>>C Missense Mutation in Lymphoblastoid Cells from Patients with Spastic Ataxia." *International Journal of Molecular Sciences* 19 (10): 3099. <https://doi.org/10.3390/ijms19103099>.
- Mali, Prashant, Luhan Yang, Kevin M. Esvelt, John Aach, Marc Guell, James E. DiCarlo, Julie E. Norville, and George M. Church. 2013. "RNA-Guided Human Genome Engineering via Cas9." *Science* 339 (6121): 823–26. <https://doi.org/10.1126/science.1232033>.
- Marques, André R. A., Mina Mirzaian, Hisako Akiyama, Patrick Wisse, Maria J. Ferraz, Paulo Gaspar, Karen Ghauharali-van der Vlugt, et al. 2016. "Glucosylated Cholesterol in Mammalian Cells and Tissues: Formation and Degradation by Multiple Cellular β -Glucosidases." *Journal of Lipid Research* 57 (3): 451. <https://doi.org/10.1194/JLR.M064923>.
- Martin, Elodie, Rebecca Schüle, Katrien Smets, Agnès Rastetter, Amir Boukhris, José L Loureiro, Michael A Gonzalez, et al. 2013. "Loss of Function of Glucocerebrosidase GBA2 Is Responsible for Motor Neuron Defects in Hereditary Spastic Paraplegia." *American Journal of Human Genetics* 92 (2): 238–44. <https://doi.org/10.1016/j.ajhg.2012.11.021>.
- Matern, Heidrun, Henrike Boermans, Friedrich Lottspeich, and Siegfried Matern. 2001. "Molecular Cloning and Expression of Human Bile Acid β -Glucosidase Downloaded From." Vol. 23. JBC Papers in Press. <http://www.jbc.org/>.
- Matern, Heidrun, Heribert Heinemann, Gü Nter Legler, and Siegfried Matern. 1997. "Purification and Characterization of a Microsomal Bile Acid-Glucosidase from Human Liver*." <http://www-jbc.stanford.edu/jbc/>.
- Maury, Yves, Julien Côme, Rebecca A Piskorowski, Nouzha Salah-Mohellibi, Vivien Chevaleyre, Marc Peschanski, Cécile Martinat, and Stéphane Nedelec. 2014. "Combinatorial Analysis of Developmental Cues Efficiently Converts Human Pluripotent Stem Cells into Multiple Neuronal Subtypes." *Nature Biotechnology* 33 (1): 89–96. <https://doi.org/10.1038/nbt.3049>.
- Meer, Gerrit van, Jasja Wolthoorn, and Sophie Degroote. 2003. "The Fate and Function of Glycosphingolipid Glucosylceramide." *Philosophical Transactions of the Royal Society of London. Series B, Biological Sciences* 358 (1433): 869–73. <https://doi.org/10.1098/rstb.2003.1266>.
- Merrill, Alfred H. 2011. "Sphingolipid and Glycosphingolipid Metabolic Pathways in the Era of

- Sphingolipidomics." <https://doi.org/10.1021/cr2002917>.
- Mielke, Michelle M., Walter Maetzler, Norman J. Haughey, Veera V.R. Bandaru, Rodolfo Savica, Christian Deuschle, Thomas Gasser, et al. 2013. "Plasma Ceramide and Glucosylceramide Metabolism Is Altered in Sporadic Parkinson's Disease and Associated with Cognitive Impairment: A Pilot Study." *PLoS ONE* 8 (9). <https://doi.org/10.1371/journal.pone.0073094>.
- Mielke, Michelle M, Norman J Haughey, V V R Bandaru, Henrik Zetterberg, Kaj Blennow, Ulf Andreasson, Sterling C Johnson, et al. 2014. "CSF Sphingolipids, β -Amyloid, and Tau in Adults at Risk for Alzheimer's Disease." *Neurobiol Aging* 35 (11): 2486–94. <https://doi.org/10.1016/j.neurobiolaging.2014.05.019>.
- Mignot, Cyril, Antoinette Gelot, and Thierry Billette De Villemeur. 2013. *Gaucher Disease. Handbook of Clinical Neurology*. 1st ed. Vol. 113. Elsevier B.V. <https://doi.org/10.1016/B978-0-444-59565-2.00040-X>.
- Mistry, Pramod K., Jun Liua, Mei Yanga, Timothy Nottolic, James McGratha, Dhanpat Jaine, Kate Zhangf, et al. 2010. "Glucocerebrosidase Gene-Deficient Mouse Recapitulates Gaucher Disease Displaying Cellular and Molecular Dysregulation beyond the Macrophage." *Proceedings of the National Academy of Sciences of the United States of America* 107 (45): 19473–78. <https://doi.org/10.1073/pnas.1003308107>.
- Mullin, S., D. Hughes, A. Mehta, and A. H.V. Schapira. 2019. "Neurological Effects of Glucocerebrosidase Gene Mutations." *European Journal of Neurology*. Blackwell Publishing Ltd. <https://doi.org/10.1111/ene.13837>.
- Nagel, Maike, Jennifer Reichbauer, Judith Böhringer, Yvonne Schelling, Inge Krägeloh-Mann, Rebecca Schüle, and Ulrike Ulmer. 2019. "Lab Resource: Multiple Cell Lines Generation of Two iPSC Lines Derived from Two Unrelated Patients with Gaucher Disease." *Stem Cell Research* 35: 101336. <https://doi.org/10.1016/j.scr.2018.10.021>.
- Okita, Keisuke, Yasuko Matsumura, Yoshiko Sato, Aki Okada, Asuka Morizane, Satoshi Okamoto, Hyenjong Hong, et al. 2011. "A More Efficient Method to Generate Integration-Free Human IPS Cells." *Nature Methods* 8 (5): 409–12. <https://doi.org/10.1038/nmeth.1591>.
- Overkleeft, Herman S, G Herma Renkema, Jolanda Neele, Paula Vianello, Irene O Hung, Anneke Strijland, Alida M Van Der Burg, Gerrit-Jan Koomen, Upendra K Pandit, and Johannes M F G Aerts. 1998. "Generation of Specific Deoxynojirimycin-Type Inhibitors of the Non-Lysosomal Glucosylceramidase*." <http://www.jbc.org/>.
- Pellegrino, Roberto Maria, Alessandra Di Veroli, Aurora Valeri, Laura Goracci, and Gabriele Cruciani. 2014. "LC/MS Lipid Profiling from Human Serum: A New Method for Global Lipid Extraction." *Analytical and Bioanalytical Chemistry* 406 (30): 7937–48. <https://doi.org/10.1007/s00216-014-8255-0>.
- Peng, Yajing, Mi Li, Ben D. Clarkson, Mariana Pehar, Patrick J. Lao, Ansel T. Hillmer, Todd E. Barnhart, et al. 2014. "Deficient Import of Acetyl-CoA into the ER Lumen Causes Neurodegeneration and Propensity to Infections, Inflammation, and Cancer." *Journal of Neuroscience* 34 (20): 6772–89. <https://doi.org/10.1523/JNEUROSCI.0077-14.2014>.
- Peotter, Jennifer L., Iryna Pustova, Molly M. Lettman, Shalini Shatadal, Mazdak M. Bradberry, Allison D. Winter-Reed, Maya Charan, et al. 2022. "TFG Regulates Secretory and Endosomal Sorting Pathways in Neurons to Promote Their Activity and Maintenance." *Proceedings of the National Academy of Sciences of the United States of America* 119 (40): 1–12. <https://doi.org/10.1073/pnas.2210649119>.
- Platt, Frances M. 2014. "Sphingolipid Lysosomal Storage Disorders." *Nature* 510 (7503): 68–75. <https://doi.org/10.1038/nature13476>.
- Porteus, Matthew H, and Dana Carroll. 2005. "Gene Targeting Using Zinc Finger Nucleases." *Nature Biotechnology* 23 (8): 967–73. <https://doi.org/10.1038/nbt1125>.
- Raju, Diana, Sophie Schonauer, Hussein Hamzeh, Kevin C Flynn, Frank Bradke, Katharina Vom Dorp, Peter Dörmann, et al. 2015. "Accumulation of Glucosylceramide in the Absence of the Beta-Glucosidase GBA2 Alters Cytoskeletal Dynamics." *PLoS Genetics* 11 (3): e1005063. <https://doi.org/10.1371/journal.pgen.1005063>.
- Ran, Caroline, Lovisa Brodin, Lars Forsgren, Marie Westerlund, Mehrafarin Ramezani, Sandra

- Gellhaar, Fengqing Xiang, et al. 2016. "Strong Association between Glucocerebrosidase Mutations and Parkinson's Disease in Sweden." *Neurobiology of Aging* 45 (September): 212.e5. <https://doi.org/10.1016/j.neurobiolaging.2016.04.022>.
- Ran, F, Patrick Hsu, Jason Wright, Vineeta Agarwala, David Scott, and Feng Zhang. 2013. "Genome Engineering Using the CRISPR-Cas9 System." *Nature Protocols* 8 (11): 2281–2308. <https://doi.org/10.1038/nprot.2013.143>.
- Rehbach, Kristina, Jaideep Kesavan, Stefan Hauser, Svetlana Ritzenhofen, Johannes Jungverdorben, Rebecca Schüle, Ludger Schöls, Michael Peitz, and Oliver Brüstle. 2019. "Multiparametric Rapid Screening of Neuronal Process Pathology for Drug Target Identification in HSP Patient-Specific Neurons." *Scientific Reports* 9 (1): 9615. <https://doi.org/10.1038/s41598-019-45246-4>.
- Reinhardt, P, M Glatza, K Hemmer, Y Tsytsyura, C S Thiel, S Hoing, S Moritz, et al. 2013. "Derivation and Expansion Using Only Small Molecules of Human Neural Progenitors for Neurodegenerative Disease Modeling." *PLoS One* 8 (3): e59252. <https://doi.org/10.1371/journal.pone.0059252>.
- Reza, Safoura, Maciej Ugorski, and Jarosław Suchański. 2021. "Glucosylceramide and Galactosylceramide, Small Glycosphingolipids with Significant Impact on Health and Disease." *Glycobiology* 31 (11): 1416–34. <https://doi.org/10.1093/glycob/cwab046>.
- Richardson, Christopher D, Graham J Ray, Mark A DeWitt, Gemma L Curie, and Jacob E Corn. 2016. "Enhancing Homology-Directed Genome Editing by Catalytically Active and Inactive CRISPR-Cas9 Using Asymmetric Donor DNA." *Nature Biotechnology* 34 (3): 339–44. <https://doi.org/10.1038/nbt.3481>.
- Schneider, Susanne A., and Roy N. Alcalay. 2020. "Precision Medicine in Parkinson's Disease: Emerging Treatments for Genetic Parkinson's Disease." *Journal of Neurology*. Springer. <https://doi.org/10.1007/s00415-020-09705-7>.
- Schöls, Ludger, Tim W Rattay, Peter Martus, Christoph Meisner, Jonathan Baets, Imma Fischer, Christine Jäggle, et al. 2017. "Hereditary Spastic Paraplegia Type 5: Natural History, Biomarkers and a Randomized Controlled Trial." *Brain* 140 (12): 3112–27. <https://doi.org/10.1093/brain/awx273>.
- Schonauer, Sophie, Heinz G Körschen, Anke Penno, Andreas Rennhack, Bernadette Breiden, Konrad Sandhoff, Katharina Gutbrod, et al. 2017. "Identification of a Feedback Loop Involving β -Glucosidase 2 and Its Product Sphingosine Sheds Light on the Molecular Mechanisms in Gaucher Disease." *The Journal of Biological Chemistry* 292 (15): 6177–89. <https://doi.org/10.1074/jbc.M116.762831>.
- Schöndorf, David C, Massimo Aureli, Fiona E McAllister, Christopher J Hindley, Florian Mayer, Benjamin Schmid, S Pablo Sardi, et al. 2014. "iPSC-Derived Neurons from GBA1-Associated Parkinson's Disease Patients Show Autophagic Defects and Impaired Calcium Homeostasis." *Nature Communications* 5 (May): 4028. <https://doi.org/10.1038/ncomms5028>.
- Schubert, Sarah F., Sabine Hoffjan, and Gabriele Dekomien. 2016. "Mutational Analysis of the CYP7B1, PNPLA6 and C19orf12 Genes in Autosomal Recessive Hereditary Spastic Paraplegia." *Molecular and Cellular Probes* 30 (1): 53–55. <https://doi.org/10.1016/j.mcp.2015.12.001>.
- Schüle, Rebecca, Sarah Wiethoff, Peter Martus, Kathrin N. Karle, Susanne Otto, Stephan Klebe, Sven Klimpe, et al. 2016. "Hereditary Spastic Paraplegia: Clinicogenetic Lessons from 608 Patients." *Annals of Neurology* 79 (4): 646–58. <https://doi.org/10.1002/ana.24611>.
- Schuster, S., E. Heuten, A. Velic, J. Admard, M. Synofzik, S. Ossowski, B. Macek, S. Hauser, and L. Schöls. 2020. "CHIP Mutations Affect the Heat Shock Response Differently in Human Fibroblasts and iPSC-Derived Neurons." *DMM Disease Models and Mechanisms* 13 (10). <https://doi.org/10.1242/dmm.045096>.
- Shi, Yanhong, Haruhisa Inoue, Joseph C Wu, and Shinya Yamanaka. 2017. "Induced Pluripotent Stem Cell Technology: A Decade of Progress." *Nature Reviews Drug Discovery*. <https://doi.org/10.1038/nrd.2016.245>.
- Shi, Yichen, Peter Kirwan, James Smith, Hugh P C Robinson, and Frederick J Livesey. 2012. "Human Cerebral Cortex Development from Pluripotent Stem Cells to Functional Excitatory Synapses." *Nature Neuroscience* 15 (3): 477–86, S1. <https://doi.org/10.1038/nn.3041>.
- Sidransky, E., M.A. Nalls, J.O. Aasly, J. Aharon-Peretz, G. Annesi, E.R. Barbosa, A. Bar-Shira, et al.

2009. "Multicenter Analysis of Glucocerebrosidase Mutations in Parkinson's Disease." *New England Journal of Medicine* 361 (17): 1651–61. <https://doi.org/10.1056/NEJMoa0901281>.
- Sidransky, Ellen. 2004. "Gaucher Disease: Complexity in a 'Simple' Disorder." *Molecular Genetics and Metabolism* 83 (1–2): 6–15. <https://doi.org/10.1016/j.ymgme.2004.08.015>.
- Sidransky, Ellen, David M. Sherer, and Edward I. Ginns. 1992. "Gaucher Disease in the Neonate: A Distinct Gaucher Phenotype Is Analogous to a Mouse Model Created by Targeted Disruption of the Glucocerebrosidase Gene." *Pediatric Research* 32 (4): 494–98. <https://doi.org/10.1203/00006450-199210000-00023>.
- Slotte, J. Peter. 2013. "Biological Functions of Sphingomyelins." *Progress in Lipid Research* 52 (4): 424–37. <https://doi.org/10.1016/j.plipres.2013.05.001>.
- Smith, Laura, Stephen Mullin, and Anthony H.V. Schapira. 2017. "Insights into the Structural Biology of Gaucher Disease." *Experimental Neurology*. Academic Press Inc. <https://doi.org/10.1016/j.expneurol.2017.09.010>.
- Spassieva, Stefka D., Xiaojie Ji, Ye Liu, Kenneth Gable, Jacek Bielawski, Teresa M. Dunn, Erhard Bieberich, and Lihong Zhao. 2016. "Ectopic Expression of Ceramide Synthase 2 in Neurons Suppresses Neurodegeneration Induced by Ceramide Synthase 1 Deficiency." *Proceedings of the National Academy of Sciences of the United States of America* 113 (21): 5928–33. <https://doi.org/10.1073/pnas.1522071113>.
- Stepanenko, A. A., and V. V. Dmitrenko. 2015. "HEK293 in Cell Biology and Cancer Research: Phenotype, Karyotype, Tumorigenicity, and Stress-Induced Genome-Phenotype Evolution." *Gene* 569 (2): 182–90. <https://doi.org/10.1016/j.gene.2015.05.065>.
- Stith, Jeffrey L., Fabiola N. Velazquez, and Lina M. Obeid. 2019. "Advances in Determining Signaling Mechanisms of Ceramide and Role in Disease." *Journal of Lipid Research* 60 (5): 913–18. <https://doi.org/10.1194/jlr.S092874>.
- Sultana, Saki, Jennifer Reichbauer, Rebecca Schüle, Fanny Mochel, Matthis Synofzik, and Aarnoud C. Van Der Spoel. 2015. "Lack of Enzyme Activity in GBA2 Mutants Associated with Hereditary Spastic Paraplegia/Cerebellar Ataxia (SPG46)." *Biochemical and Biophysical Research Communications* 465 (1): 35–40. <https://doi.org/10.1016/j.bbrc.2015.07.112>.
- Sun, Angela. 2018. "Lysosomal Storage Disease Overview." *Annals of Translational Medicine* 6 (24): 476–476. <https://doi.org/10.21037/atm.2018.11.39>.
- Symington, Lorraine S, and Jean Gautier. 2011. "Double-Strand Break End Resection and Repair Pathway Choice." <https://doi.org/10.1146/annurev-genet-110410-132435>.
- Synofzik, Matthis, Michael A Gonzalez, Charles Marques Lourenco, Marie Coutelier, Tobias B Haack, Adriana Rebelo, Didier Hannequin, et al. 2014. "PNPLA6 Mutations Cause Boucher-Neuhauser and Gordon Holmes Syndromes as Part of a Broad Neurodegenerative Spectrum." *Brain : A Journal of Neurology* 137 (Pt 1): 69–77. <https://doi.org/10.1093/brain/awt326>.
- Takahashi, Kazutoshi, Koji Tanabe, Mari Ohnuki, Megumi Narita, Tomoko Ichisaka, Kiichiro Tomoda, and Shinya Yamanaka. 2007. "Induction of Pluripotent Stem Cells from Adult Human Fibroblasts by Defined Factors." *Cell* 131 (5): 861–72. <https://doi.org/10.1016/j.cell.2007.11.019>.
- Takahashi, Kazutoshi, and Shinya Yamanaka. 2006. "Induction of Pluripotent Stem Cells from Mouse Embryonic and Adult Fibroblast Cultures by Defined Factors." *Cell* 126 (4): 663–76. <https://doi.org/10.1016/j.cell.2006.07.024>.
- Terns, Michael P, and Rebecca M Terns. 2011. "CRISPR-Based Adaptive Immune Systems." <https://doi.org/10.1016/j.mib.2011.03.005>.
- Tesson, Christelle, Magdalena Nawara, Mustafa a M Salih, Rodrigue Rossignol, Maha S. Zaki, Mohammed Al Balwi, Rebecca Schule, et al. 2012. "Alteration of Fatty-Acid-Metabolizing Enzymes Affects Mitochondrial Form and Function in Hereditary Spastic Paraplegia." *American Journal of Human Genetics* 91 (6): 1051–64. <https://doi.org/10.1016/j.ajhg.2012.11.001>.
- Thompson, Sarah L., and Duane A. Compton. 2011. "Chromosomes and Cancer Cells." *Chromosome Research*. NIH Public Access. <https://doi.org/10.1007/s10577-010-9179-y>.
- Urnov, Fyodor D, Edward J Rebar, Michael C Holmes, H Steve Zhang, and Philip D Gregory. 2010. "Genome Editing with Engineered Zinc Finger Nucleases." *Nature Reviews. Genetics* 11 (9): 636–46. <https://doi.org/10.1038/nrg2842>.

- Votsi, Christina, Eleni Zamba-Papanicolaou, Lefkos T. Middleton, Marios Pantzaris, and Kyproula Christodoulou. 2014. "A Novel GBA2 Gene Missense Mutation in Spastic Ataxia." *Annals of Human Genetics* 78 (1): 13–22. <https://doi.org/10.1111/ahg.12045>.
- Wagner, Matias, Daniel P.S. Osborn, Ina Gehweiler, Maike Nagel, Ulrike Ulmer, Somayeh Bakhtiari, Rim Amouri, et al. 2019. "Bi-Allelic Variants in RNF170 Are Associated with Hereditary Spastic Paraplegia." *Nature Communications* 10 (1). <https://doi.org/10.1038/s41467-019-12620-9>.
- Warren, Luigi, Philip D Manos, Tim Ahfeldt, Yui-Han Loh, Hu Li, Frank Lau, Wataru Ebina, et al. 2010. "Highly Efficient Reprogramming to Pluripotency and Directed Differentiation of Human Cells Using Synthetic Modified mRNA." *Cell Stem Cell* 7 (5): 618–30. <https://doi.org/10.1016/j.stem.2010.08.012>.
- Weely, Sonja Van, Johannes M.F.G. Aerts, Marinella B. Van Leeuwen, Judith C. Heikoop, Wilma E. Donker-Koopman, John A. Barranger, Tager Joseph M., and André W. Schram. 1990. "Function of Oligosaccharide Modification in Glucocerebrosidase, a Membrane-associated Lysosomal Hydrolase." *European Journal of Biochemistry* 191 (3): 669–77. <https://doi.org/10.1111/j.1432-1033.1990.tb19173.x>.
- Weely, Sonja Van, Margreet Brandsma, Anneke Strijland, Joseph M Tager, and Johannes M F G Aerts. 1993. "Demonstration of the Existence of a Second, Non-Lysosomal Glucocerebrosidase That Is Not Deficient in Gaucher Disease." *Biochimica et Biophysica Acta*. https://ac.els-cdn.com/092544399390090N/1-s2.0-092544399390090N-main.pdf?_tid=fb430b58-e092-43db-8f19-0ae1c2b82308&acdnat=1533039824_f420d3606e0982ecb82cd8e16a041bd1.
- Westbroek, Wendy, Ann Marie Gustafson, and Ellen Sidransky. 2011. "Exploring the Link between Glucocerebrosidase Mutations and Parkinsonism." *Trends in Molecular Medicine* 17 (9): 485–93. <https://doi.org/10.1016/j.molmed.2011.05.003>.
- Witte, Martin D., Wouter W. Kallemeijn, Jan Aten, Kah Yee Li, Anneke Strijland, Wilma E. Donker-Koopman, Adrianus M.C.H. Van Den Nieuwendijk, et al. 2010. "Ultrasensitive in Situ Visualization of Active Glucocerebrosidase Molecules." *Nature Chemical Biology* 6 (12): 907–13. <https://doi.org/10.1038/nchembio.466>.
- Woeste, Marina A., Sina Stern, Diana N. Raju, Elena Grahn, Dominik Dittmann, Katharina Gutbrod, Peter Dörmann, et al. 2019. "Species-Specific Differences in Nonlysosomal Glucosylceramidase GBA2 Function Underlie Locomotor Dysfunction Arising from Loss-of-Function Mutations." *Journal of Biological Chemistry* 294 (11): 3853–71. <https://doi.org/10.1074/jbc.RA118.006311>.
- Woeste, Marina A, Sina Stern, X N Diana Raju, Elena Grahn, Dominik Dittmann, Katharina Gutbrod, X Peter Dörmann, et al. 2019. "Species-Specific Differences in Nonlysosomal Glucosylceramidase GBA2 Function Underlie Locomotor Dysfunction Arising from Loss-of-Function Mutations." <https://doi.org/10.1074/jbc.RA118.006311>.
- Yahata, Kensei, Kiyoshi Mori, Hiroshi Arai, Susumu Koide, Yoshihiro Ogawa, Masashi Mukoyama, Akira Sugawara, et al. 2000. "Molecular Cloning and Expression of a Novel Klotho-Related Protein." *Journal of Molecular Medicine* 78 (7): 389–94. <https://doi.org/10.1007/s001090000131>.
- Yang, Yi-Jing, Zhi-Fan Zhou, Xin-Xin Liao, Ying-Ying Luo, Zi-Xiong Zhan, Mu-Fang Huang, Lu Zhou, Bei-Sha Tang, Lu Shen, and Juan Du. 2016. "SPG46 and SPG56 Are Rare Causes of Hereditary Spastic Paraplegia in China." *Journal of Neurology* 263 (10): 2136–38. <https://doi.org/10.1007/s00415-016-8256-3>.
- Yildiz, Yildiz, Per Hoffmann, Stefan Vom Dahl, Bernadette Breiden, Roger Sandhoff, Claus Niederau, Mia Horwitz, et al. 2013. "Functional and Genetic Characterization of the Non-Lysosomal Glucosylceramidase 2 as a Modifier for Gaucher Disease." *Orphanet Journal of Rare Diseases* 8 (1): 151. <https://doi.org/10.1186/1750-1172-8-151>.
- Yildiz, Yildiz, Heidrun Matern, Bonne Thompson, Jeremy C. Allegood, Rebekkah L. Warren, Denise M O Ramirez, Robert E. Hammer, F. Kent Hamra, Siegfried Matern, and David W. Russell. 2006. "Mutation of ??-Glucosidase 2 Causes Glycolipid Storage Disease and Impaired Male Fertility." *Journal of Clinical Investigation* 116 (11): 2985–94. <https://doi.org/10.1172/JCI29224>.
- Yu, Junying, Maxim A. Vodyanik, Kim Smuga-Otto, Jessica Antosiewicz-Bourget, Jennifer L. Frane, Shulan Tian, Jeff Nie, et al. 2007. "Induced Pluripotent Stem Cell Lines Derived from Human

- Somatic Cells." *Science* 318 (5858): 1917–20. <https://doi.org/10.1126/science.1151526>.
- Yu, Robert K, Yoshihiko Nakatani, and Makoto Yanagisawa. 2009. "The Role of Glycosphingolipid Metabolism in the Developing Brain." <https://doi.org/10.1194/jlr.R800028-JLR200>.
- Yue, Wyatt W., Sabrina Mackinnon, and Gustavo A. Bezerra. 2019. "Substrate Reduction Therapy for Inborn Errors of Metabolism." *Emerging Topics in Life Sciences*. Portland Press Ltd. <https://doi.org/10.1042/ETLS20180058>.
- Zaslavsky, Kirill, Wen-Bo Zhang, Fraser P. McCready, Deivid C. Rodrigues, Eric Deneault, Caitlin Loo, Melody Zhao, et al. 2019. "SHANK2 Mutations Associated with Autism Spectrum Disorder Cause Hyperconnectivity of Human Neurons." *Nature Neuroscience* 22 (4): 556–64. <https://doi.org/10.1038/s41593-019-0365-8>.
- Zhou, Hongyan, Shili Wu, Jin Young Joo, Saiyong Zhu, Dong Wook Han, Tongxiang Lin, Sunia Trauger, et al. 2009. "Generation of Induced Pluripotent Stem Cells Using Recombinant Proteins." *Cell Stem Cell* 4 (5): 381–84. <https://doi.org/10.1016/j.stem.2009.04.005>.
- Zhu, Peng-Peng, Kyle R Denton, Tyler Mark Pierson, Xue-Jun Li, and Craig Blackstone. 2014. "Pharmacologic Rescue of Axon Growth Defects in a Human iPSC Model of Hereditary Spastic Paraplegia SPG3A." *Human Molecular Genetics* 23 (21): 5638–48. <https://doi.org/10.1093/hmg/ddu280>.
- Zimran, Ari, and Deborah Elstein. 2015. "Gaucher Disease and Related Lysosomal Storage Diseases | Williams Hematology, 9e | AccessMedicine | McGraw-Hill Medical." 2015. <https://accessmedicine.mhmedical.com/content.aspx?bookid=1581§ionid=108067441>.

List of figures

| | |
|---|----|
| Fig. 1: Overview of the most frequent pathways disturbed in hereditary spastic paraplegia with examples of affected proteins. | 8 |
| Fig. 2: Application opportunities for iPSC. Somatic cells from either a patient or a healthy control subject can be reprogrammed and differentiated in a second step towards specialized cells. .. | 17 |
| Fig. 3: Comparison of the current drug development approach to a new strategy using iPSC in a clinical trial in a dish (CTiD) approach. | 18 |
| Fig. 4: Schematic representation of different gene editing approaches. | 20 |
| Fig. 5: Restriction fragment length polymorphism strategy to pre-screen picked iPSC colonies after each CRISPR approach. | 28 |
| Fig. 6: Characterization and validation of genomic integrity and pluripotency of reprogrammed iPSC from GBA1-deficient fibroblasts. | 36 |
| Fig. 7: Summary of pathogenic <i>GBA2</i> variants present in iPSCs generated from two unrelated families. | 37 |
| Fig. 8: Western Blot analysis demonstrated restoration of GBA2 protein in isogenic controls of iPSC-derived cortical neurons in three independent lysates. | 40 |
| Fig. 9: Comparing assay conditions for measuring GBA2 activity. | 41 |
| Fig. 10: Enzymatic characterization of patient-derived cortical neurons and their respective isogenic controls. | 43 |
| Fig. 11: GBA1 and GBA2 activity in GBA1-deficient neuronal cells. | 44 |
| Fig. 12: Mass Spectrometry data of three independent lysates of cortical neurons depicted in a Volcano Blot analysis. | 46 |
| Fig. 13: Comparison of hexosylceramide levels in plasma and CSF derived from different patients carrying bi-allelic <i>GBA2</i> variants to age and sex matched healthy control samples. | 48 |
| Fig. 14: Lipid mass spectrometry analysis of three independent treatment approaches in cortical neurons with G418, an aminoglycoside for translational read-through; Arimoclomol, as a co-inducer for the heat shock response and Miglustat, as substrate reduction treatment. | 51 |

List of tables

| | |
|--|----|
| Tab. 1: Selection of therapeutic approaches to target GBA1-deficiency in GBA-PD (adapted and modified from (Schneider and Alcalay 2020)). | 11 |
| Tab. 2: Overview of diseases resulting from disturbances of the sphingolipid metabolism (modified from (Platt 2014) and complemented by (Kolter and Sandhoff 2006)). | 13 |
| Tab. 3: Primers used to verify pathogenic <i>GBA</i> variants in reprogrammed iPSC via Sanger Sequencing. | 23 |
| Tab. 4: Primers used to exclude unintentional plasmid integration. | 23 |
| Tab. 5: RT-qPCR primer to compare pluripotency marker on a transcriptional level. | 24 |
| Tab. 6: Antibodies used to demonstrate pluripotency of generated GBA1-deficient iPSC by immunohistochemistry staining. | 25 |
| Tab. 7: Antibodies used for immunohistochemistry to stain neuronal markers. | 26 |
| Tab. 8: CRISPR approach and sequence-specific parts of the gRNA to correct pathogenic <i>GBA2</i> variants (NM_020944.3) in patient-derived iPS cells (PAM-sequence in grey). | 27 |
| Tab. 9: ssODNs used as repair templates to correct patient-specific variants in GBA2-deficient iPSC. | 27 |
| Tab. 10: Primers used in this study to pre-screen via RFLP, to confirmed variants in patient-derived cells and check for unintentional plasmid integration. | 28 |
| Tab. 11: Locus and primers used to confirm potential predicted off-target sites. | 29 |
| Tab. 12: Antibodies used in GBA2 Western Blot analysis. | 32 |
| Tab. 13: List of patients from which skin-derived iPSCs were generated in this project. | 34 |
| Tab. 14: Overview and efficiency of CRISPR experiments to generate isogenic controls. | 38 |
| Tab. 15: Overview over iPS cell lines used in this study. | 39 |
| Tab. 16: Evaluation of tested assay conditions to optimize the enzymatic assay for quantification of GBA2 activity. | 42 |
| Tab. 17: GBA1 and GBA2 activity in GBA2-deficient cortical neurons and a chemical GBA2 inhibited (AMP-DNM) control line. Mean and standard deviation (StDev) measured in patient-derived cells. | 42 |
| Tab. 18: GBA1 and GBA2 activity in GBA1-deficient cortical neurons and control cells treated with a GBA1 inhibitor (CBE). In these patient-derived cells GBA1 and GBA2 activity are displayed as mean with standard deviation (StDev). | 44 |

Tab. 19: Lipid classes and their respective fold changes in patient-derived cortical neurons versus isogenic controls are measured in a lipid mass spectrometry approach. Lipid classes with a fold change greater than two are highlighted. 47

Tab. 20: Overview of measured biofluid samples via mass spectrometry of GBA2-deficient patients and matching controls. 47

Acknowledgements

First I would like to thank my supervisor Prof. Dr. Rebecca Schüle for giving me the wonderful opportunity to perform my PhD thesis in her lab.

I am grateful for her trust and freedom to start this exciting project in her lab and for everything what I learned throughout this time.

Another word of thanks goes to Prof. Dr. Ludger Schöls for supporting me especially in the beginning of my thesis. Encouraging me with all his knowledge and advices throughout the thesis. Working in a closer collaboration together with the groups of Prof. Dr. Ludger Schöls and Prof. Dr. Matthis Synofzik contributed to an enthusiastic work environment of support and motivation.

I would like to thank Dr. Alaa Othman (Institute of Molecular Systems Biology, ETH Zurich) for our collaboration and his expertise, which was highly appreciated at all times.

A very special thanks goes to my advisory board members Prof. Dr. Stefan Liebau und Prof. Dr. Doron Rapoport. Thank you for guiding me throughout my thesis with all your feedback and advice. I highly appreciated the support of Prof. Dr. Stefan Liebau in process of finalizing my thesis. Further thanks to the Graduate Training Center of Neuroscience for their great support during this process.

A further special thank to Tom Wahlig foundation for hosting their unforgettable symposia and creating a familiar and welcoming atmosphere and not least for funding a part of my research.

A special thanks to all my colleagues and lab members for making this time memorable, especially: Selina, Jenny, Melanie, Maïke, Steffi, Philip, Stefan and Yvonne. Not only for all your scientific support, but also your listening, joking and keeping me motivated in all these years.

Finally I would like to thank my friends and family. Your constant support and motivation during made this journey possible and created so may unforgettable memories. I am deeply grateful for having you in my life.